Fisheries and Oceans Canada / Pêches et Océans Canada

Ecosystems and Oceans Science / Sciences des écosystèmes et des océans

Canadian Science Advisory Secretariat (CSAS)

Research Document 2021/058

Pacific Region

Vessel presence and acoustic environment within Southern Resident Killer Whale (*Orcinus orca)* critical habitat in the Salish Sea and Swiftsure Bank area

Svein Vagle[1], Rianna Burnham[1], Pramod Thupaki[1], Christine Konrad[2], Scott Toews[2], Sheila J. Thornton[2]

[1]Institute of Ocean Sciences
Fisheries and Oceans Canada
9860 W Saanich Road
Sidney, BC V8L 5T5

[2]Pacific Science Enterprise Centre
Fisheries and Oceans Canada
4160 Marine Drive
West Vancouver, BC V7V 1N6

October 2021

Canada

Foreword

This series documents the scientific basis for the evaluation of aquatic resources and ecosystems in Canada. As such, it addresses the issues of the day in the time frames required and the documents it contains are not intended as definitive statements on the subjects addressed but rather as progress reports on ongoing investigations.

Published by:

Fisheries and Oceans Canada
Canadian Science Advisory Secretariat
200 Kent Street
Ottawa ON K1A 0E6

http://www.dfo-mpo.gc.ca/csas-sccs/
csas-sccs@dfo-mpo.gc.ca

ISSN 1919-5044
ISBN 978-0-660-40238-3 Cat. No. Fs70-5/2021-058E-PDF

Correct citation for this publication:

Vagle, S., Burnham, R., Thupaki, P., Konrad, C., Toews, S., Thornton, S.J. 2021. Vessel presence and acoustic environment within Southern Resident Killer Whale (*Orcinus orca*) critical habitat in the Salish Sea and Swiftsure Bank area. DFO Can. Sci. Advis. Sec. Res. Doc. 2021/058. x + 66 p.

Aussi disponible en français :

*Vagle, S., Burnham, R., Thupaki, P., Konrad, C., Toews, S., Thornton, S.J. 2021. Présence de navires et environnement acoustique dans l'habitat essentiel de l'épaulard résident du Sud (*Orcinus orca*) dans la zone de la mer des Salish et du banc Swiftsure. Secr. can. de consult. sci. du MPO. Doc. de rech. 2021/058. xi + 69 p.*

TABLE OF CONTENTS

GLOSSARY vii
PREFACE ix
ABSTRACT x
1. INTRODUCTION 1
2. METHODS 4
  2.1. SOUNDSCAPE CHARACTERIZATION 4
    2.1.1. Passive Acoustic Mooring (PAM) Network 4
  2.2. VESSEL PRESENCE AND SPEED 7
    2.2.1. Automatic Identification System (AIS) tracked vessels 7
    2.2.2. Small Vessel Analysis 9
  2.3. VESSEL NOISE MODEL 10
    2.3.1. Model Setup and Validation 10
    2.3.2. Scenario Modeling 10
3. RESULTS 11
  3.1. SOUNDSCAPE CHARACTERIZATION 11
    3.1.1. Minimum Ambient 12
    3.1.2. Soundscape composition 12
    3.1.3. Characterization of natural conditions and sound transmission 13
    3.1.4. Acoustic presence of vessels 13
  3.2. VESSEL PRESENCE AND SPEED 13
    3.2.1. AIS Vessels 13
    3.2.2. Small Vessel Presence 14
  3.3. VESSEL NOISE MODEL 15
    3.3.1. Model Results and Validation 15
    3.3.2. Scenario Modeling Results 15
4. DISCUSSION 16
5. ACKNOWLEDGMENTS 20
6. TABLES 22
7. FIGURES 28
8. REFERENCES CITED 59

LIST OF TABLES

Table 1: Frequency ranges of acoustic metrics used in this analysis 22
Table 2: Geoacoustic properties used to define the propagation of acoustic waves 23
Table 3: A list of vessel noise model and extrapolation inputs 24
Table 4: Periods of recording at each location for each summer month of analysis. 25
Table 5: Comparison between observed and simulated SPL at mooring locations 35
Table 6: Results of acoustic scenario modelling 36

LIST OF FIGURES

Figure 1: The study area in the Salish Sea 28
Figure 2: Example of the PAM moorings being deployed. 29
Figure 3: Knudsen curves relating wind speed to deep water 30
Figure 4: Example of method used to determine abiotic and anthropogenic noise 31
Figure 5: Bottom substrate type defined in the model. 32
Figure 6: Ambient noise levels averages for May to October each year.................................... 33
Figure 7: Rhythm plots to compare bimonthly sound pressure levels (SPLs)............................ 34
Figure 8: Comparison of sound pressure levels (SPLs) for days of the week. 35
Figure 9: Hourly SPLs in the SRKW communication range to compare day and night. 36
Figure 10: The L_{99} ambient noise at each site used to form a ‘minimum ambient’ 37
Figure 11: Soundscape composition derived from a Knudsen curve... 37
Figure 12: Averaged summer wind speeds (m/s) in the Salish Sea bimonthly. 38
Figure 13: Wind-noise derived additions in SRKW communication band in bimonthly periods.. 38
Figure 14: Wind-derived acoustic additions in SRKW echolocation band in bimonthly periods . 38
Figure 15: Averaged rainfall amounts (mm/hr) in the Salish Sea 39
Figure 16: Diurnal comparison for SRKW communication and echolocation bands 39
Figure 17: Average daily presence of AIS Class A large commercial vessels........................... 40
Figure 18: Average daily presence of AIS Class A (non-mandatory) vessels in the study area . 41
Figure 19: Average daily presenceof AIS Class B vessels in the study area 42
Figure 20: Average daily AIS vessel presence in the study area by month 43
Figure 21: Relative composition of AIS Class A and AIS Class B vessel presence 44
Figure 22: The change in average vessel presence of AIS Class A large commercial vessels.. 45
Figure 23: The change in average presenceof AIS Class A (non-mandatory) vessels.............. 46
Figure 24: The change in daily presence of AIS Class B vessels in 2020 47
Figure 25: Average speed over ground (SOG) of AIS Class A and AIS Class B vessels........... 48
Figure 26: Average daily distance traveled by AIS Class A large commercial vessels.............. 49
Figure 27: Average daily distance traveled by AIS Class A (non-mandatory) small vessels 50
Figure 28: Average daily distance traveled by AIS Class B vessels 51
Figure 29: Survey coverage of National Aerial Surveillance Program flights............................. 52
Figure 30: Vessel sightings per unit effort for National Aerial Surveillance Program flights 52
Figure 31: Approximated survey coverage of DFO Creel Survey overflights in the study area .. 53
Figure 32: Average count of vessels observed per DFO Creel Survey overflight....................... 54
Figure 33: Example of vessel model output. 55
Figure 34: Comparison between observed and simulated SPL 56

Figure 35: Vessel noise additions at 10 kHz in SRKW communication range 57
Figure 36: Vessel noise additions in the 50 kHz in SRKW echolocation range 57
Figure 37: Track of additional (outgoing) TMX tankers 58

GLOSSARY

1/3 octave band – a frequency band that is 1/3 of an octave wide, centered around a frequency of interest.

Automatic Identification System (AIS) – an automatic tracking system that uses transceivers to send information on vessel identity, location and planned route to Vessel Traffic Services.

Ambient noise – the level of background noise of an area, where single noise sources are not discerned.

Creel Survey - fishery catch survey that consists of aerial overflights to evaluate fishing effort, and an access point survey, where returning sport fishing parties are interviewed at boat access points (marinas, boat ramps, etc.) to estimate fishing effort and total catch.

Critical habitat (CH) - the habitat that is necessary for the survival or recovery of a listed extirpated, endangered, or threatened species, and that is identified as CH in a Species at Risk recovery strategy or action plan.

Comodulation masking release – a decrease in expected masking of a signal that occurs when noise sources demonstrate variation in their amplitude over a range of frequencies.

Exceedance levels – used to represent quartiles or percentiles for a proportion of time where a given ambient noise level has been reached.

Knudsen curves – empirical models that parameterize ambient noise as a function of frequency based on abiotic conditions.

L_1 – representation of the 1% of the data where the amplitude of the ambient noise in the range of interest is at its greatest.

L_5, L_{95} – The upper and lower 5% of the ambient noise values respectively in the frequency range of interest.

L_{50} – used to express the median value, or 50% of the time when recordings surpass a value.

L_{25}, L_{75} – used to represent the upper and lower quartiles, representing the value exceed 25% of the time and the value exceed 75% of time (or not exceeded 25% of the time) respectively.

L_{99} – used to represent background ambient noise. The noise level that 99% of the recordings analyzed exceed.

Masking – when the threshold of detection and interpretation of a sound or call is raised by the presence of another sound.

Minimum ambient - a L_{99} sound level used in this analysis to represent a level of ambient noise where vessel noise additions are absent and wind noise is negligible.

Noise – an unwanted addition to a frequency band of interest. With respect to masking, noise is used to describe the masking sound.

Passive acoustic monitoring (PAM) – an unobtrusive means to listen, describe and characterize the underwater sound field and vocalizing marine mammals within it.

Power spectral density (PSD) – the sound power divided by the bandwidth to describe how the power of a sound is distributed with frequency.

Sound Pressure Level (SPL) – the received pressure of a given sound, expressed in decibels (dB) relative to a reference pressure of 1μPa.

Source level (SL) – the amount of sound radiated by a source, defined as the intensity of the radiated sound at a distance of 1 m from the source.

Spatial masking release - a decrease in expected masking, or release, that occurs when the signal and noise source are in different locations.

Temporal masking release - a decrease in expected masking, or release, that occurs when the signal and noise source are present at different times. Similar to comodulation.

PREFACE

The Southern Resident Killer Whale (SRKW) population consists of 75 individuals (2021) and is listed as Endangered under the Canadian *Species at Risk Act* (SARA). Areas of coastal and inland waters around Vancouver Island are now legally designated as SRKW critical habitat (CH) under SARA. These areas support important life history events, and have been identified as necessary for the survival and recovery of the population.

The Salish Sea is the collective name for the inland waters around southern Vancouver Island, the Juan de Fuca Strait and the Strait of Georgia in Canada and the San Juan Islands and Puget Sound in Washington State in the United States, and is bounded to the west by a line from Cape Flattery to Carmanah Point. This collective name will be used to refer to these waterways throughout this document. The area of SRKW CH to the west of this line encompasses La Perouse Bank, Swiftsure Bank, and various canyons and submarine features. For ease of reference, this portion of SRKW CH is referred to as 'the Swiftsure Bank area' throughout this document. The phrase 'the study area' is used in this document to encompass portions of both of these areas.

This report is part of a series of three documents that together examine the threat of vessel presence and acoustic disturbance on SRKW using areas of the Salish Sea from May to October (hereafter referred to as 'summer'). First, the presence and habitat use of SRKW in the Salish Sea and Swiftsure Bank area was determined, identifying the monthly frequency of occurrence and areas where foraging or travelling behaviours are dominant. This was determined through sighting information and behavioural observations, as described in Thornton et al. (2021a[1]). Vessel-related threats to recovery within the study area were examined with a focus on physical and acoustic disturbance in this document. Also, the presence of vessels and their transiting speeds through the study area was characterized. Here, ambient noise levels were characterized for the study area for May to October. The relative contributions of natural and anthropogenic (vessel) noise sources to the soundscape were examined, particularly in frequency ranges important to killer whale communication (500 Hz to 15 kHz) and echolocation (15-100 kHz). The results from this soundscape characterization were then further analyzed as part of a co-occurrence analysis by Thornton et al. (2021b[2]) to better understand the potential impacts the change in ambient noise conditions arising from natural and anthropogenic sources may have on SRKW habitat use, and on their communication and echolocation range. The co-occurrence analysis also examined vessel presence in areas used most frequently by SRKW as an assessment for the potential for ship strike.

---

[1] Thornton, S.J., Toews, S., Stredulinsky, E., Gavrilchuk, K., Konrad, C., Burnham, R.E., Vagle, S. 2021a Southern Resident Killer Whale (*Orcinus orca*) summer distribution and habitat use in the southern Salish Sea and the Swiftsure Bank area (2009 to 2020). CSAS Working paper. In prep.

[2] Thornton, S.J., Toews, S., Burnham, R.E., Konrad, C., Stredulinsky, E. Gavrilchuk, K., Thupaki, P., Vagle, S.. 2021b. Areas of elevated risk for vessel-related physical and acoustic impacts in Southern Resident Killer Whale (*Orcinus orca*) critical habitat. CSAS Working paper. In prep.

ABSTRACT

The soundscape of an area is defined by acoustic additions from natural and human-derived noise. Six moorings were deployed in the Salish Sea and the Swiftsure Bank area to describe the soundscape, and additions from abiotic and anthropogenic sources for May-October for 2018-2020. Commercial vessels transit international shipping lanes to ports including Victoria, Vancouver, Nanaimo, Port Angeles, Tacoma and Seattle through these waterways. In addition, the coastal cities are hubs for ferries, recreational, and whale watching vessels. The Salish Sea and the Swiftsure Bank area also contain protected critical habitat for Southern Resident Killer Whales (SRKW), including on La Perouse and Swiftsure Banks, and in Juan de Fuca Strait and Haro Strait.

Patterns in the soundscape through the summer were considered. The contributions from wind and rain were examined using data from the Environment and Climate Change Canada (ECCC) forecast model. Visualization of weather patterns showed considerable wind additions around Sooke in mid-summer, whereas offshore winds dominated in late-spring and early fall.

Vessel presence was quantified from Automatic Identification System (AIS) data. For the AIS non-mandatory smaller and recreational vessel types, aerial surveillance data were used to estimate presence. However, this was still considered to represent the minimum use of the study area by these vessel types. Acoustic metrics were also considered to track vessel presence.

To better appreciate the soundscape experienced by SRKW, the additions from natural and vessel noise in frequency ranges used for social communication (500 Hz to 15 kHz) and echolocation (15-100 kHz) were examined. This highlighted areas most impacted, and provided a means of evaluating relative quality of the acoustic environment within CH. Analysis of vessel presence and movements demonstrated the impacts of vessel presence.

A numerical vessel noise model was developed to allow for soundscape estimates in areas other than those monitored directly by passive acoustic recorders. Scenarios of forecasted changes in vessel presences in this area were also explored. A near-future expected increase in tanker traffic from approximately one weekly passage to one passage daily through the Salish Sea, corresponding to increases in shipping as a result of the Trans Mountain expansion project, was modelled.

Principal threats to survival and recovery of SRKW include physical and acoustic disturbance and vessel strike. Our analyses form the basis for discussions on acoustic disturbance and masking, resulting in reduced SRKW calling and echolocation extents.

1. INTRODUCTION

Oceanic ambient noise levels, or ocean soundscapes, are dynamic, and influenced by natural and anthropogenic contributions. The calls of marine mammals, fish and other invertebrates, and noises resulting from their movements and prey handling, are natural biological additions. There are also natural abiotic agents of noise, such as geological noise, precipitation, and wind and wave effects. The non-natural, or anthropogenic, noise contributions are increasing in their distribution and abundance. Vessel noise is the most pervasive in this category, with background levels now several decibels (dB) above pre-industrial levels (Richardson et al.,1995). Contributions are often greatest along shipping routes, and in waters close to major port cities and inhabited coastal areas (Pine et al., 2016). As ocean soundscapes are a dynamic combination of these natural biological and non-biological, and human-derived components, the noise input that dominates will vary over time and space, due to variation in sound field conditions and oceanic properties, and the acoustic frequency bands of concern.

Abiotic noise additions from wind, waves and water movement can be a major component of overall ocean noise. Sea state and near-surface ocean dynamics, related to winds, can influence the soundscape, with additions from air bubbles, spray, splash, surface waves, and turbulence (Carey et al., 1993). These additions can be complex, although sound levels from wind have been shown to be highly correlated with wind speed, fetch and water depth, but are also dependent on currents, including tidal currents, which will modulate the surface wave field (Wenz, 1962; Vagle et al., 1990; Richardson et al., 1995; Wysocki et al., 2007; Coers et al., 2008; Lugli, 2010; Ladich, 2013).

The first non-military study of the underwater soundscape was published by Knudsen et al. (1948). They established that the high frequencies of the ambient noise spectrum (500 Hz – 50 kHz) is mainly produced by wind, describing a relationship between the noise intensity spectrum and wind presence. The relationship between wind speed and noise levels was later refined by Vagle et al. (1990).

Precipitation can also add significantly to the overall noise field at a range of acoustic frequencies, ranging from approximately 500 Hz and up to as high as 50 kHz, depending on the type of rainfall (Amitai et al., 2007). However, the acoustic inputs are typically focused in the frequency range 15-22 kHz (Scrimger et al., 1989; Medwin et al., 1992; Nystuen, 1993, 1996; Quartly et al., 2000; Nystuen and Ma, 2002; Ma and Nystuen, 2005; Ma et al., 2005; Pensieri et al., 2015).

Anthropogenic noise can dominate soundscapes within a wide acoustic frequency band. In many places the background noise levels are now several decibels above pre-industrial levels, even in areas with no nearby human-made noise sources (Richardson et al., 1995). This dramatic change was precipitated largely by the addition of motorized commercial shipping, which has transformed the soundscapes in both the open ocean and closer to shore (Richardson et al., 1995; Hildebrand, 2009). Large-vessel noise adds predominantly to ambient noise levels in the low frequencies (< 500 Hz), with noise generated primarily from propeller cavitation and propulsion. These vessels also contribute energy at higher acoustic frequencies; up to 100 kHz (Ross, 1976; Gray and Greeley, 1980; Richardson et al., 1995; Arveson and Vendittis, 2000; Farina, 2014; Veirs et al., 2016). However, due to much higher range-dependent transmission losses at these frequencies, the contributions tend to be more local in nature. It is suggested that global ambient noise levels have risen 10- to 100-fold in frequencies below 500 Hz as a result of vessel presence (Jasny, 2005; Tyack, 2008). Coastal waters and shipping lanes have seen an estimated increase of 10 dB re 1 μPa per decade compared to observations made in the mid-1970’s (Ketten, 2002). The underwater noise levels in the Pacific have seen significant rises, particularly in the last 50-years, as a result of increased shipping (Andrew et al., 2002; Jasny, 2005; NRC, 2005; McDonald et al., 2006; Chapman and Price, 2011; Frisk, 2012; Merchant et al., 2014).

Increases in vessel traffic, and the number of transits of different vessel types can be tracked using the Automatic Identification System (AIS), whereby certain vessels are required to carry AIS Class A transceivers that relay information on their vessel name, type, identification number, location, and intended destination every 5-30 seconds. The International Maritime Organization (IMO) regulations state that an AIS Class A transceiver must be carried by every vessel over 150 gross tonnage (GT) that is carrying at least 12 passengers and engaged on an international voyage, and every vessel over 300 GT engaged on an international voyage. Within Canadian waters, Transport Canada also requires AIS Class A to be carried by every vessel over 500 GT not engaged on an international voyage, but exempts fishing vessels from the requirement to carry AIS. In the United States, the AIS carriage requirements include, but are not limited to, vessels of at least 65 feet in length and engaged in commercial service, towing vessels of at least 26 feet in length and greater than 600 horsepower and engaged in commercial service, or vessels with capacity of at least 150 passengers.

Carriage of AIS transceivers is not mandatory on smaller vessels; however, it offers considerable safety benefits through increased visibility by other vessels and elevated awareness of vessel traffic in the area. For recreational vessels, AIS Class B transceivers are more commonly used than Class A, but this system reports information less frequently, with a lower priority in the transmission stream, and with a lower transmission power. Therefore, the data transmissions are received less frequently and over shorter spatial ranges. However, they are more affordable than the Class A transceivers and so are often preferentially used by recreational boaters. Vessels that are not required to carry AIS are underrepresented in analyses of vessel presence and noise impacts, even though they can far outnumber larger vessels in some regions (Serra-Sogas et al., 2018) and can be significant contributors to the ambient noise levels (Erbe et al., 2012).

Passive acoustic monitoring (PAM) techniques are used to describe the ocean soundscape, and spatiotemporal changes in the level of ambient noise. The contributions of each of the abiotic, biotic and anthropogenic sources can be estimated, and representative frequencies or frequency ranges can be used as metrics to characterize inputs over time and space. This may help to understand the effects of human-induced noise on the marine environment and the organisms that inhabit it. These passive acoustic observations also allow for a non-invasive way of surveying the presence of marine mammals in an area, or assessing ecosystem health (Pijanowski et al., 2011; Sueur and Farina, 2015).

Extrapolation from single hydrophone moorings, or systems used in networks or arrays, to other non-monitored areas can be achieved through modelling exercises. Validated by observed noise levels, where these exist, these models allow us to predict the pathways and transmissions of underwater noise, to characterize the inputs from different sources, and to examine how different sources alone or together may influence the soundscape. Ocean noise mapping exercises (e.g., Erbe et al., 2012) use AIS data as a means to assess ambient noise levels resulting from shipping. Underwater noise levels are derived as a function of cumulative shipping transits and the acoustic characteristics of the vessel inputs by class. These models can be used to identify and describe areas with elevated noise levels, to predict changes in soundscapes, or test scenarios based on expected changes to the fleet, including the addition of more and larger vessels.

The inland waters around southern Vancouver Island, including Juan de Fuca Strait and the Strait of Georgia in Canada, and waters around San Juan Islands and Puget Sound of northern

Washington State, collectively referred to as the Salish Sea, are heavily impacted by anthropogenic activity. Neighbouring areas to the west of Juan de Fuca Strait in the Swiftsure Bank area also experience heavy vessel traffic loads. This is primarily driven by vessels transiting to ports including Vancouver, Victoria, Nanaimo, Port Angeles, Tacoma, and Seattle, and the proximity to other coastal cities and ports that are hubs for recreational boating and whale watching. Commercial deep-sea vessels transiting international shipping lanes are the dominant contributor, with ferries and tugs also making significant contributions in certain areas (MacGillivray et al., 2016). On average, an estimated 20 AIS Class A vessels transit through Haro Strait in the Salish Sea each day, or approximately one an hour, most of which are associated with the Port of Vancouver (Veirs and Veirs, 2006; Erbe et al., 2012; Veirs et al., 2016). These transits are mostly bulk carriers and container ships, with each transit elevating noise levels relative to ambient by about 20 dB re 1uPa (Veirs et al., 2016). The noise emitted from these vessels is typically in the 125 Hz to 20 kHz frequency range, often concentrated below 10 kHz (Veirs et al., 2016). Ferry traffic and cruise liners also contribute to the ambient noise level, with these and other passenger vessels typically transiting more frequently during the summer months compared to the winter. The presence and additions to the soundscape of smaller vessels, which typically emit higher frequency noise, are underestimated in current noise models for this area, but could have a significant impact on overall ambient noise levels (Erbe et al., 2012; Cominelli et al., 2018). Vessels transiting to and from both American and Canadian ports are present in the study area. Cumulative sound exposure maps by Erbe et al. (2012) showed the Salish Sea, more than any other area on the British Columbia coast, to consistently exceed 100 dB in the 63- and 125-Hz centered 1/3 octave bands, a target maximum level set out in the EU Marine Strategy Framework Directive (Tasker et al., 2010).

The Salish Sea is part of the range of the Southern Resident Killer Whale (SRKW). Their small population size, decreasing population trajectory, and the prevalence of anthropogenic threats in areas critical to their life histories led SRKW to be listed as Endangered under the *Species at Risk Act* (SARA) (COSEWIC, 2001). The waters of Swiftsure Bank, Juan de Fuca Strait, and Haro Strait were recognized as foraging areas and have since been designated as critical habitat (DFO 2017a,b, Fisheries and Oceans Canada 2018). These core feeding areas, and other areas where the whales have been commonly observed, such as Boundary Pass and Swanson Channel in the southern Gulf Islands (Hauser et al., 2007; Olson et al., 2018), overlap with the international shipping lanes and areas of heavy traffic (Cominelli et al., 2018). As mandated under the SARA, the Government of Canada produced a Recovery Strategy (Fisheries and Oceans Canada, 2018), which identified physical and acoustic disturbance, primarily from vessels, as a threat to SRKW survival and recovery. The Recovery Strategy also identified decreased prey availability and the persistent presence of contaminants in their environment as threats (Fisheries and Oceans Canada, 2018). In addition, a review of the effectiveness of recovery measures for SRKW undertaken in 2017 identified vessel strike as an additional threat to recovery of the population (DFO 2017a,b; Raverty et al., 2020).

Acoustics is the main means by which SRKW send and receive information, either communicating, using whistles or pulsed calls, or using echolocation ‘clicks’. Noise additions in the frequency ranges that they use for communication and echolocation may hinder their conspecific contact, and prey- and way-finding abilities. Vessel noise can mask or obscure calls or acoustic cues, such that the whales fail to detect or interpret them. When noise is a chronic addition to the soundscape it can also cause physiological stress or damage, alter hearing sensitivity, induce injury, or disturb behavioural patterns (Richardson et al., 1995; Simmonds et al., 2004; Southall et al., 2007, Rolland et al., 2012). In addition, the physical presence of vessels has been shown to alter cetacean behaviour (e.g., Dahlheim et al., 1984; Morete et al., 2007; Christiansen et al., 2013, 2014; Dahlheim and Castellote, 2016), and exposes SRKW to the risk of vessel strike.

A network of passive acoustic recorders deployed in the Salish Sea and on Swiftsure Bank as part of the Government of Canada's Ocean Protection Plan Marine Environmental Quality (OPP/MEQ) program aid the characterization of the soundscape of the SRKW CH. This study examined the acoustic contributions from both abiotic and anthropogenic sources to the overall broadband soundscape (10 Hz - 100 kHz), specifically wind and rain, and vessel noise. The noise contributions to the frequencies SRKW use for communication and echolocation (Heise et al., 2017) were given focus. The acoustic impact of larger commercial (AIS Class A) and smaller, often recreational (Class B and non-mandatory carriers), vessels were considered.

A numerical acoustic vessel noise model was used to interpret the additions from AIS Class A traffic at locations other than where direct observations are available. Our modelling approach was also used to forecast the potential impacts of future increased traffic loads through the Salish Sea and Swiftsure Bank area. In particular, a scenario of a seven-fold increase of tanker traffic, which is expected from the Trans Mountain expansion project (TMX), was modelled. The results of these analyses will feed into the discussions of the impact of shipping and elevated ambient noise levels on SRKWs and their use of the Salish Sea.

2. METHODS

The study area encompassed portions of the SRKW CH in the Salish Sea including Juan de Fuca Strait, Haro Strait, Boundary Pass, the southern portion of the Strait of Georgia, and waters around the southern Gulf Islands. The SRKW CH also encompasses the waters of Swiftsure Bank, La Perouse Bank, and surrounding canyons and bathymetric features. The region examined in this analysis was the area bounded by 49.0°N, 125.5°W in the northwest, 49.0°N, 123.0°W in the northeast, 48.0°N, 125.5°W in the southwest and 48.0°N, 123.0°W in the southeast (Figure 1).

2.1. SOUNDSCAPE CHARACTERIZATION

2.1.1. Passive Acoustic Mooring (PAM) Network

The acoustic recordings used in this study were from six PAM moorings that have been deployed in the study area since February 2018 (Figure 1). The recordings were made using Autonomous Multichannel Acoustic Recorders (AMAR, JASCO Applied Sciences, G4) equipped with GeoSpectrum Technologies M36-100 hydrophones. These were mounted on a quiet mooring system manufactured by Oceanetic Measurement Ltd., which positioned the hydrophone approximately 2 m from the sea floor (Figure 2).

Each system was calibrated by the manufacturer, and then again using a 250 Hz piston phone prior to each deployment. Recordings were made continuously at a sample rate of 256 kHz with 24-bit resolution and stored on internal SD memory cards as wav files. A servicing schedule of approximately 2-3-months was maintained for the moorings, whereby data were downloaded and new batteries installed, allowing recordings to be consistently collected. On recovery, the wav files were post-processed with custom Python scripts, modified from those used by Merchant et al. (2015). One-minute power spectra were computed using a 1 second Hanning window, with a 50% overlap and Welch's averaging, from which sound pressure level (SPL) metrics were calculated and used in the subsequent soundscape analysis. Minute-wise data were aggregated on hourly, daily, monthly, bimonthly and six-monthly scales to address questions in characterizing the soundscape.

Acoustic Analysis

The focus of the present analysis was passive acoustic recordings made between May 1 and October 31 for 2018, 2019 and 2020 to cover the time periods when SRKW are most frequently observed in the Salish Sea. The soundscape was characterized by several applicable metrics, including broadband ambient noise levels in the frequency range 10 Hz to 100 kHz. It has been suggested that noise additions in this frequency range may initiate behavioral or physiological changes in SRKW (Heise et al., 2017; Table 1). Killer whale calling is typically within the frequency range of 500 Hz -15 kHz. This frequency range was therefore considered for its potential for acoustic inputs to obscure conspecific calling or social behaviors, such as group cohesion and coordination. Echolocation occurs in the frequency range of 15-100 kHz, and so noise levels in this range were considered for possible masking of echolocation click echoes. Increased noise levels within these three bands may impair navigation and orientation, as well as prey location and capture (Heise et al., 2017; Table 1).

Abiotic noise additions were considered in the 7,500-8,500 Hz range for wind, having previously been seen to correlate with wind speeds between 4-15 ms^{-1} (Vagle et al., 1990). Additions to the soundscape from precipitation noise were examined for in frequencies centered around 20 kHz (Vagle et al., 1990; Table 1). Vessel presence metrics were also considered. The 100-1000 Hz decadal band was used to indicate vessel presence without being influenced by water turbulence noise (Merchant et al., 2012). Also, metrics used by the EU Marine Strategy Framework Directive were included; considering the sound levels in the 63-Hz and 125-Hz centered 1/3 octave bands (Merchant et al., 2012, 2015). Vessel-mounted echosounders operating at 50 kHz are frequently used in this area, so frequencies centered around this value were examined as an indicator of vessel presence, especially smaller, recreational boats (Table 1).

To assess the changes in soundscapes, a level when ambient noise was at its lowest (hereafter 'minimum ambient') was first established. This was when natural noise was negligible (low to no wind or wave additions, no precipitation) and anthropogenic noise sources were absent. The minimum was derived from the L_{99} exceedance level from recordings collected from the acoustic moorings in the study area. In this analysis, the L_{99} exceedance level represents the natural ambient noise level which was exceeded 99% of the time. Recordings from each mooring were aggregated over the six months (May to October) and averaged over the three years (2018-2020). The results from each site were compared, and that with the lowest SPL used to form the 'minimum ambient' reference. This reference was used as a constant comparator across the study site to establish the impact of wind, precipitation, and vessel noise to the sound field.

In addition, L_1 and L_{50} exceedance levels were considered to represent the most acute additions to the soundscape, present for only 1% of the time, and the median level of noise in the sound field respectively.

Soundscape Composition

The proportional contributions of abiotic and vessel noise to the soundscape were estimated at each mooring using the relationship between the SPLs at 8 kHz and 20 kHz. The spectral slope relationship between wind speed and sound spectrum level in deep water, initially described by Knudsen et al. (1948) and refined to $(\text{frequency})^{-1.9}$ by Vagle et al. (1990, Equation 27), as indicated in Figure 3 for wind speeds of 10 and 15 ms^{-1}, was also used. An example output of the method is shown in Figure 4, showing the points with exponents smaller than -1.9 below the slope in green and those with a greater exponent in red. Departures from the spectral slope was used as a first-order method to separate different sound sources, whereby low-frequency vessel noise contributions would fall below the slope, and higher-frequency contributions attributed to precipitation and small vessel noise would fall above the slope (Vagle et al., 1990; Nystuen et al., 2010). The number of points on, above or below the slope were then expressed as proportions (Figure 4 example) and then aggregated into monthly values to be displayed and compared for each summer.

Characterization of abiotic conditions and sound transmission

The sound propagation characteristics and the local sound speeds within the study site were derived from data describing water depth and water properties. Bottom type data were also used to define how sound would interact with the seafloor. High resolution bathymetric data were obtained from the Canadian Hydrographic Service (CHS 2020[3]). These data were interpolated to give water depths on a uniform grid for the full study area with a 15-arc second spacing, or approximately 300 m resolution (Haugerud, 1999; Olson et al., 2018). The water column sound speed profiles were calculated from salinity, temperature and depth (CTD) profiles. Both observational data, routinely collected during the mooring servicing trips, and modelled water properties were used in the analysis. When high spatial and/or temporal resolution was needed, the required sound speed field was obtained from the results of the SalishSeaCast hydrodynamic model (Soontiens et al., 2016; Soontiens and Allen, 2017). The SalishSeaCast system is a three-dimensional biochemical and hydrodynamic model which has integrated long hindcast hourly wind data, ocean carbon, chemistry, and physics data from 2007 onwards (Soontiens and Allen, 2017). Temperature and salinity data were taken from the LiveOcean model (Siedlecki et al., 2015), low-pass filtered and tides removed, and then applied on a daily scale (Olson et al., 2018). Model results were downloaded from the SalishSeaCast model ERDDAP server with a spatial resolution of approximately 440 m by 500 m and 40 vertical levels through the water column between 0.5 and 500 m, formed from hourly data. Data for this analysis were retrieved for the period from April to November 2018 (accessed in February 2020 from the data set ubcSSg3DTracerFields1hV18-06). Results from the vertical data layers near the surface had a 1 m resolution, and those at the deepest depths had a 24 m resolution (Soontiens and Allen, 2017). Water-column properties were converted into sound speed and water density fields using the Intergovernmental Oceanographic Commission standard TEOS-10 (McDougall and Barker, 2011). The acoustic frequency dependent absorption was derived from Francois and Garrison (1982) using a pH value of 8.

The bottom sediment composition was also characterized throughout the study area, to add to predictions of how sound would be propagated through the unconsolidated sediment that forms the ocean floor in the Salish Sea. For this analysis three broad regions of bottom-type classification were used, formed from work conducted by Haggarty et al. (2018). The Fraser River deposition zone in the Strait of Georgia is predominantly silt and mud, the area around the southern Gulf Islands, the near-shore areas of the Strait of Juan de Fuca, Haro Strait and Boundary Pass can be characterized as predominantly rocky, and the main channel of Juan de Fuca Strait connecting to the Pacific Ocean shelf region is dominated by a sandy substrate (Figure 5). The geoacoustic properties of each of these substrate types were derived by work conducted by Hamilton (1980) and Jensen et al. (2011), and focused on the propagation of low frequencies (60-500 Hz) through unconsolidated sediment via both the faster compressional (longitudinal) P waves, and slower, shear (transverse) S waves, and the associated attenuation factor related to the acoustic wavelength λ (Table 2). These parameters were tuned for each PAM recorder location by comparing modeled and observed SPLs at the different sites.

Wind speed data accessed from the Environment and Climate Change Canada (ECCC) model available through the SalishSeaCast model allowed the visualization of spatiotemporal patterns of wind in the study area from May to October. These data were then used to derive the

[3] Canadian Hydrographic Service, retrieved from CHS NONNA Data Portal.

acoustic additions that wind would make at 10 kHz and 50 kHz. These frequencies were used to represent SRKW communication and echolocation range respectively. The use of 10 kHz is representative of the fundamental frequency range for SRKW whistles (2-17 kHz; Ford, 1989; Thomsen et al., 2001). The frequencies around 50 kHz are near the center of the high-frequency range in which SRKW echolocation clicks are produced. Echolocation signals have modal peaks between 20-30 kHz and 40 and 60 kHz (Au et al. 2004). The use of 50 kHz is in line with previous work by Au et al. (2004). The same analysis was replicated with precipitation data also accessed from the ECCC model.

Acoustic presence of vessels

The presence of vessels over time was derived acoustically from mooring data by examining frequency ranges believed to be the focus of their acoustic additions to the soundscape (Table 1). The appropriateness of the application of these metrics for data from our study area was demonstrated by Burnham et al. (2021), through non-parametric correlations between AIS data and SPL in the vessel bands. The 100-1000 Hz band is considered to represent vessel presence, while excluding noise from water turbulence in the lower frequencies, while the 63-Hz and 125-Hz 1/3 octave bands (57-71 Hz and 114-141 Hz respectively) have been applied in previous studies, as well as being set by the EU Marine Strategy Framework (Merchant et al., 2012, 2015). The frequency range 49500-50500 Hz was used to mark vessel presence of small vessels which emit higher frequency noise. This frequency range also represents the most common echosounder frequency used in this area, focused around 50 kHz.

Temporal patterns in the acoustic presence of vessels were examined for at monthly, weekly, within-week, and diurnal scales. Within-month temporal patterns determined for May to October were compared to February for a broad summer-winter comparison. We assumed that acoustic additions from small vessels would be low or absent in winter, and so if additions were present in the summer recordings in frequencies focused around 50 kHz, it would further support the use of this frequency range as a metric to track the presence of this vessel type. The implications of vessel-derived acoustic patterns were also examined for in the SRKW relevant frequencies.

For diurnal patterns, four four-hour sections were considered: 00:00-04:00, pre-dawn using nautical sunrise, and a time presumed to lack small vessels; 06:00-10:00, post-dawn morning; 12:00-16:00, afternoon; and 18:00-22:00, nautical twilight dusk to sunset. The comparison was made between mid-summer (August) and mid-winter (January) months to help determine the source of the increase.

2.2. VESSEL PRESENCE AND SPEED

2.2.1. Automatic Identification System (AIS) tracked vessels

Quality control and vessel categorization

Vessel presence in the study area was quantified from AIS data collected by Canadian Coast Guard terrestrial receivers (Figure 1). The raw AIS data for the study area during the period of interest (May through October, 2018-2020) were cleaned and binned from the received time intervals into 5-minute periods for each vessel. Speed over ground (SOG) and acceleration over ground (AOG) were calculated for each of the five-minute binned AIS records using the distance between GPS locations (after conversion to suitable orthogonal co-ordinate system) and elapsed time. Any data that appeared erroneous, for example due to stated vessel location (e.g., over land), or with an excessive speed or acceleration (e.g., SOG > 50 knots or AOG >100 knots/hr), were removed. For Class A data, any missing data points were interpolated from neighboring time periods and missing vessel information was determined from internet searches and online databases where possible, using unique vessel identifiers, such as Maritime Mobile Service Identity (MMSI) numbers. For vessel types that carry AIS Class B, vessel classification information is often absent from the AIS data and can be unreliable when present (Konrad, 2020). Therefore, for Class B vessels, only classification information that could be determined and confirmed using online databases was used to assign vessel type.

The AIS-derived vessel data were used in several aspects of the analysis. Initially, Class A vessels were categorized into thirteen vessel types: 1) Bulk carriers, 2) Container ships, 3) Ferries, 4) Fishing vessels, 5) Government/Research, 6) Naval vessels, 7) Passenger vessels, 8) Recreational vessels, 9) Tankers, 10) Tugs, 11) Vehicle carriers, 12) Registered whale watching vessels, 13) Others and vessels of unknown type. Class B vessels, primarily pleasure crafts, but also fishing vessels and smaller commercial vessels, were classified as their own vessel type. These categories were adapted or aggregated for different aspects of the analysis.

For the analysis of vessel presence and SOG, vessel types were divided into two broad categories: those required to carry an AIS transceiver, and those for which this was optional. According to Canadian AIS carriage requirements, the following vessel types were considered AIS-mandatory: container ships, bulk carriers, vehicles carriers, tankers, ferries, passenger vessels, and other cargo (e.g., refrigerated, general, or open hatch cargo, or heavy load carrier). All remaining Class A vessel types and all Class B vessels were considered AIS-optional. This latter category included non-commercial, fishing, and small commercial vessels, such as tugs.

Analysis of the presence and SOG of AIS vessels was conducted in R (Version 3.6.0; R Core Team, 2019), using the ‘sf’ (Pebesma, 2018) and ‘raster’ (Hijmans, 2020) packages. All AIS vessel presence and vessel strike risk analysis outputs were generated using a 1 km^2 grid, based on the NAD83 UTM Zone 10N projected coordinate reference system.

Vessel Hours Quantification

The presence of AIS-tracked vessels was expressed as function of time that each vessel was present in each 1 km^2 grid cell. The average daily vessel hours ($\overline{VessHr}$) for each grid cell was quantified for each month (from May to October) of each year (from 2018 to 2020), according to the formula:

$$\overline{VessHr} = \frac{\sum VessPoints \times \frac{5}{60}}{Days}, \quad (1)$$

where $\sum VessPoints$ is the sum of all vessel points (each representing five minutes of vessel presence, including vessels not making way), and $Days$ is the number of days of available AIS data.

Timestamps, at one-hour resolution, were used to calculate the number of days of available AIS data for each month for each AIS data type (Class A and Class B), so that temporal gaps in the AIS dataset were accounted for when determining average rates of vessel presence. Monthly raster layers of average daily vessel hours per grid cell were calculated for: (1) AIS Class A large commercial vessels, (2) AIS-optional Class A vessels and (3) AIS Class B vessels. For each of these vessel categories, for each month, values for each grid cell were averaged across all three years (2018-2020) to form one raster layer.

To assess any differences in vessel traffic patterns in 2020, expected due to the impacts of regulations related to the COVID-19 pandemic, a cell-wise comparison of average vessel hours in 2020 for each month and vessel category was made to the corresponding average value for 2018 and 2019. Restrictions related to COVID-19 were in force from April 6, 2020, and eased for Canadian recreational traffic June 24, 2020; cruise ship traffic remained prohibited for the entirety of the study period.

Additionally, non-spatial summary statistics were calculated to examine vessel presence trends across months and by vessel type. In these summaries, vessels not making way, with a SOG of 1 knot or less, were excluded from the analysis. To examine seasonal trends and the relative rates of presence for each of the three vessel categories, the average rate of daily vessel hours was calculated for each month, across the whole study area and all years. To examine vessel presence by vessel type, the average rate of daily vessel hours for each vessel type was calculated across the whole study area and duration. These averages were expressed as a percentage of the average total vessel hours for each AIS class.

Vessel Speed Over Ground

Raster layers of monthly averaged vessel speeds were generated using the SOG values (in knots) calculated from the AIS vessel positions. For each month (May-October) of each year (2018-2020), the SOG values associated with all vessel points (including vessels not making way) in a given 1 km^2 grid cell were collectively averaged. This averaged speed layer was then multiplied by the value from average daily vessel hours layer for the corresponding grid square, to generate a derived distance layer of averaged daily nautical miles traveled in each cell. For each month, the values for all three years were then averaged to generate an average daily value for each grid cell, for each month across the three-year period (2018-2020).

2.2.2. Small Vessel Analysis

Aerial Surveys

Data from opportunistic aerial summer surveys were used to estimate presence of non-AIS vessels in the study area. Aerial survey data collected in April through September by the National Aerial Surveillance Program (NASP) and previously reported by Serra-Sogas et al. (2018) were used to map vessels per unit effort (SPUE) for AIS and non-AIS vessels in our study area. The flight tracks were used to estimate effective sighting distances and quantify search effort using conventional distance sampling methods (Buckland et al., 2001) based on the perpendicular distances of sightings from the flight path (Serra-Sogas et al., 2018). Flights occurred only during daylight hours, and were spread evenly across days of the week.

Overflight data from DFO Creel Surveys of recreational fishing vessels from May through October in 2018-2020 were also used in this analysis. During Creel Survey overflights, vessel positions were manually recorded on paper, and then approximate latitude and longitude were digitized for each vessel or cluster of vessels (Shardlow et al., 1989). The precision of these approximations has not been quantitatively assessed; it was estimated to be within ± 500 m for nearshore areas, but uncertainty in the approximations is believed to increase for sightings made in more offshore waters. The use of this data was limited to recreational fishing vessels due to inconsistency in the recording of other vessel types. In the absence of flight tracks, survey effort was estimated from approximated paths from generalized survey routes using a 4 km^2 grid over the study area. A 7.4 km buffer was used to estimate sighting distance, which was informed by sightings distances calculated for NASP flights (Serra-Sogas et al., 2018). For each month, the number of vessels recorded in each 4 km^2 grid cell was summed across all years. To estimate flight effort for each cell, all buffered flight path polygons that covered the center of the 4 km^2 grid cell were summed. Monthly raster layers of vessels sighted per flight were derived by dividing vessel number by flight effort.

2.3. VESSEL NOISE MODEL

2.3.1. Model Setup and Validation

A shipping noise model was developed to characterize the sound field in the study area, without being restricted to any particular mooring location. The model implemented was similar to the acoustic model developed by Collins (1993) using a Range-dependent Acoustic Model (RAM) and further refined by Aulanier et al. (2017). The RAM model uses the Pade split-stepping method to solve the range-dependent parabolic equation for sound propagation in cylindrical coordinate system on a vertical plane. The horizontal direction was divided into 120 vertical planes, equally distributed to achieve a full 360 degrees coverage around each source (ship position). This approach to simulating 3D sound propagation does not account for out-of-plane refraction and sound around barriers such as island and sharp coastline features and therefore, it is often called a 2.5D or quasi-3D acoustic model. Realistic environmental data based on high resolution bathymetry, sediment composition, and water property data from the SalishSeaCast NEMO model were included in the RAM model to accurately simulate quasi-3D sound propagation in the domain (Table 3). Source sound levels due to shipping traffic were estimated by integrating the AIS Class A data from the area of interest. The processed and cleaned AIS records were used to provide source positions to estimate the soundscape in the domain every 30 minutes over the 6-month simulation period between May and October, 2018. Results from 20 vertical (z-levels) depths were extracted and processed for further analysis. These levels started at 0.5 m and went down to 500 m (Table 3).

The following vessel classes were used in the modeling exercise: Container ships, Ferries, Fishing vessels, Naval vessels, Government/Research vessels, Cargo, Passenger vessels, Tankers, Tugs, and Vehicle carriers. Source levels by vessel type were obtained from MacGillivray and Li (2018). Vessel transit SOG was calculated from the AIS records and source levels for vessels in transit derived using the simple linear relationship described by Veirs et al. (2016), whereby sound levels were increased by 0.93 dB/knot (or +1.8 dB per ms^{-1}) of increased speed over ground. When the vessel type was not reported in the AIS record, the source level was estimated using the relationship between ship speed and size characteristics and vessel noise outputs as described by Simard et al. (2016). The vessel noise model was used to evaluate ambient noise levels at water depths relevant to SRKWs (7.5 m, 20 m, 50 m, 100 m) using AIS vessel information for May to October 2018. Data from the 125-Hz centered 1/3 octave frequency band from recordings from the six PAM moorings were used to validate the model outputs and tune the bottom characteristic parameters used in the model (Table 3).

The current vessel noise model was limited to simulating SPL at lower acoustic frequencies (125 Hz, was used here), but to explore possible impacts on the higher frequency ranges associated with SRKW communication and echolocation extents much higher acoustic frequencies needed to be used. To give a first-order estimate of high-frequency vessel noise, and representation of the worst-case scenario of vessel-derived acoustic additions, a simple extrapolation to higher frequencies was used (Figure 3). Using the 125-Hz modeled SPL at a given location the SPL at the higher frequencies were estimated using a simple $(\text{frequency})^{-2.0}$ relationship (Wenz, 1962). Noise levels at 10 kHz were calculated to represent the SPL at SRKW communication range and at 50 kHz for SRKW echolocation. Vessel noise at the L_5, L_{50}, L_{95} exceedance levels and arithmetic mean (L_{eq}) were computed.

2.3.2. Scenario Modeling

To highlight the usefulness of vessel noise models, noise levels for a near-future scenario representing the expected increase in tanker traffic to and from Vancouver as a result of increased oil shipments associated with the TMX project were estimated. Tanker traffic related to TMX operations currently transit the route from Vancouver to La Perouse Bank approximately once a week. It is expected that when the new pipe line is operational, this will increase to approximately 1 tanker per day leaving the Burrard Inlet loading site and transiting the study area. This 7-fold increase scenario was simulated by creating a proxy AIS record that simulated a once-a-day transit by a TMX tanker to be included in the model inputs.

3. RESULTS

3.1. SOUNDSCAPE CHARACTERIZATION

Each mooring was set to record continuously from May to October, 2018-2020. However, data gaps occurred when maintenance of the recorders was delayed, or there were technical issues resulting in data loss. In the spring of 2020, scheduled mooring servicing trips were severely delayed due to restrictions during the COVID-19 pandemic, resulting in significant gaps in data for most of the moorings (Table 4).

Boundary Pass and Haro Strait showed the greatest range in broadband ambient noise levels (10 Hz to 100 kHz), recording both the highest and the lowest SPL levels. The peaks in SPL at these sites were short-lived, acute acoustic additions resulting from vessel passes, predominantly from commercial and other AIS-vessel transits. This contrasted to recordings from Swiftsure Bank and Sooke which reported elevated SPL in this range consistently when compared to the other moorings. Recordings made at Port Renfrew and Jordan River showed a high degree of consistency in the SPL for soundscape and acoustic metrics, with vessel noise consistently present.

The similarities of the recordings at Boundary Pass and Haro Strait, and for those made at Swiftsure Bank, Port Renfrew and Jordan River, created an inner- and outer-strait distinction in the soundscape of the study area (also see Burnham et al. 2021). The inner strait recorders of Haro Strait and Boundary Pass were generally in more protected waters and are not subject to the offshore effects of those on Swiftsure Bank and in Juan de Fuca Strait.

Broadband noise exceedance levels of L_1, L_{50}, L_{99} and the arithmetic mean (L_{eq}) were calculated for the entire recording period (May-Oct) each year (Figure 6). The exceedance levels of the range 10 Hz to 100 kHz showed moorings in Juan de Fuca and outer strait sections to have increased power spectral density (PSD) levels in the lower frequencies (< 1000 Hz, Figure 6). The largest peak was seen for Swiftsure Bank in 2020 (Figure 6). This peak in PSD was much less apparent in recordings made at Haro Strait and Boundary Pass, and not evidenced at all when considering only the quietest moments (L_{99} values). Peaks were seen in the higher frequencies (> 10000 Hz), and into the echolocation frequency range of SRKW (> 15 kHz) for all moorings. These were most present during 2020 (Figure 6). Boundary Pass and Haro Strait showed the lowest background noise levels (L_{99}) of the sites, but also the highest PSD levels at the L_1 exceedance level. Sooke consistently had the highest PSD levels of the moorings in Juan de Fuca Strait, with similar distributions of SPL across frequencies as seen for Port Renfrew, Jordan River and Swiftsure Bank (Figure 6).

Temporal analysis showed ambient noise levels in the frequency range 10 Hz to 100 kHz to decrease from 2018 to 2020 (Figure 7). Bimonthly comparison showed similarities between periods for each location (Figure 7). Again, recordings of Port Renfrew and Jordan River soundscapes were comparable and typically showed lower ambient noise levels than other sites for each period (Figure 7). The SPLs of the overall broadband soundscape (10 Hz to 100 kHz) were typically highest, followed by SPLs in the frequencies for SRKW communication (500 Hz to 15 kHz), and echolocation (15-100 kHz, Figure 7).

Comparisons between days of the week indicated elevated SPL for weekends when compared to week days (also see Burnham et al. 2021). This was most prominent for recordings in Juan de Fuca Strait and especially on Swiftsure Bank (Figure 8). Broadband SPL was significantly higher on Sundays during the early to mid-summer period (May-September, Figure 8), with notable elevation also for Mondays, which may represent statutory holidays (Figure 8). More consistency in the overall sound field was seen between the days of the week for later summer periods (September-October; Figure 8). Elevated SPLs were seen for SRKW communication and echolocation frequency ranges in the recordings for Friday and Saturday, with the greatest differences between days were seen between mid-week to weekend values (Figure 8). Similar results to those seen at Swiftsure Bank were found for Port Renfrew and Jordan River, however the eastern strait moorings showed more consistent soundscape levels between days, with no weekly patterns seen in Boundary Pass recordings (Burnham et al. 2021).

Diurnal patterns were also examined using 05:00-16:59 local time (UTC 12:00 to 23:59) as day. and 17:00-04:59 local time (UTC 00:00 to 11:59) as night (Figure 9). Elevation in soundscape levels have been reported for moorings in Juan de Fuca Strait during daylight hours for May to October (Burnham et al. 2021). Examination of the SPL levels in the SRKW communication call frequencies showed a similar day-time increase for all moorings, and most prominently for Swiftsure Bank, Port Renfrew and Jordan River (Figure 9). This range encompassed acoustic additions from both commercial (AIS) and recreational (non-AIS) vessel traffic. The day to night differences were most pronounced in Swiftsure Bank and Port Renfrew recordings in July and August, whereby a sharp increase in noise was seen at 07:00 local time, and the lowest soundscape levels were recorded between approximately midnight and 02:00 local time in all cases (Figure 9). Recordings made in May-June were similar in their soundscape characteristics to those made in September and October, with less diurnal patterning also seen for these two periods (Figure 9; also see Burnham et al. 2021).

3.1.1. Minimum Ambient

The L_{99} exceedance level measured at each station indicated peaks in noise at low frequencies (approximately 30-300 Hz) for moorings in Juan de Fuca, especially at Sooke. Peaks were also present around 1000 Hz (Figure 10). The absence of the low frequency peaks in Boundary Pass and Haro Strait recordings, and lesser increases at 1000 Hz (Figure 10a) suggested the L_{99} exceedance levels for these recorders were the most indicative of the ambient background noise levels without anthropogenic input and substantial wind or wave acoustic additions (Figure 10a). The L_{99} exceedance level at Boundary Pass and Haro Strait were therefore considered the best to form the 'minimum ambient' reference ambient noise level. As the L_{99} exceedances at these sites showed congruence, a composite PSD frequency line was calculated to form the reference level to be applied in further analysis (Figure 10b).

3.1.2. Soundscape composition

The soundscape composition, derived from Knudsen curves and the relationship between 8 kHz and 20 kHz, at Swiftsure Bank, Port Renfrew and Jordan River showed a greater proportion of the mid-frequency noise, attributed to the presence of rain and smaller vessels (Figure 11a-c). However, for the recordings assessed, these mid-frequencies additions were the smallest contributor to the soundscape for all moorings (Figure 11). The soundscape at Sooke, Haro Strait, and Boundary Pass showed low-frequency noise additions from commercial traffic to be more prevalent than the moorings in Juan de Fuca Strait and on Swiftsure Bank (Figure 11d-f). Indeed, Swiftsure Bank had the lowest proportion of commercial vessel-derived additions for the period analysed (Figure 11a). A proportion of the soundscape was unaccounted for in the broad groups of large vessels, wind, and rain; a number of other factors such as water turbulence, wave noise, or vessel traffic could form some of these acoustic contributions. The proportion of this ‘unknown’ class was generally at its greatest for recordings made in 2020. Sooke recordings consistently showed the smallest proportion of soundscape attributable to unknown sources, with both additions from commercial shipping and wind noise dominating (Figure 11d).

3.1.3. Characterization of natural conditions and sound transmission

The ECCC model, accessed through the SalishSeaCast NEMO model, showed the south-eastern portion of the Strait of Juan Fuca and areas around San Juan Islands to experience greatest average wind speeds, approximately 6 ms^{-1}, from May to August (Figure 12). Wind-derived additions were greatest at Sooke during May and June, with recordings made on the Jordan River and Haro Strait moorings also possibly influenced by elevated wind speeds (Figures 12-14). September and October showed a greater offshore wind influence, especially at Swiftsure Bank (Figure 12). The acoustic additions from the wind during this time extended from Swiftsure Bank to Jordan River (Figures 12-14). Wind noise additions in the SRKW communication frequency range were greatest between July and August around Sooke (Figure 13). Wind generated noise at echolocation frequencies was greatest around Sooke for May and June (Figure 14). Wind acoustic additions in the communication and echolocation frequencies were greatest in the offshore regions from September; in 2020 this extended eastward into Juan de Fuca Strait as far as Jordan River (Figures 13-14). The amplitude of wind additions was typically greater in the communication call frequency range rather than in the frequency range used for echolocation (Figure 13-14).

Precipitation data from the SalishSeaCast model showed small pockets of rain in the Gulf Islands for May and June, whereas more offshore weather systems were observed for July and August, which were then heightened for September and October (Figure 15). Noise additions from rain would therefore be expected to follow this pattern, with precipitation adding to the mid- to high-frequencies most in September and October in Juan de Fuca Strait.

3.1.4. Acoustic presence of vessels

No significant differences between bi-monthly periods for acoustic additions were attributable to AIS tracked vessels (63-Hz and 125-Hz 1/3 octave bands, Figure 7). During the summer months considered here, Swiftsure Bank, Port Renfrew and Jordan River showed a week-weekend distinction in frequency bands attributed to vessel traffic, with weekend SPL in frequencies around 50 kHz elevated (Figure 8). The broadband SPL increases in ambient noise seen during the day were concurrent to increases in mid- to high-frequencies (Figure 9) and noise levels in the frequency ranges used to represent vessel presence (Burnham et al. 2021).

In addition to the non-parametric correlations confirming the relationship between the vessel metrics (Table 1) and vessel presence (see Burnham et al. 2021), a comparison showed that the day-time elevation seen in the vessel frequency range 49500-50500 Hz present during August was not present during January, further implicating this increase in SPL to result from small vessel presence (Figure 16).

3.2. VESSEL PRESENCE AND SPEED

3.2.1. AIS Vessels

Vessel Presence

Both AIS Class A and Class B vessels contributed considerably to vessel presence in the Salish Sea and the Swiftsure Bank area (Figures 17-19). The presence of large commercial vessels was relatively constant across months (Figures 17, 20), and was largely confined to the shipping lanes and ferry routes. The presence of non-mandatory AIS Class A vessels was more variable, particularly around Port Renfrew and in the Swiftsure Bank area (Figures 18, 20). The presence of AIS Class B vessels varied greatly across months, with the greatest presence in July and August (Figures 19-20). However, the representation of AIS-optional small commercial and recreational vessels from AIS data was considered the minimum presence of these vessel types.

Overall, ferries, bulk carriers and tugs were the greatest contributors to AIS Class A vessel presence (Figure 21), with fishing vessels, containerships, passenger vessels, government and research vessels, tankers, recreational vessels and naval vessels contributing to a lesser extent (Figure 21).

During the study period, 5980 unique vessels transmitting AIS Class B were recorded in the study area. Of these, 28.8% were successfully matched to online records with information on vessel type. These vessels accounted for 45.6% of all AIS Class B vessel presence in the study area over time, and were predominantly recreational vessels (Figure 21). This category encompassed both sailing and motor vessels, including recreational fishing vessels. The next most common vessel types, in descending order, were small passenger vessels (which included whale watching vessels), fishing vessels, coast guard and other safety/rescue vessels and tugs (Figure 21). Naval, research/survey, antipollution, small cargo, diving operations, and supply vessels and pilot tenders were aggregated as ‘Other’ Class B vessels (Figure 21).

In 2020 average vessel presence was reduced relative to 2018 and 2019 (Figures 22-24). This was particularly true for the early months of the study. There was a clear decrease in vessel presence along ferry routes (Figure 22), resulting from COVD-19 restrictions. The AIS Class B vessel presence among the Gulf Islands and around Victoria was also less compared to previous years (Figure 24). Vessel presence around the San Juan Islands, however, was higher in 2020 than in 2018 and 2019, from July onwards (Figure 24).

Vessel Speed

Average vessel speed varied by type (Figure 25). Large commercial vessels, specifically container ships, tankers, bulk carriers, passenger vessels and ferries, demonstrated the highest average speeds among AIS Class A vessel types. For AIS Class B vessels, the highest average speeds were attributed to small passenger vessels, and coast guard and other safety/rescue vessels (Figure 25). Average daily distance traveled calculated from vessel speeds per square kilometer followed a similar pattern to vessel presence (Figures 26-28). Ferry routes (Figure 26) and AIS Class B vessel traffic around the Gulf Islands (Figure 28) were areas of heightened traffic.

3.2.2. Small Vessel Presence

Aerial Surveys

The data from the National Aerial Surveillance Program (NASP) showed a difference in spatial distribution and volume of AIS and non-AIS vessel (Figures 29-30). However, survey effort in the study area was low (Figure 29). Non-AIS vessels were more prevalent than those transmitting AIS, with their presence greatest around the Gulf Islands, and near Sooke and Port Renfrew (Figure 30). The DFO Creel Survey overflights added to the overall survey effort (Figure 31), recording presence of recreational fishing vessels (Figure 32). The surveys targeted this vessel type (99.3% of vessel data), and noted if these fishing vessels were actively fishing (76.5%) or transiting (22.8%). Limited presence of whale watching (0.2%), and active commercial fishing (0.5%) vessels were also recorded. The areas with the highest recorded recreational fishing vessel presence for the study period were again off Sooke and Port Renfrew

(Figure 32). Vessel presence in the Swiftsure Bank area was high for June to September when surveys were conducted (Figure 31-32). The data analysis was limited by flight coverage and to the results that had been digitized. Data were not available for August-October 2018, and were limited to Juan de Fuca Strait and the Gulf Islands for both 2018 and 2019 datasets (Figure 32).

3.3. VESSEL NOISE MODEL

3.3.1. Model Results and Validation

Outputs of the vessel noise model at 125-Hz were given for depths of 7.5 m, 20 m, 50 m and 100 m (Figure 33). Areas around Discovery Island, into Haro Strait and Boundary Pass showed the greatest SPLs in surface layers, with values lessening with depth. The southern boundary of Juan de Fuca Strait, along the US coast, also showed consistently elevated levels in this May 2018 example (Figure 33). The changes in SPL with depth are due to reduced propagation losses in the water column, the effect of the bottom sediment boundary, and the effect of bathymetric features.

Comparisons between observed and modelled median SPL at the different locations during May 2018 demonstrated the percentage error in simulated SPL at the mooring locations were within 5% of observed median values at 3 of the 6 locations (Port Renfrew, Jordan River, Sooke; Table 5). The performance improved when comparing the 95th percentile (Table 5). The model consistently over-predicted SPL at all locations with the performance weakened further in locations with a large number of islands or other barriers. This can be attributed to the lack of advanced three-dimensional physics (out-of-plane refraction) in the quasi-3D model being currently used to simulate the propagation of sound waves in the model domain. This will be addressed through refinements in future iterations of the model.

The modelled probability density function of SPL at Swiftsure Bank, Port Renfrew, Jordan River and Sooke showed a similar Gaussian distribution, however with a modified skew and kurtosis (Figure 34). These differences could be due again to the simplified physics used to simulate the 3D acoustic wave propagation in the water and sediment media.

Vessel Noise at SRKW relevant frequency ranges

First-order estimates of vessel noise levels at 10 kHz (Figure 35) and 50 kHz (Figure 36) for surface waters (to 7.5 m) showed the vessel noise additions to be greatest in echolocation frequencies. The L_{95} and L_{eq} exceedance levels especially highlighted the commercial shipping lanes as sources of noise for both frequency ranges (Figures 35-36). Noise levels in the echolocation frequencies was also heightened in shallow water areas and regions where vessels turn (Figure 36).

3.3.2. Scenario Modeling Results

The vessel noise model was used to examine the impact to the Salish Sea sound field resulting from a projected increase in oil tanker traffic due to the expanded TMX pipeline capacity. This future growth in vessel traffic was simulated by increasing the frequency of tanker traffic from approximately one vessel per week to one vessel per day representing increased TMX pipeline capacity, and plotting a path of additional TMX tanker traffic passage (Figure 37). Using traffic recorded in May 2018 as a baseline, this would mean an increase in the total number of tankers passing through the study area from 197 to 228. Mean SPL values at a number of locations throughout the study area, identified to be important areas for SRKW, were found to increase by approximately 0.80% with the increased tanker traffic simulated here. The expected increases varied between 0.36% and 1.14% for the locations of interest (Table 6).

4. DISCUSSION

Underwater soundscapes are the composites of abiotic, biological and man-made sound. The soundscape of the Salish Sea varies with space and time dependent on acoustic additions from wind as natural noise and vessel presence from human use of the study area. The increased wind-speeds at the eastern extent of Juan de Fuca (Figure 12) explained the increased broadband soundscape conditions seen at Sooke (Figure 6, 10a) during the study period, and the distinction of the sound field at this site compared to neighbouring moorings (Figures 6-7). The contribution of wind noise in the SRKW ranges was heightened in areas of shallow water and hard substrate (Figure 5, 14-15) which may alter the way these additions are expressed in the sound field and influence the soundscape interpretation by the whales. The offshore wind influence was seen most strongly in the early and latter parts of the study period, with additions present in the acoustic record as far east as Jordan River (Figures 13-14).

Mid-frequency additions around 20 kHz were not considerable to the soundscape at any of the mooring locations (Figure 11). The source of the noise around this frequency can be difficult to discern between rain and small vessels, as additions can appear very similar, depending on the amount and type of rain (Nystuen, 1986; Medwin et al., 1990, 1992; Ma et al., 2005). The SalishSeaCast model demonstrates how localised the acoustic additions can be, especially given the nature of intense rain showers and squalls. Therefore, comparison between SPL and precipitation may need an increased resolution. Acoustically distinguishing high-frequency additions from precipitation and those from small vessels may be aided by the use of the SalishSeaCast model. Precipitation was low from May through August (Figure 15), and therefore it is more likely that this acoustic addition could be attributed to small vessels, particularly in the early- to mid-summer.

The anthropogenic component of the soundscape is determined by the volume of traffic and properties of the sound field as well as topography and sediment type. The commercial AIS Class A vessels add to the soundscape in the lower frequencies, showing good agreement when AIS-derived vessel number was correlated with the acoustic vessel metrics (Merchant et al., 2012, 2015; Burnham et al. 2021). Vessel transits of AIS Class A are predominantly restricted to the shipping lanes following the traffic separation scheme and so spatial presence, and therefore acoustic additions were predictably represented (Figures 18-19, 33). Whereas Swiftsure Bank, Port Renfrew and Jordan River recordings demonstrated the chronic nature of vessel noise, Boundary Pass and Haro Strait showed the more acute nature of additions from direct transits of vessels over the mooring site. In Juan de Fuca Strait, the acoustic impact of commercial vessels may be lower, with fewer peaks in PSD in the lower frequencies (Port Renfrew and Jordan River, Figure 6), but the influence of Class B and recreational vessel traffic shaped the sound field at these locations (Figures 18-19; also see Burnham et al. 2021), with PSD peaks for additions in the mid- to high-frequencies (Figure 6). The 20 kHz contributions seen in the soundscape composition analysis (Figure 11) and the patterns seen for the 50 kHz frequency range, also add evidence of increased small vessel presence in the acoustic record for the study area for May to October (Figures 7-8). Considered together this shows how influential this vessel type can be in the soundscape, and likely how under-represented in acoustic analyses they currently are (Erbe et al., 2012; Cominelli et al., 2018). The AIS Class B and recreational vessels contribute substantially in the higher-frequencies, and to those relevant to the SRKW on more local spatial and short-term temporal scales (see L_{75}, 50 kHz; Figure 17b). The use of 50 kHz as a metric to track small vessel presence showed their contribution to the cumulative soundscape experienced by SRKW could be significant, especially during daylight hours. These acoustic additions are likely from pleasure craft, recreational fishing vessels, and whale watchers, few of which carry AIS transceivers. Indeed, in much of our study area, non-AIS carrying vessels have been recorded to outnumber those vessels that could be tracked through AIS (Serras-Sogas et al., 2018). Seeing at least 50 vessels of these types near SRKW is not uncommon during summer weekends and holidays in the Salish Sea (Koski et al., 2006; Holt et al., 2009). Better quantification of small vessel presence, to tie to the acoustic additions made by this vessel type, is still needed.

The vessel presence of AIS Class A vessels decreased between 2018 and 2019, resulting in reductions in the overall soundscape, in both broadband (10 Hz to 100 kHz) measures and those more pertinent to SRKW (Vagle, 2020; Burnham et al. 2021). The vessel noise model suggests greater additions in the frequencies used in echolocation, with this having the potential to mask echoes or decrease the extent over which echolocation could be effectively used. Reduced efficacy in echolocation could have implications for success in navigation and foraging behaviours (see Thornton et al., 2021b**Error! Bookmark not defined.**), with reduced traffic levels offering a possible reprieve. In 2020, vessel passages were impacted by the COVID-19 pandemic. Measures announced in early April (April 6, 2020) restricted recreational vessel activities and prohibited all commercial marine vessels with a capacity of more than 12 passengers including cruise ships and ferries. This period of 'anthropause' (Rutz et al., 2020), has led to suggestions of benefits for wildlife including reduced human disturbance (Bates et al., 2020). In our study area, the presence of AIS-tracked vessels declined immediately following the announcement, but recovered as the summer progressed (Figures 23-25), demonstrating only a short-term reduction in human-use. Overall, AIS Class A vessel transits in 2020 met or exceed numbers seen in previous years, with SRKW and other cetacean species in the Salish Sea therefore not likely to have had significant benefit from restrictions. The reduced presence of smaller, recreational vessels may have resulted in the greatest benefit (Figure 24), but this is hard to quantify due to them not being tracked by AIS and limited NASP and Creel data to draw from (Figures 29, 31).

The presence of AIS Class A small commercial and non-commercial vessels as well as AIS Class B vessels presented in this analysis should be assumed to represent a minimum estimate of presence. Many of these vessels are not required to carry AIS transceivers, and so are considerably underrepresented in AIS datasets in the Salish Sea especially during the spring and summer (Serras-Sogas et al., 2018). An expansion of AIS carriage requirements enforced from June 15, 2019 by Transport Canada now requires vessels traveling at least 1 nm from shore to carry AIS (either Class A or Class B type) if they are certified to carry more than 12 passengers or are at least eight metres in length and carrying passengers (Government of Canada, 2019). This applies to many whale watching vessels and will increase the number of Class B vessels tracked by the AIS. In this analysis, AIS-non mandatory vessel presence was higher in Juan de Fuca Strait in American waters compared to Canadian (Figures 18-19), which may represent true differences in vessel number, or simply that a greater range of vessels are regulated to carry AIS transceivers in the US, and were within line-of-sight of the terrestrial receivers. However, another expansion of Canadian AIS carriage requirements came into effect on April 26, 2021, such that AIS Class A is now required for vessels at least 20 m in length (with the exception of pleasure crafts), tugs at least 8 m in length, and vessels carrying more than 50 passengers (Government of Canada, 2020). This will provide a more complete picture of Canadian vessel presence and brings requirements closely in line with those already in force in American waters, allowing for more equitable comparisons of American and Canadian vessel traffic in the future. However, the exclusion of pleasure crafts from the expanded requirements results in a continued need for other means of quantifying recreational vessel traffic.

Aerial surveys have the potential to provide valuable information to supplement vessel data collected via AIS. The aerial survey data shown in this study highlight the presence of smaller vessels in the study area, however, the data currently available have limitations in their application to this analysis. Again, these data are considered to be a minimal representation of vessel types not required to carry AIS transceivers, because the DFO Creel Survey overflights focus only on recreational fishing vessels and the NASP surveys avoiding areas of high vessel density. This highlights the unknowns about non-AIS vessel presence in both number and location. Further planned improvements, such as more accurate flight track recording and expansion of vessel types recorded by DFO Creel Survey overflights, will further add to these types of vessel presence analyses in addition to expansion of the vessel types required to carry AIS.

Reduced representation of AIS vessel presence data between Port Renfrew and Sooke, especially in AIS Class B vessel data along the coast southeast of Port San Juan (Figure 19), corresponds to an area of reduced coverage by the AIS receivers, not necessarily a lack of vessels. Terrestrial AIS works on approximately line-of-sight coverage, where here the greater distance between base stations (Figure 1) and weaker signal in the Class B transceivers resulted in limited data reception. Although the data were checked for inaccuracies before use, they were also still subject to error or instrumentation failure (Aarsæther and Moan, 2009; McGillivary et al., 2009; Silber et al., 2010; Robards et al., 2016).

The vessel noise model highlights the acoustic impact that AIS Class A commercial vessels have on the soundscape in the Salish Sea. The acoustic additions were considerable at all depths examined. The acoustic disturbance was greater in the upper 20 m or so, within the typical dive depths of SRKW (Baird et al., 2005). Data from DTags have shown foraging dives to be initiated at approximately 7.5 m depth, and dive depths were frequently limited to the upper 30 m (Baird et al., 2003, 2005; Tennessen et al., 2019). Slow echolocation click use related to prey searching in the upper water column has been recorded for shallow dives (2.5-3.5 m), but maximum dive depth for prey capture has been recorded to exceed 150 m (Tennessen et al., 2019). Resting and travelling behaviours also occurred within these shallower depths near the surface (Baird et al., 2003), and most other dives recorded for travelling were within the top 10 m of the water column (Tennessen et al., 2019). Foraging SRKW will dive to depth following Chinook salmon (*Oncorhynchus tshawytscha*) prey, but typically these dives will not exceed 150 m (Baird et al., 2003, 2005). These depths match what has been presented in this analysis (Figure 33). Diving to depth, the soundscape is more likely to be to be dominated by more distance noise sources, coming from vessel traffic in the outbound shipping lane (Vagle et al., in prep[4]).

The SPL level of 110 dB has been suggested as a threshold value beyond which behavioural modifications may occur in SRKW (Hemmera Environchem Inc., 2014), with areas in the study area exceeding this level in both the observed and the model results. Changes in behaviour, or a transition from foraging to travelling in the presence of vessels (Williams et al., 2014), or abandonment of prey-rich areas would tax an already stressed population. Areas of Swiftsure Bank, Juan de Fuca Strait and Haro Strait are known foraging areas (Olson et al., 2018; Thornton et al., 2021b**Error! Bookmark not defined.**) that also demonstrate elevated vessel presence.

Prey detection and conspecific communication needed for prey sharing may also be impacted, as demonstrated by the vessel noise model's application to the SRKW communication and echolocation ranges (Figures 35-36). It also demonstrated how noise can concentrate in areas due to the physical geographies of the inlets and waterways.

The vessel noise models presented here represent the worst-case scenario for SRKW foraging or transiting the Salish Sea. First, the modelled values in all cases represent an overestimation

[4] Vagle, S., Burnham, R.E., O'Neill, C., Yurk, H. Variability in anthropogenic underwater noise due to bathymetry and sound speed characteristics. Manuscript in preparation.

of the ambient noise values arising from vessel presence compared to that measured by the moorings (Table 5). The overestimate remained in the extrapolation to the representative frequencies of SRKW communication and echolocation. Iterative model refinements hope to address some of this overestimate in the future. Also, the vessel noise modelling does not assume any spatial, temporal, or comodulation masking release for SRKW (Erbe et al., 2016). Instead, the model depicts vessel presence to be consistent based on the transit numbers derived from the AIS data, and so is considered here as more of a chronic rather than transient input when considering vessel noise levels monthly. The model does not take into account whale location or the dynamics of calling, including directionality (Miller, 2006; Wellard et al., 2020), or parameters of calls such as inter-pulse-interval (Lammers et al., 2004; Madsen et al., 2005; Morisaka et al., 2011), which are altered to assist with localisation and particularly during prey capture. Instead, the maximum abiotic and ambient noise levels that might be experienced by a whale in all locations during anytime of the time period shown were depicted. These worst-case scenarios were also used in Thornton et al. (2021b**Error! Bookmark not defined.**) to further evaluate the noise levels present in the study area, and how they may alter the acoustics use of SRKW. It is assumed in the model results that there was no release mechanism from the masking noise, and that hearing, calling and sound reception is omnidirectional. Also, no directionally or change in amplitude in signal output either from the whale (e.g., Miller and Tyack, 1998; Miller, 2002; Jensen et al., 2018) or vessels were included.

The noise model was limited to AIS Class A vessels only. Inclusions of AIS Class B and recreational vessels to better represent all anthropogenic noise sources is an ongoing endeavour. Other sources of vessel noise, for example such as berthing from vessel maneuvering or at anchor, from the pump and generator, were not quantified here as they are not thought to be relevant to the vessels in the study area.

The vessel-noise model used in this analysis is limited to about 500 Hz. Therefore, the necessary extrapolations to the higher frequency bands used by SRKW introduce significant uncertainties when using the present model outputs to evaluate impacts on SRKW (Table 3, Figure 3). However, work is presently underway to expand the modeling capability to better represent the 3D nature of the ocean landscape and to be able to demonstrate noise additions to at least 5 kHz, which will allow a more direct evaluation of the vessel noise impact on the soundscape at SRKW relevant frequencies. In addition, the model would benefit greatly from a means to account for Class B and non-AIS vessel presence. The addition from these vessel types is considerable, with their presence still underrepresented in the current analysis physically and acoustically. Killer whales vocalise and have demonstrated hearing sensitivity into the low frequencies (<1 kHz, Miller et al., 2006; Branstetter et al., 2017), but are presumed to have the most acute hearing capacity in the frequencies in which they vocalise. The acoustic additions from smaller vessels are more likely to fall into these higher frequency ranges.

Together the interpretation of the soundscape components in the frequency ranges known to be used by SRKW informs our understanding of the whales' appreciation of the sound field, the relative impact each component has, and the potential level of acoustic disturbance vessels present. Global increases in ambient noise levels in low-frequency ranges have been seen over the last fifty years, in the order of 10-12 dB re 1 µPa, coincident to the doubling of the global shipping fleet (Notarbartolo di Sciara and Gordon, 1997; Rolland et al., 2012). This is set to continue with cargo capacity predicted to triple, and vessel passage rate to double in the next 20-years (Jasny, 2005). Models like the vessel noise model presented here could be used to predict the soundscape increases that might result from changes in shipping schedules and pressures. Noise emissions from vessels varies depending on ship size, class, engine type, hull design, propeller configurations, operating conditions, and speed of travel (Badino et al., 2012; McKenna et al., 2013; Lidtke et al., 2016; Veirs et al., 2016). Scenarios with alterations of one or more of these factors could be modelled to determine the soundscape impacts before changes are made. Here a scenario of TMX tanker traffic being increased seven-fold was presented, in-line with what has been predicted to occur as the Trans-Mountain pipeline expansion (TMX) project proceeds. The impacts of this increase in tanker traffic were found to occur mostly at Swiftsure Bank and the Port Renfrew and Jordan River moorings in Juan de Fuca Strait (Table 6).

Vessel noise models can also be used to evaluate the impact of potential reductions in traffic or actions taken to mitigate vessel noise. Measures undertaken by the Vancouver Fraser Port Authority's Enhancing Cetacean Habitat and Observation (ECHO) program, for example, to reduce impacts to SRKW critical habitat include voluntary ship slowdowns and inshore lateral displacement for tug operators, designed to reduce vessel noise contributions and to shift vessel transits further from SRKW habitat, respectively. In addition, Transport Canada has implemented temporary vessel exclusion zones (Interim whale Sanctuary Zones, ISZs). These measures have shown more limited success principally because a lack of participation in the trial by AIS Class B and recreational vessels (Vagle and Neves, 2019; Vagle, 2020; Burnham et al., in review[5]). Vessel noise models, like that used in this report, could be used to identify the regions where measures like these might be most effective. The use of other operational mitigations, such as vessel convoys or greater restrictions in timing or routes of transit could also be explored by modeling to establish their potential benefit. The model may also be used to explore the benefits of retrofitting vessels or removing the oldest vessels in the fleet as part of source-based mitigation actions (Veirs et al., 2017; Burnham et al., in review[5]).

The work presented here provides an insight into the level of anthropogenic noise resulting from vessels, in addition to the ambient natural noise levels. It also describes the patterns of physical presence of vessels. Coastal and on-shelf waters show greater variation in ambient noise levels compared to deeper more offshore sites, and are subject to a greater concentration of shipping and industrial activity (Urick, 1983; Jensen et al., 2011; Merchant et al., 2012). The wind and precipitation models helped to appreciate the additions and level of variation over time and space from these natural noise additions. The attempt to quantify AIS and non-AIS vessel traffic, and comparisons to the acoustic data, will help increase knowledge on vessel-derived noise. Considered together the components of chronic and more acute or transient noise sources, all overlapping in time in frequency, that form the soundscape in the Salish Sea at times when SRKW were most frequently present can be presented. There is increasing evidence that cetaceans perceive anthropogenic noise as a risk or form of threat (Tyack, 2008). Therefore, the results of these analyses can be used to examine how noise additions from natural and human-derived sources add to the frequency ranges used by SRKW, and initiate the discussion of how that might have implications in their ability to navigate, find prey and communicate with conspecifics. On a broader scale, acoustic and physical disturbance from vessels have been listed as main threats to the SRKW population. The results presented here add to the consideration of the impacts of vessel presence, and both the short- and long-term implications for acoustic masking of conspecifics' calls or sound cues in fecundity and survival in an acoustically degraded habitat.

5. ACKNOWLEDGMENTS

The authors would like to thank Caitlin O'Neill, Peter Van Buren, Christie Morrison and Harald Yurk for help with acquiring the PAM data. Thanks also must go to the officers and crew on

[5] Burnham, R.E., Vagle, S., O'Neill, C., Trounce, K. The efficacy of management measures to reduce vessel noise in critical habitat of southern resident killer whales in the Salish Sea. In Review.

CCGS VECTOR for all their help with servicing our hydrophone moorings in the Salish Sea. Florian Aulanier and Pierre Mercure-Boissonnault helped with setting up the vessel noise model and Emmanuel Rosetti and Guillaume Godbout retrieved the Coastguard AIS vessel data and provided information on AIS coverage. The authors also acknowledge Patrik Zetterberg and Brenda Wright for coordinating the collection of the DFO Creel Survey overflight data, Kristopher Hein, Matthew Clarke and Karin Mathias for managing and provision of that dataset, Norma Serra-Sogas for providing NASP survey data, and Adrian Nicoll for providing a python script for validating vessel information.

6. TABLES

Table 1: Frequency ranges of acoustic metrics used in this analysis to describe changes and additions to the soundscape.

Frequency range (Hz)	Metric	Description
10-100,000	Soundscape, SRKW	General ambient noise metric, range where behavioural change in SRKW may be observed if noise additions are present (Heise et al., 2017)
500-15,000	SRKW	Range for SRKW communication calls (Heise et al., 2017)
15,000-100,000	SRKW	Echolocation range for SRKW (Heise et al., 2017)
100-1,000	Vessel	Vessel presence marker, excluding water turbulence (Merchant et al., 2012)
57-71	Vessel	63 1/3 octave band (Merchant et al., 2012, 2015, EU's Marine Strategy Framework Directive)
113-141	Vessel	125 1/3 octave band (Merchant et al., 2012, 2015, EU's Marine Strategy Framework Directive)
10-100	Abiotic	Low-frequency wind, wave and water turbulence (Merchant et al., 2012)
4,9500-50,500	Vessel	Representative of the 50 kHz signal used in depth sounders
7,500-8,500	Abiotic	Correlated to wind speed (Vagle et al., 1990)
19,500-20,5000	Abiotic	Precipitation noise, centered around 20000 Hz (Vagle et al., 1990)

Table 2: Geoacoustic properties used to define the longitudinal and shear wave propagation of low frequency acoustic waves through the different sediment types present in the study area. λ is the wavelength of a given acoustic wave penetrating into the substrate.

Sediment Type	Density (dB/λ)	P-wave speed (m/s)	P-wave attenuation (dB/λ)	S-wave speed (m/s)	S-wave attenuation (dB/λ)
Rocky	2200	2275	0.1	500	3.4
Sandy	1900	1700	0.9	250	2.2
Silt and Mud	1640	1550	0.8	125	1.2

Table 3: A list of vessel noise model and extrapolation inputs, the sources of the data, assumptions under which the data was applied and the sensitivity of the model to each of the inputs.

Model Input	Data Input	Source	Assumption	Model sensitivity (approx.)
Bathymetry	15 s arc, 300 m resolution	Canadian Hydrographic Service, 2020	Interpolated to model grid	Low
Sediment data	Sediment type, on a 300m resolution	Haggarty et al., 2018	Sediment type approximated into different zones	High
Geoacoustic sediment properties	Low frequency (60-500 Hz) propagation of P and S waves	Hamilton, 1980; Jensen et al., 2011	Properties tuned to fit acoustic observations	High
Water properties	Temperature, salinity, wind data	Live Ocean model, SalishSeaCast model	Interpolated from hydrodynamic model grid to acoustic model grid	Medium
Water column properties	40 vertical layers	McDougall and Barker, 2011	Variable layer thickness	Low
Acoustic transmission properties	Acoustic frequency dependent absorption for pH value of 8	Francois and Garrison, 1982	Assumes constant pH	Low
Vessel source levels	Derived source levels, considering SOG	Veirs et al., 2016 ; Simard et al., 2016 ; MacGillivray and Li, 2018	-	High
Vessel presence	Cleaned AIS vessel presence data. AIS Class A only	CCG	-	High

Table 4: Periods of recording at each location for each summer month of analysis. Full represents data was recorded continuously for that month without interruption, otherwise the days of the month with recordings are indicated. Asterisks (*) indicate periods lost due to COVID-19

Year	Month	Swiftsure Bank	Port Renfrew	Jordan River	Sooke	Haro Strait	Boundary Pass
2018	May	Full	Full	Full	Full	Full	Full
	June	Full	1-20	1-6, 9-30	Full	Full	Full
	July	1-29	None	Full	Full	Full	Full
	Aug.	17-31	19-31	Full	Full	Full	Full
	Sept.	Full	Full	Full	Full	Full	Full
	Oct.	Full	Full	Full	Full	Full	Full
2019	May	Full	Full	Full	1-18, 31	Full	Full
	June	Full	Full	Full	Full	Full	Full
	July	Full	Full	Full	Full	Full	1-2, 18-31
	Aug.	Full	Full	Full	1-9, 17-31	Full	Full
	Sept.	Full	Full	Full	1-7, 10,13-15,17-30	Full	Full
	Oct.	Full	Full	Full	1, 18-19, 22-31	Full	Full
2020	May	None*	None*	14-31*	14-31*	None	12-31*
	June	21-30*	21-30*	Full	Full	None	Full
	July	Full	Full	Full	Full	16-31	Full
	Aug.	Full	Full	Full	Full	Full	Full
	Sept.	Full	Full	Full	Full	Full	Full
	Oct.	1-26	1-26	1-22	1-23	1-23	1-29

Table 5: Comparison between observed and simulated SPL from the vessel noise model at mooring locations for May 2018. Median (L_{50}) and 95th percentile/L_5 exceedance level are shown.

Mooring Location and approx. depth (m)	Observed SPL (dB)125Hz, L_{50} exceedance level	Observed SPL (dB) 125Hz, L_5 exceedance level	Percentage Error, L_{50} exceedance level (%)	Percentage Error, L_5 exceedance level (%)
Swiftsure (70m)	80.46	100.44	8.10	1.79
Port Renfrew (155m)	85.25	96.36	1.17	4.00
Jordan River (112m)	85.40	99.23	4.78	1.05
Sooke (163m)	88.90	101.83	2.89	1.72
Haro Strait (224m)	81.46	102.43	13.55	6.69
Boundary Pass (181m)	81.66	105.53	19.28	4.91

Table 6: Results of acoustic scenario modelling, showing the impact of higher TMX-related tanker traffic, and the percentage increases from the model results of current traffic levels.

Location	Mean Scenario SPL (dB)	% increase in total vessel noise
Swiftsure	85.71	0.82
Port Renfrew	84.51	1.14
Jordan River	87.62	0.90
Sooke	89.40	0.36
Haro Strait	88.48	0.60
Boundary Pass	94.94	0.47

7. FIGURES

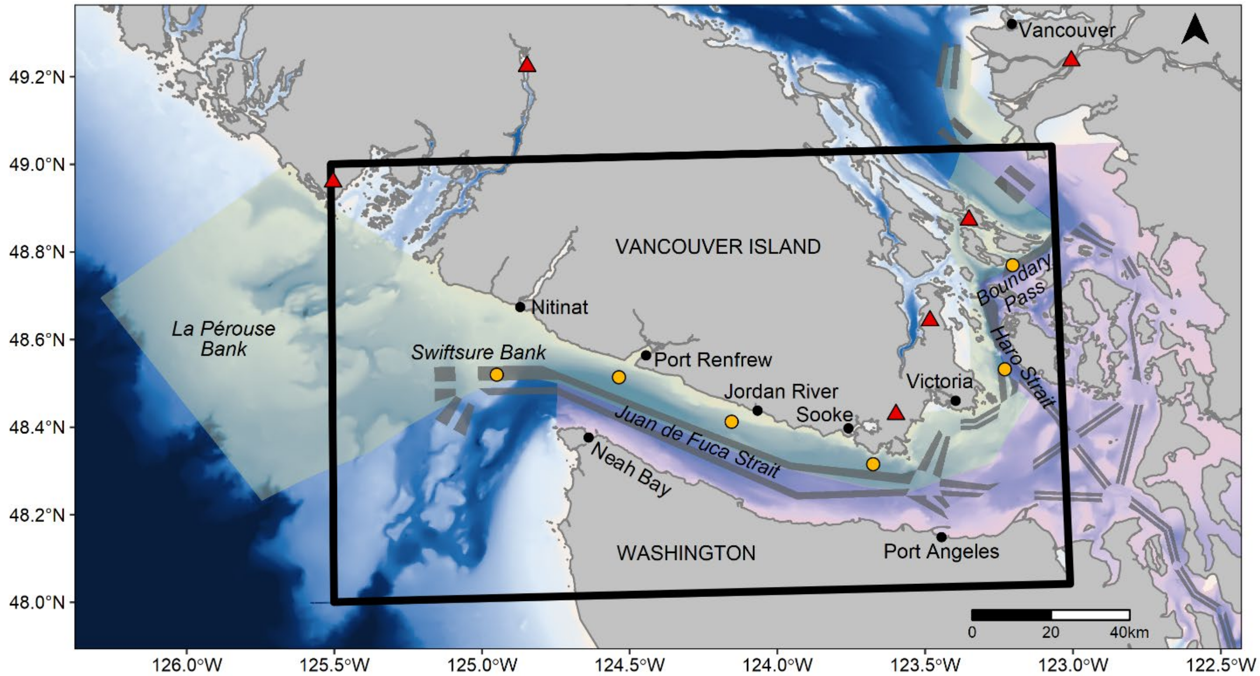

Figure 1: The study area (bounded by a black box, 49.0°N, 125.5°W; 49.0°N, 123.0°W; 48.0°N, 125.5°W; 48.0°N, 123.0°W) in the Salish Sea. The acoustic moorings (yellow circles), AIS receivers (red triangles) and shipping lanes (grey lines) are shown. SRKW critical habitat in Canadian waters (yellow shading) and American waters (pink shading) is also indicated.

Figure 2: One of the PAM moorings being deployed. Each mooring is equipped with four white floatation spheres to keep the moorings vertical on the sea floor and equipped with a dual set of acoustic releases for redundancy during recovery and held down by a 100 kg anchor. The hydrophone is positioned 2 m above the sea floor.

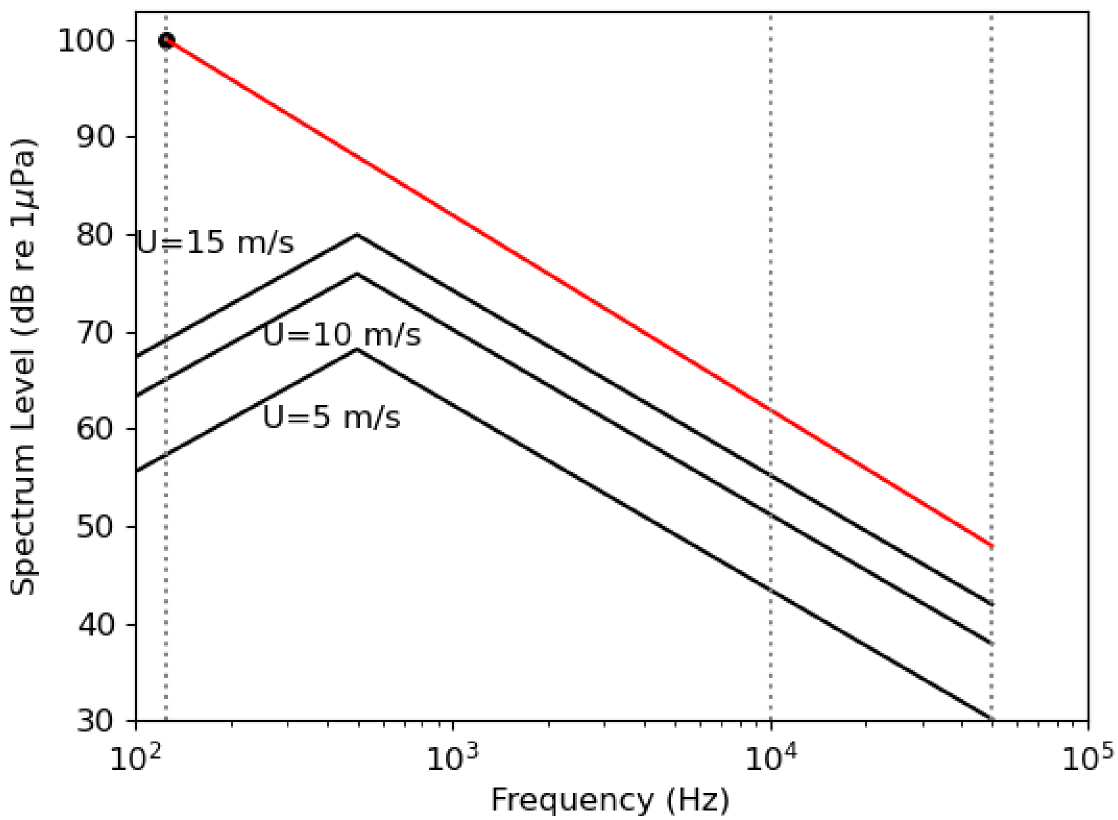

Figure 3: Knudsen curves relating wind speed (U) to deep water noise spectrum level used in the present analysis (black lines). Curves are shown for 3 different wind speeds. Also shown is the assumed frequency dependent spectrum level characteristics used to extrapolate modeled vessel noise at 125 Hz to higher frequencies associated with SRKW (red line). The three frequencies used in the analysis (125, 10,000 and 50,000 Hz) are shown as vertical dotted lines

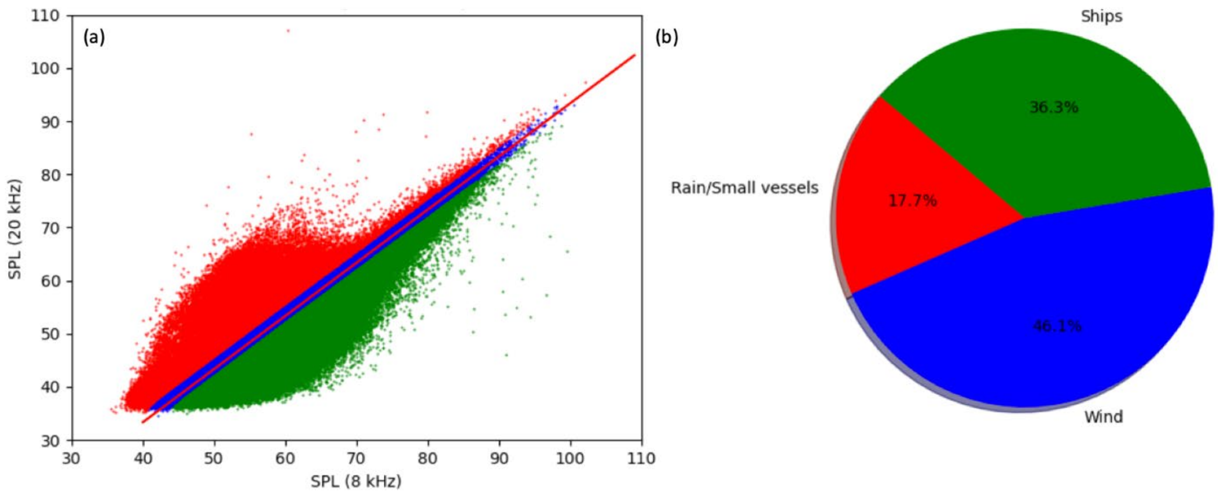

Figure 4: Example of method used to determine abiotic and anthropogenic acoustic additions to the soundscape with the SPL in the wind (8 kHz, blue) and rain (20 kHz, red) and commercial vessel noise (green) frequency ranges plotted for matching minute-wise minimum broadband (10 Hz to 100 kHz) ambient noise level for each hour of data. The number of the points from (a) are expressed as a proportion in (b)

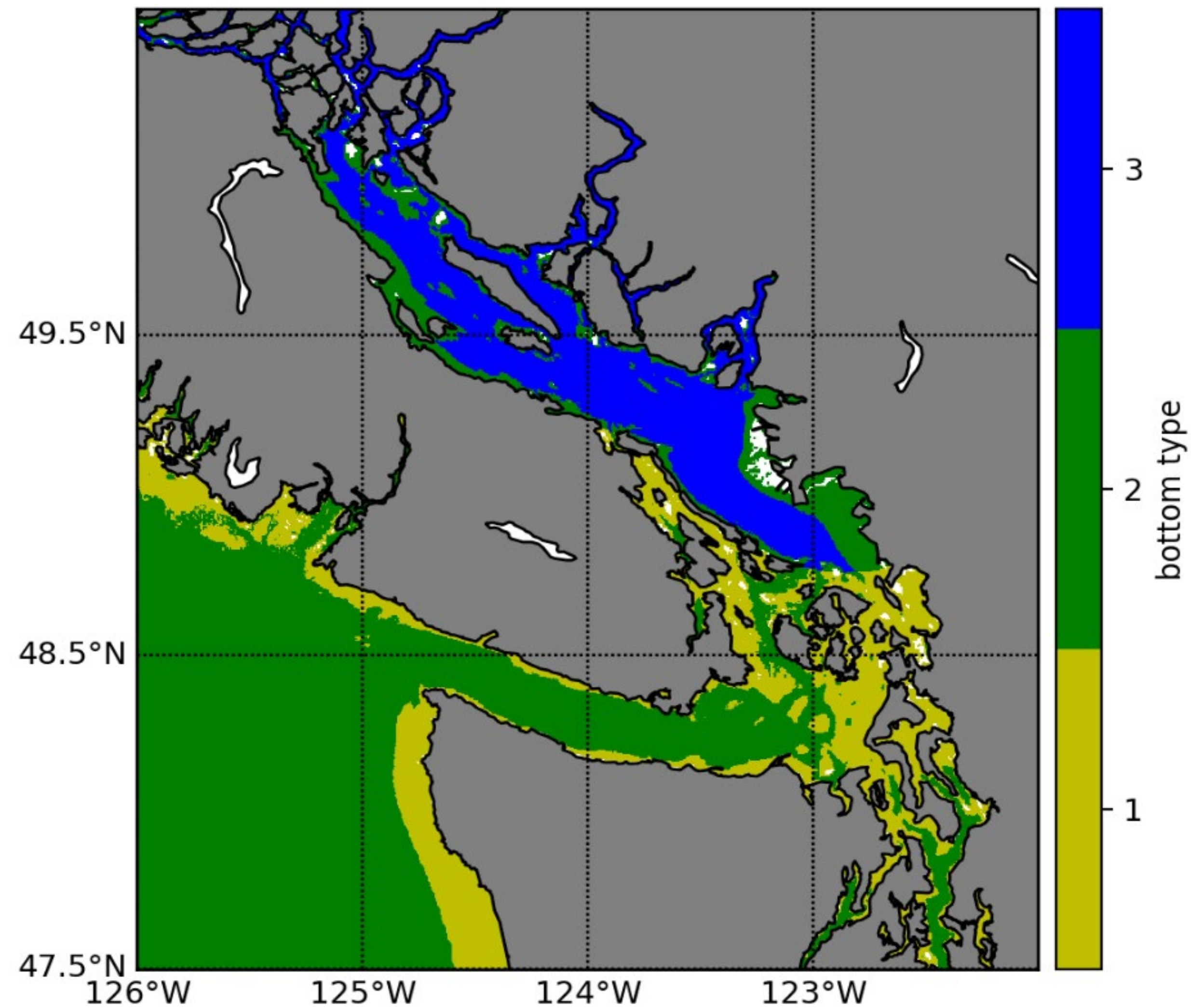

Figure 5: Bottom substrate type defined in the model. Substrate type 1 (yellow) is rock, substrate type 2 (green) is sand, and substrate type 3 (blue) is silt and mud.

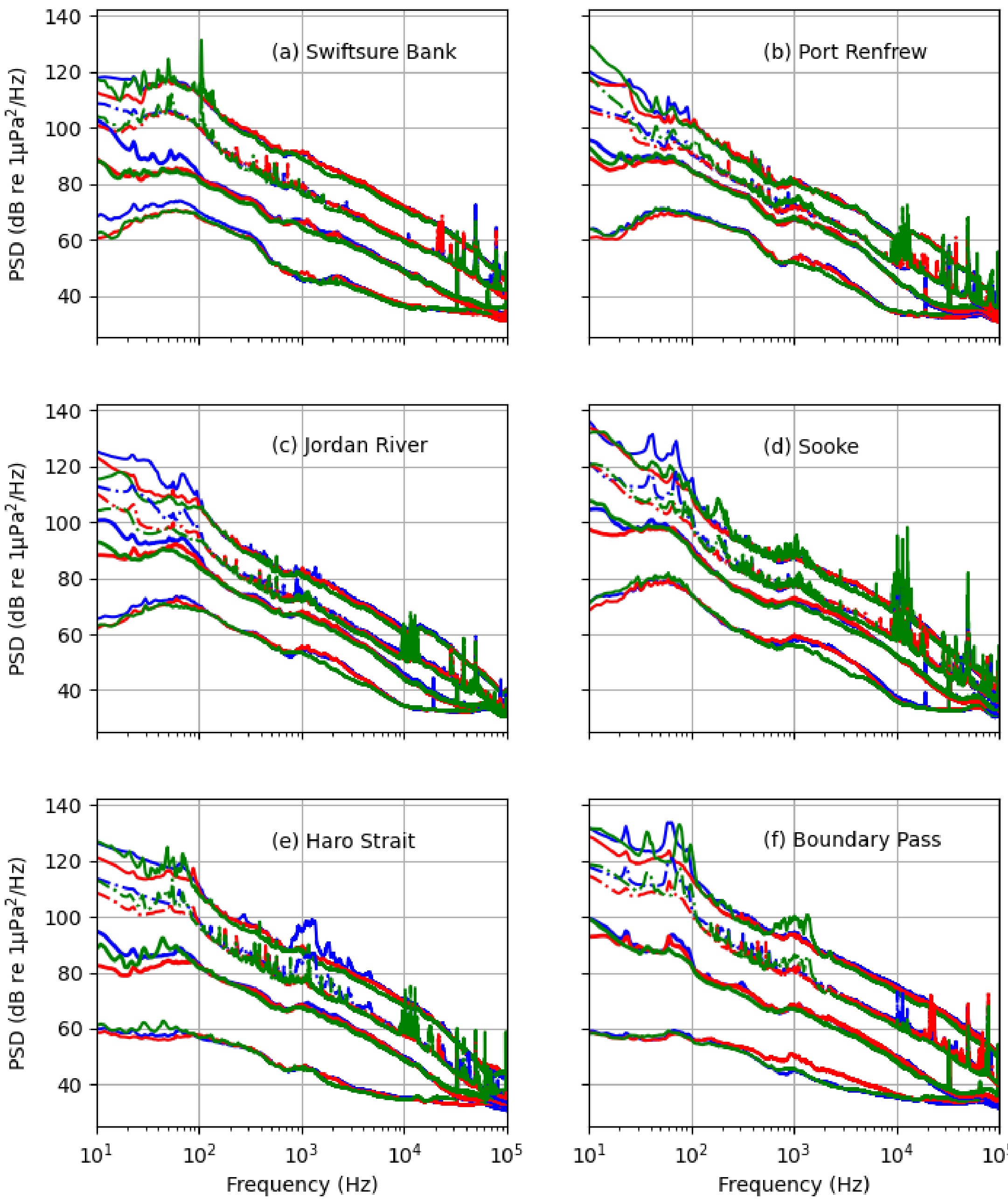

Figure 6: Ambient noise levels averaged from recordings made May to October for each year. Noise exceedance levels L_1, L_{50}, L_{99}, and the arithmetic mean L_{eq} are displayed. Each year is represented by a colour whereby blue is 2018, red is 2019, and green is 2020.

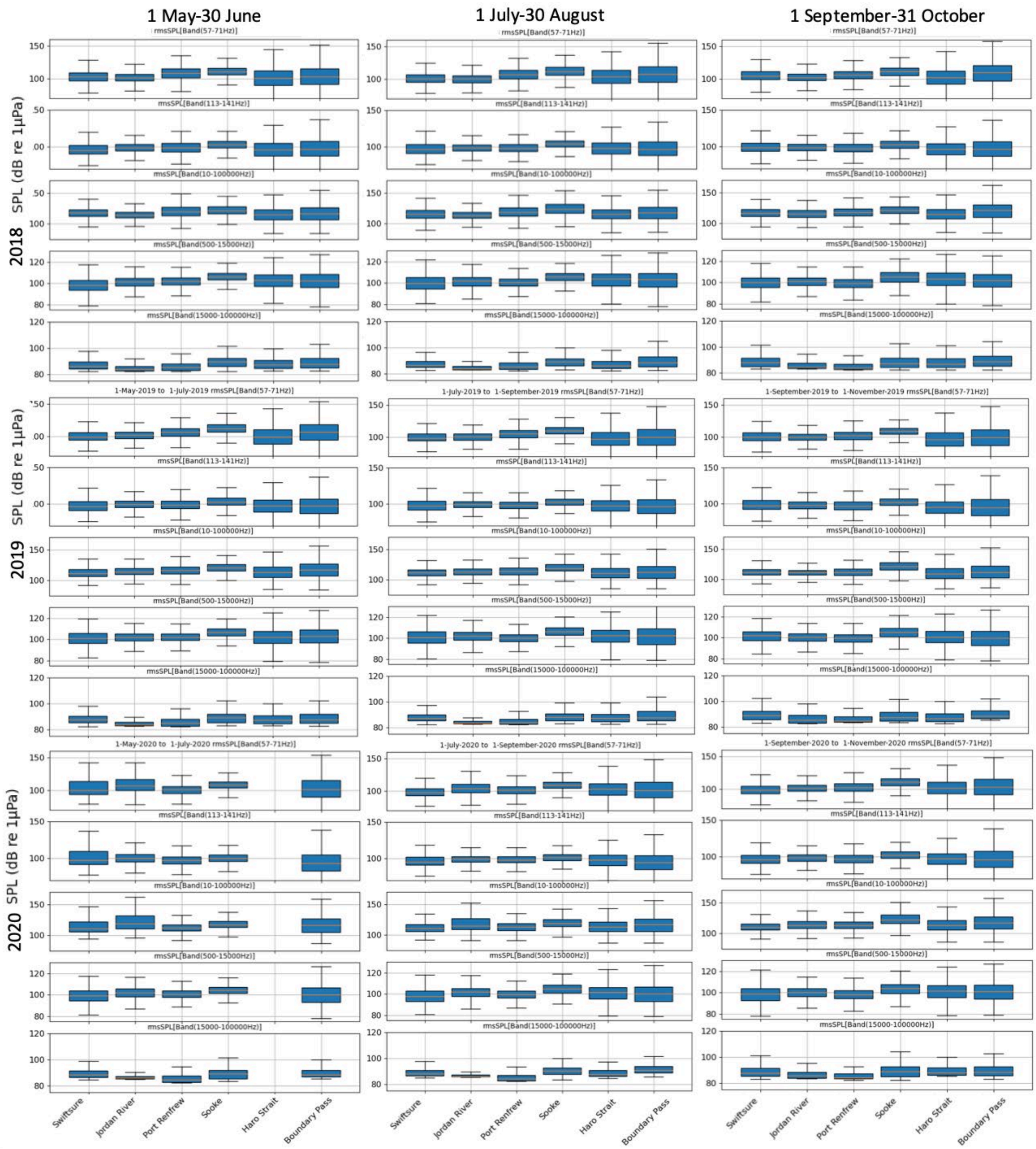

Figure 7: Rhythm plots to compare exceedance levels L_{25}, L_{50} and L_{75} of bimonthly sound pressure levels (SPLs) in vessel frequency ranges (57-71 Hz, 113-141 Hz) broadband soundscape (10-100000 Hz) and SRKW communication (500 Hz-15 kHz) and echolocation (15-100 kHz) ranges. Comparisons are made between years and mooring locations.

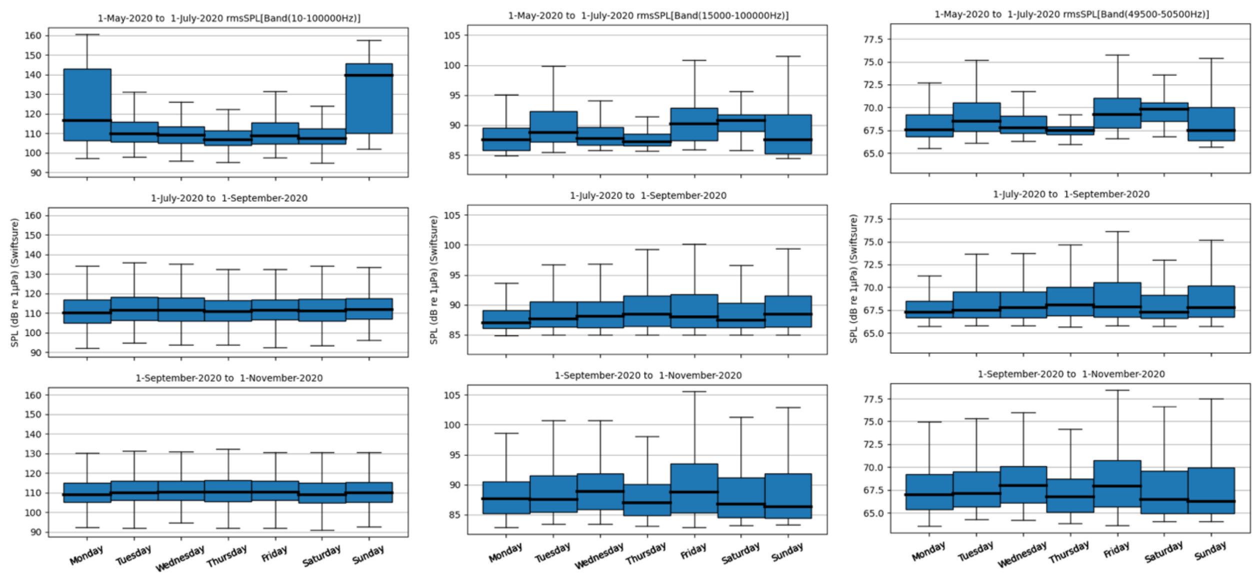

Figure 8: Comparison of exceedance levels L_{25}, L_{50} and L_{75} of sound pressure levels (SPLs) for broadband soundscape and frequency ranges with the possibility to disturb SRKW behaviour (10-100 kHz), communication (500 Hz-15 kHz) and echolocation (15-100 kHz) over days of the week made for Swiftsure Bank recordings from summer 2020.

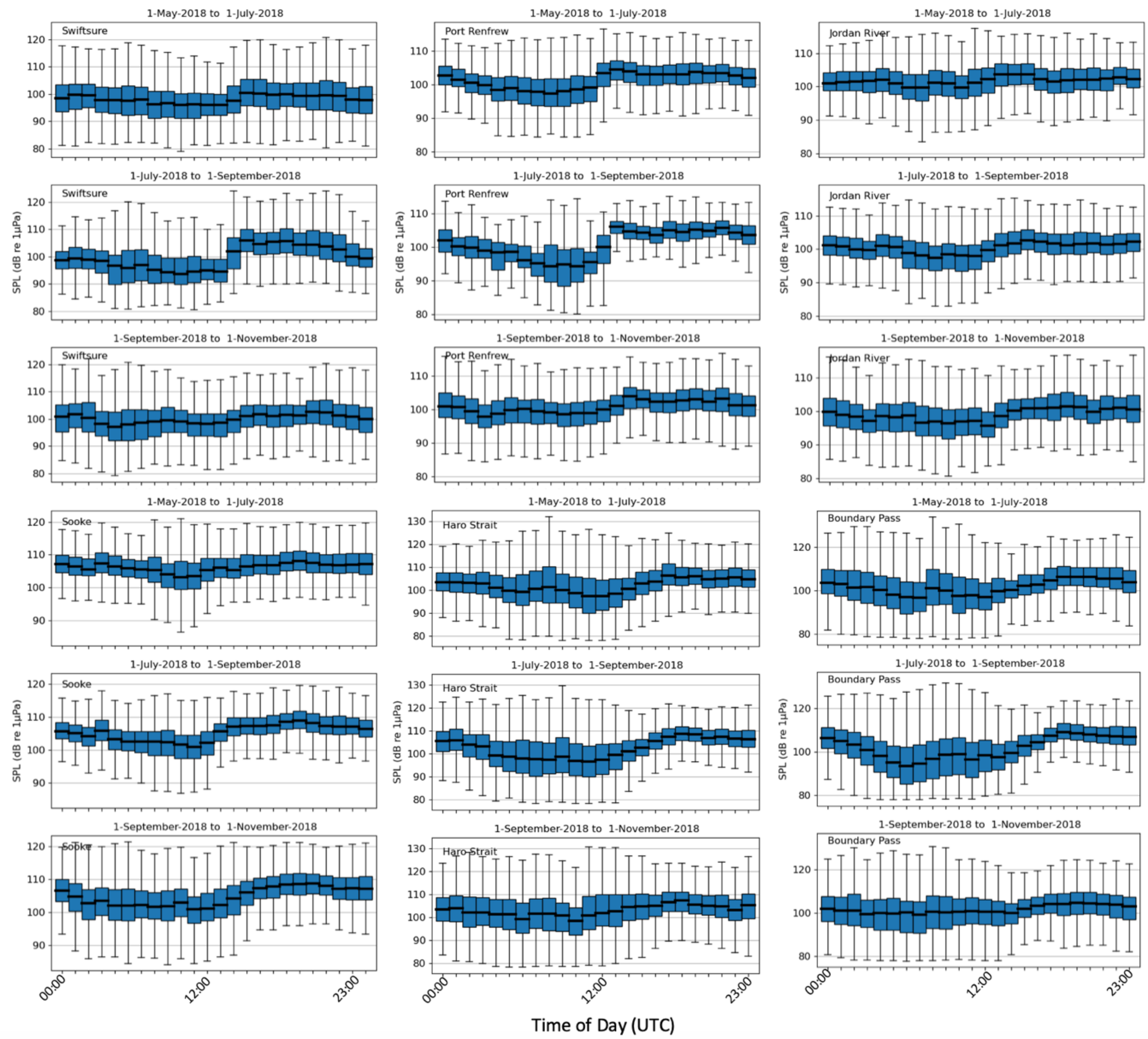

Figure 9: Hourly SPLs in the SRKW communication (500 Hz-15 kHz) frequency range to compare ambient noise levels during a day, particularly between day and night. Time is expressed in UTC, with 12:00-00:00 representing day, and 00.00-12:00 representing night for this analysis.

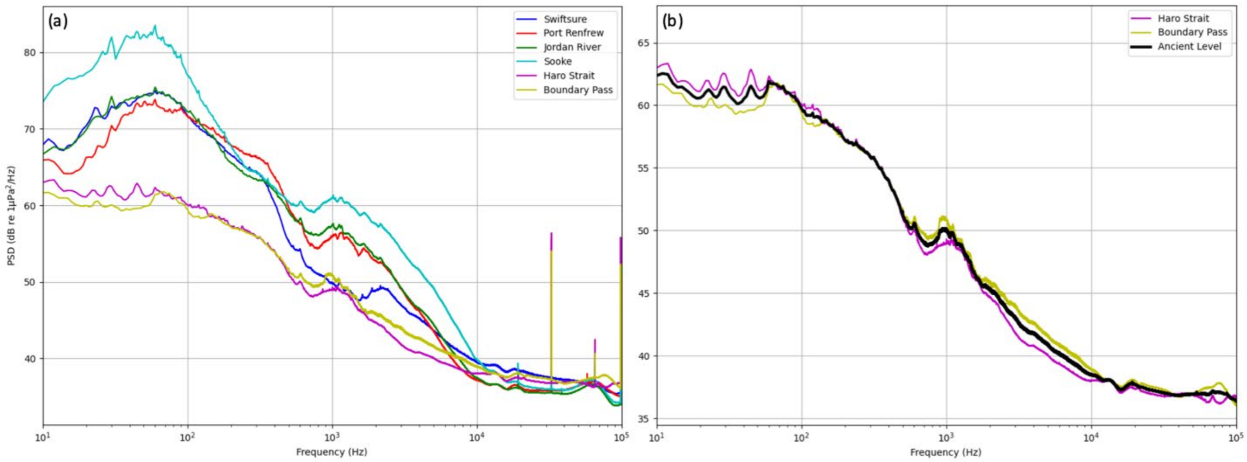

Figure 10: (a) The L_{99} exceedance levels for ambient noise levels of each site aggregated over May to September for 2018-2020 and (b) the use of a composite of L_{99} exceedance levels of ambient noise levels from Boundary Pass and Haro Strait as the 'minimum ambient' noise level.

Figure 11: Soundscape composition, with proportions derived from the relationship between the SPL at 8 kHz and 20 kHz against a Knudsen curve. Results were aggregated to give proportional soundscape additions by shipping (blue), wind (orange) rain (green) and unknown sources (red) monthly for the summers of 2018-2020 for Swiftsure Bank (a), Port Renfrew (b), Jordan River (c), Sooke (d), Haro Strait (e) and Boundary Pass (f).

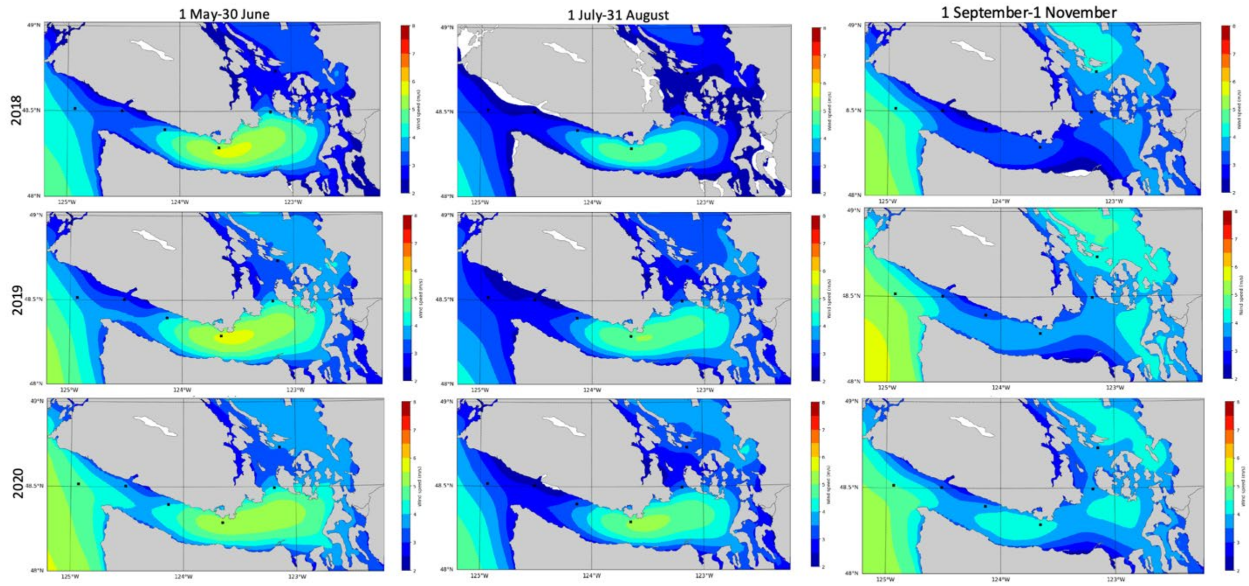

Figure 12: Averaged summer wind speeds (m/s) in the Salish Sea derived from the SalishSeaCast NEMO model (Soontiens et al., 2016; Soontiens and Allen, 2017), displayed in bimonthly increments for 2018-2020.

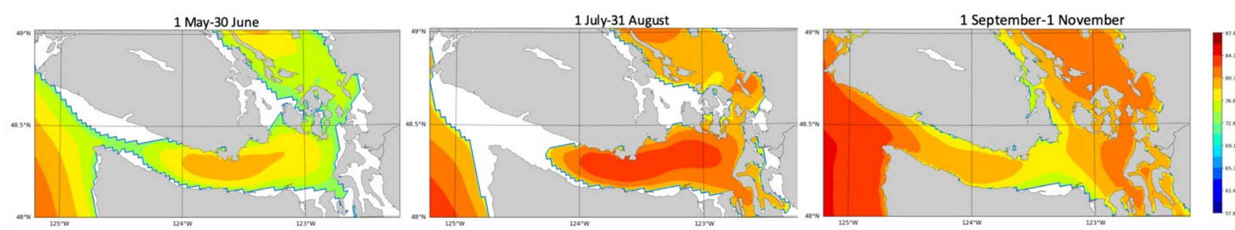

Figure 13: Wind-noise derived additions at 10 kHz, to represent the SRKW communication band in bimonthly periods through the summer season aggregated for 2018-2020.

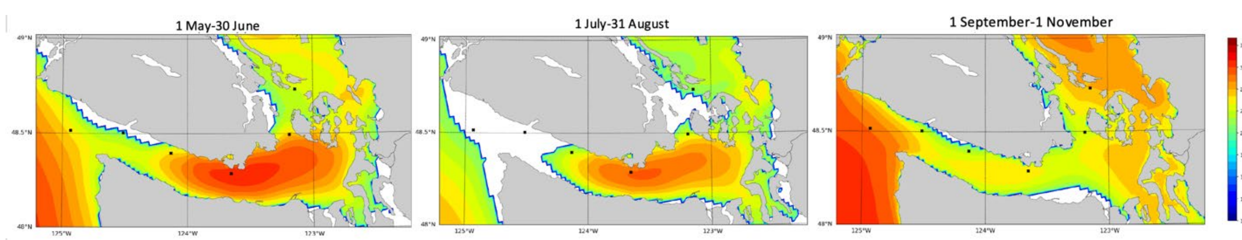

Figure 14: Wind-derived acoustic additions at 50 kHz, to represent the SRKW echolocation band in bimonthly periods through the summer season aggregated for 2018-2020.

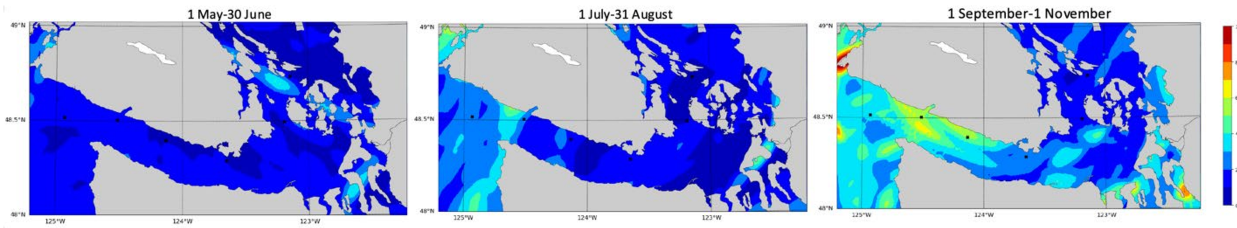

Figure 15: Averaged rainfall amounts (mm/hr) in the Salish Sea derived from the SalishSeaCast NEMO model (Soontiens et al., 2016; Soontiens and Allen, 2017), displayed in bimonthly increments for 2018-2020.

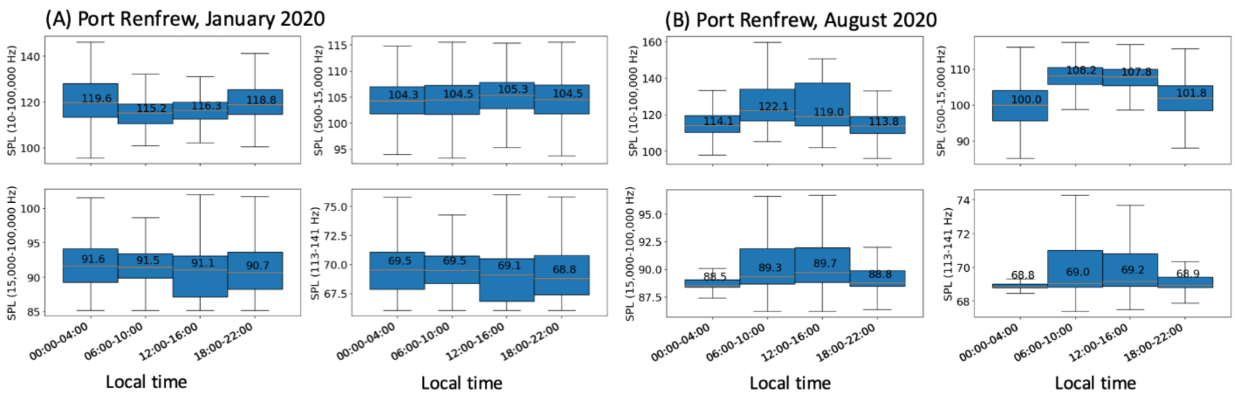

Figure 16: Diurnal comparison, using four 4-hour periods (00:00-04:00; 06:00-10:00; 12:00-16:00; 18:00-22:00) to compare noise levels in the overall soundscape, SRKW communication and echolocation bands, and frequencies focused around 50 kHz. The same comparison was made for January (A) and August (B) 2020 to explore seasonality in the differences between day-night SPL.

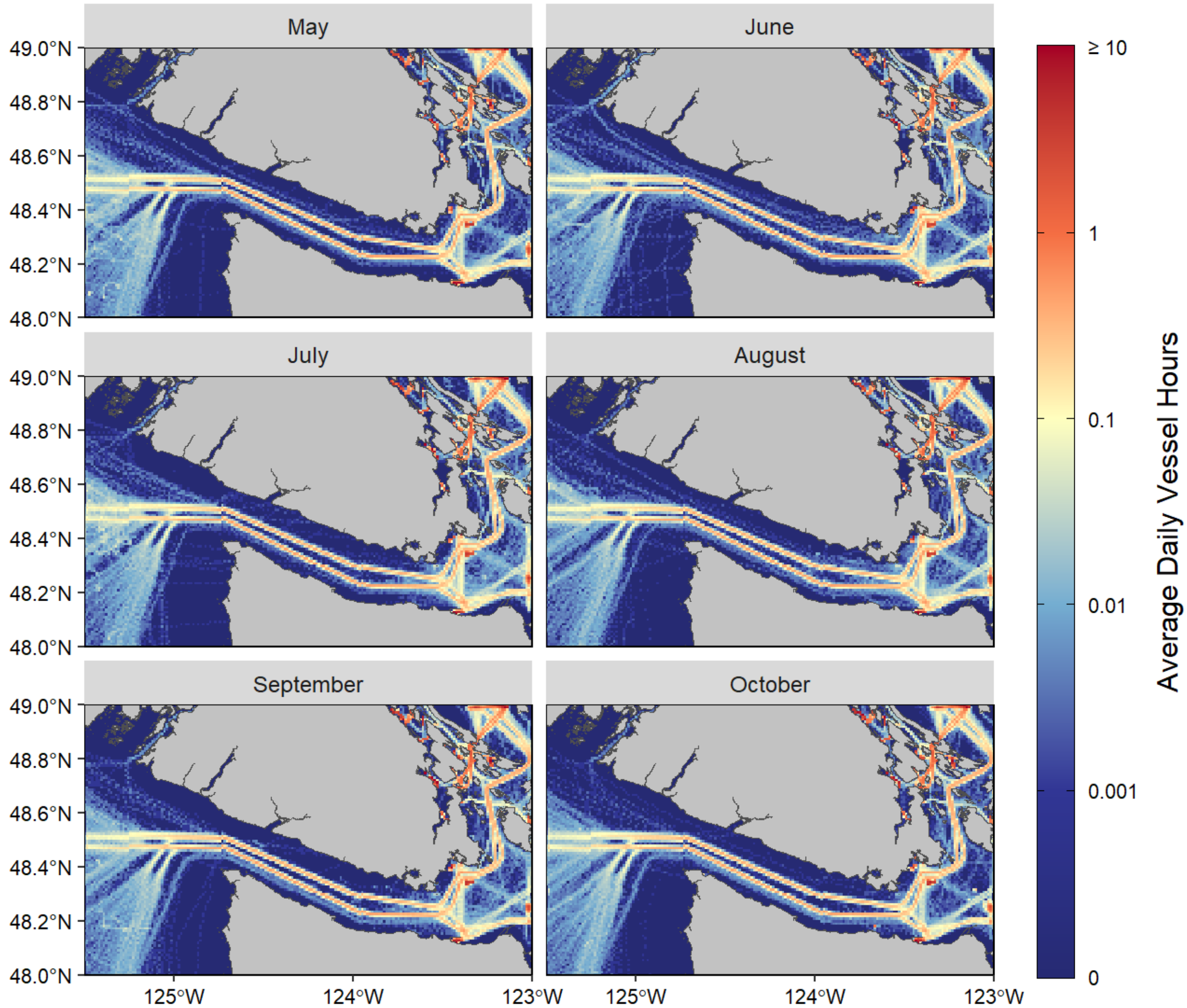

Figure 17: Average daily presence (hours/day/km²) of AIS Class A large commercial vessels in the study area, for May to October, 2018-2020. This includes cargo vessels, tankers, ferries, and cruise ships.

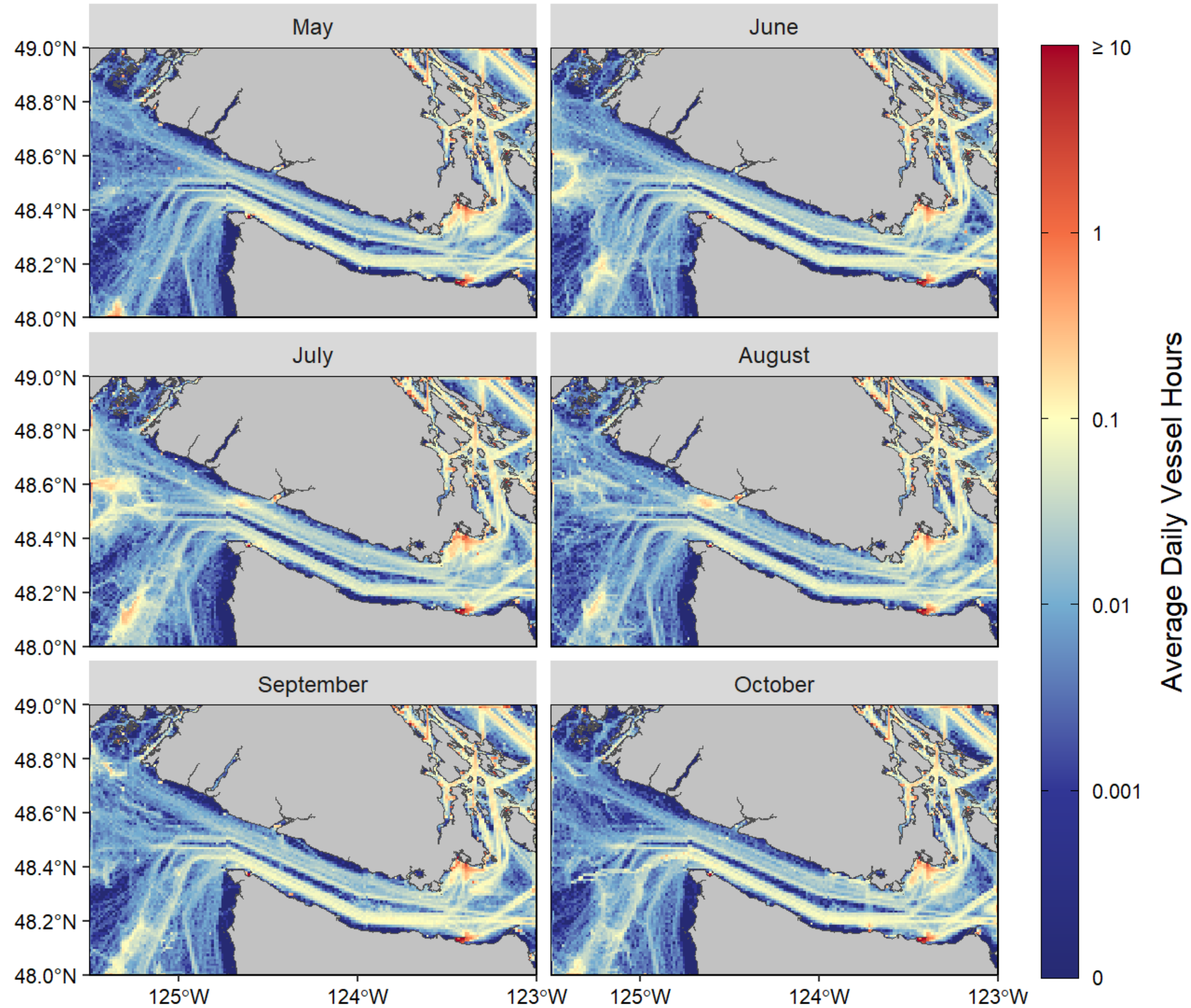

Figure 18: Average daily presence (hours/day/km^2) of AIS Class A (non-mandatory) small commercial and non-commercial vessels in the study area, May through October, 2018-2020. This includes tugs, fishing vessels, government/research vessels, recreational vessels, naval vessels and other vessel types. These vessels are generally not required to carry AIS and so are incompletely captured here.

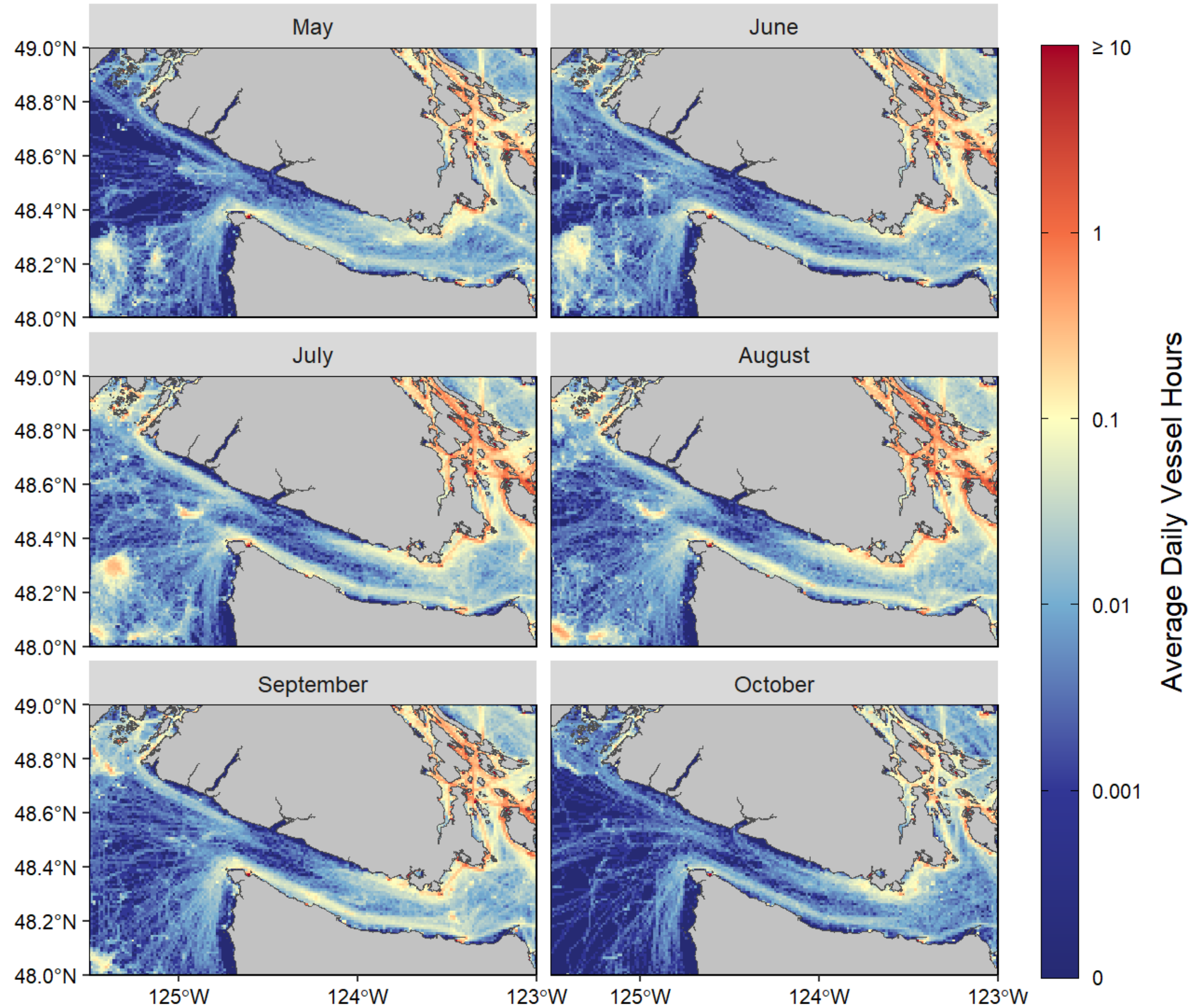

Figure 19: Average daily presence (hours/day/km^2) of AIS Class B vessels in the study area, May through October, 2018-2020. This includes recreational, small passenger, fishing, and coast guard vessels, tugs and other vessel types not required to carry AIS transceivers.

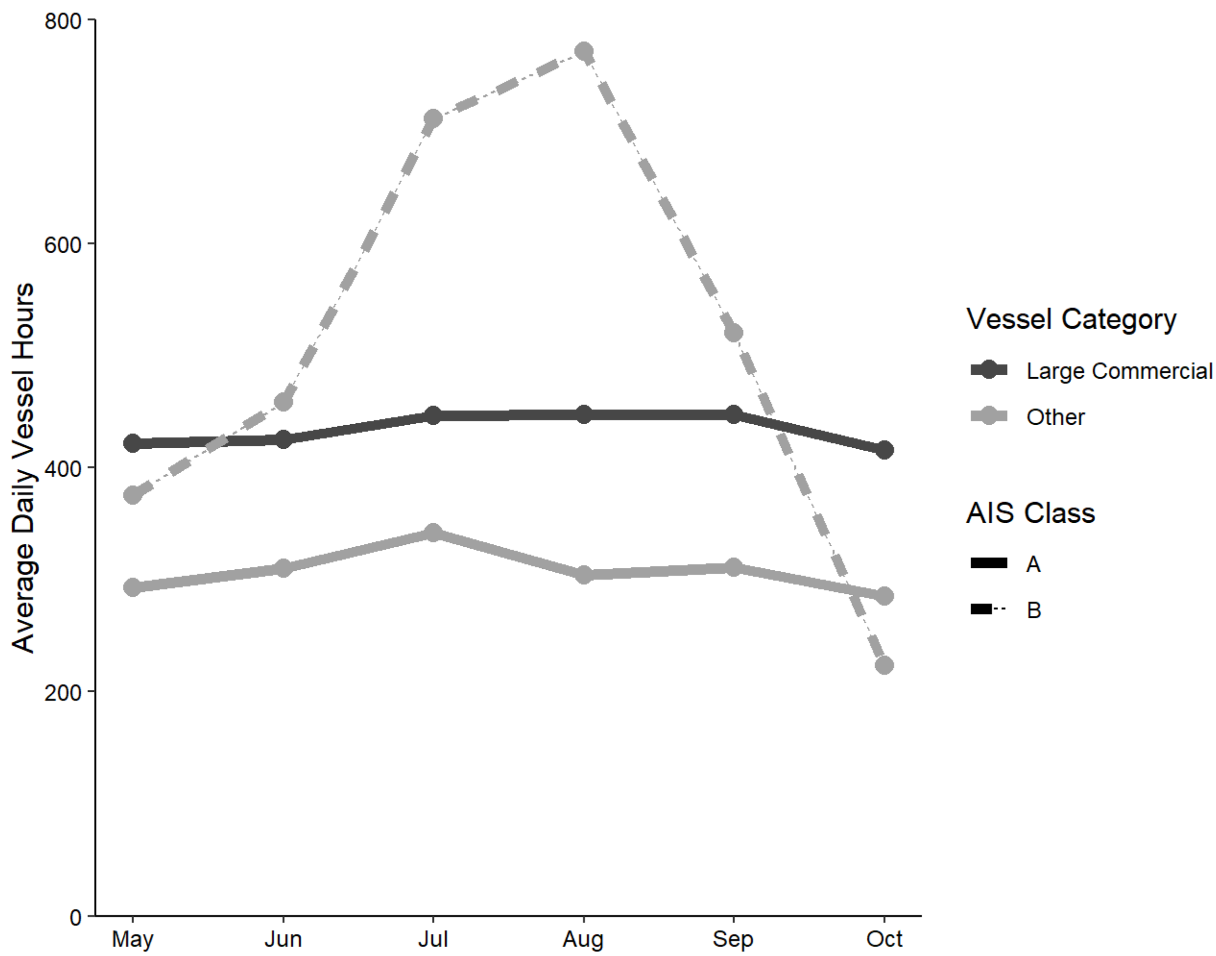

Figure 20: Average daily AIS vessel presence in the study area by month averaged across 2018-2020, for vessels making way (SOG > 1 knot). For large commercial vessels, AIS is generally mandatory, but for vessels labeled 'Other' it is not.

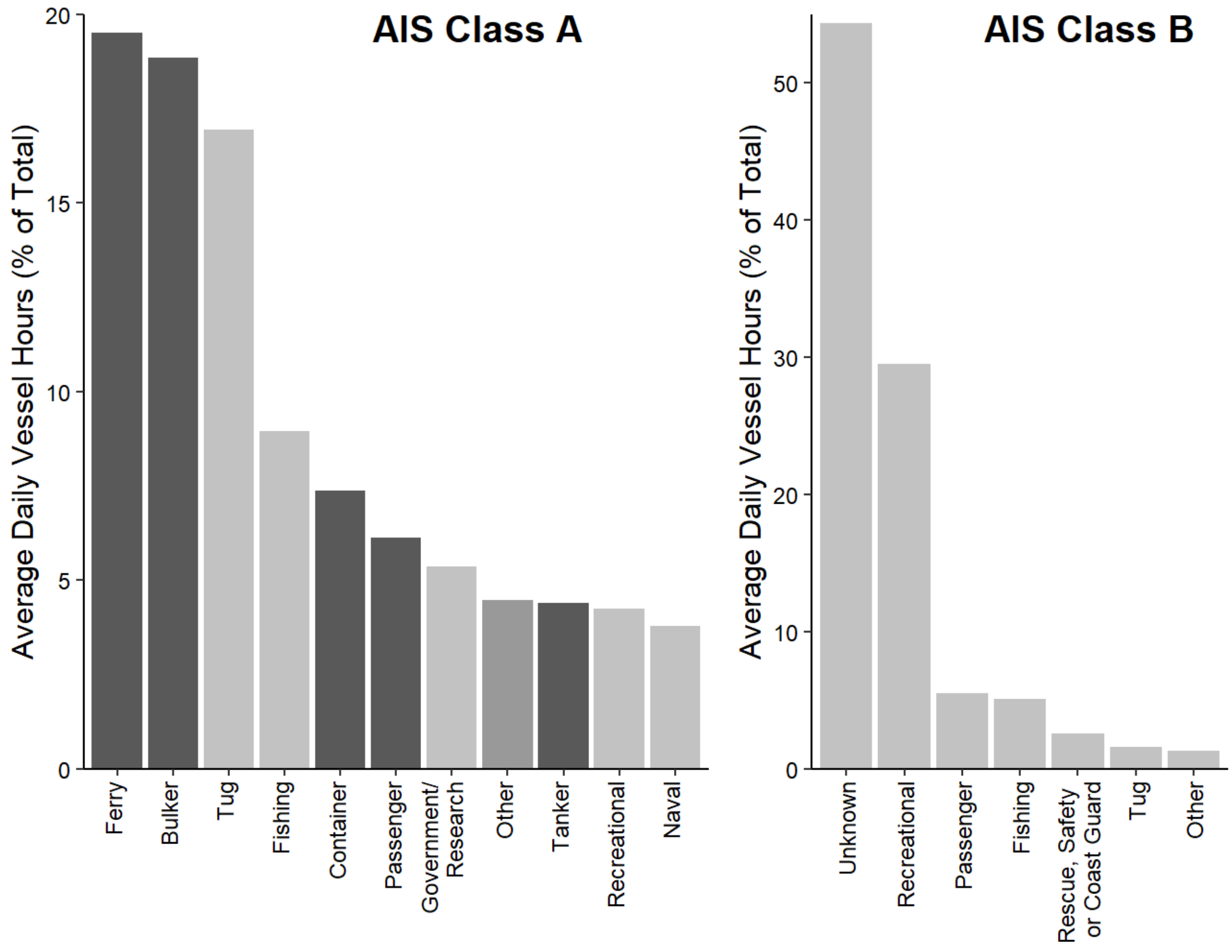

Figure 21: Relative composition of AIS Class A and AIS Class B vessel presence by type, in the study area, May through October, 2018-2020. AIS is generally mandatory for large commercial vessels (dark grey bars), but not for vessel types light grey bars. AIS Class A 'Other' vessels (mid-grey bar) represents large commercial vessels and other vessel types. The data were filtered to exclude vessels not making way (i.e. SOG < 1 knot). Only the top 10 Class A, and top 5 for Class B vessel types are shown, all others are represented as 'Other'.

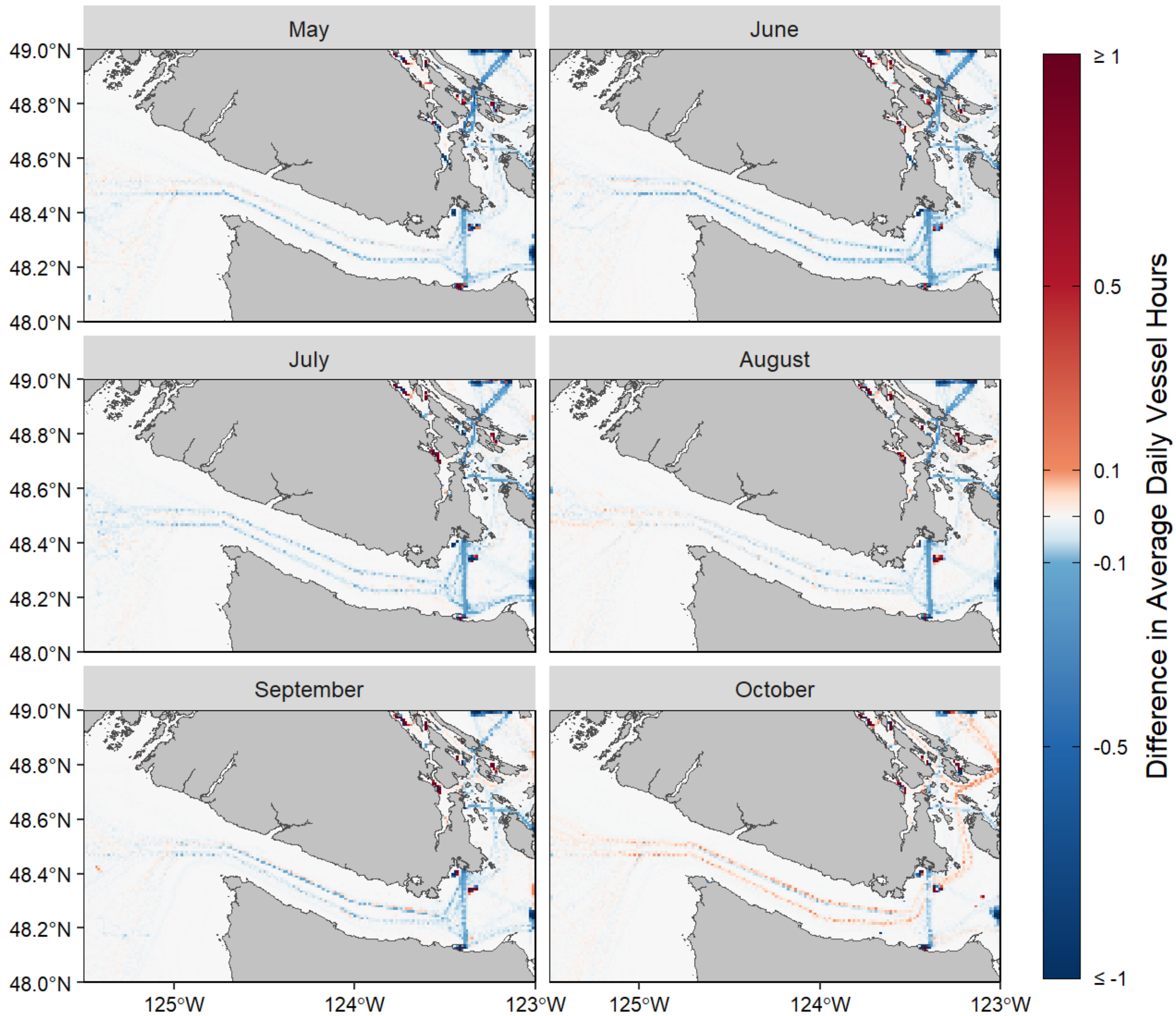

Figure 22: The change in average vessel presence (hours/day/km^2) of AIS Class A large commercial vessels in 2020 compared to values for 2018 and 2019, expressed as a relative deviation. This includes cargo vessels, tankers, ferries, and cruise ships.

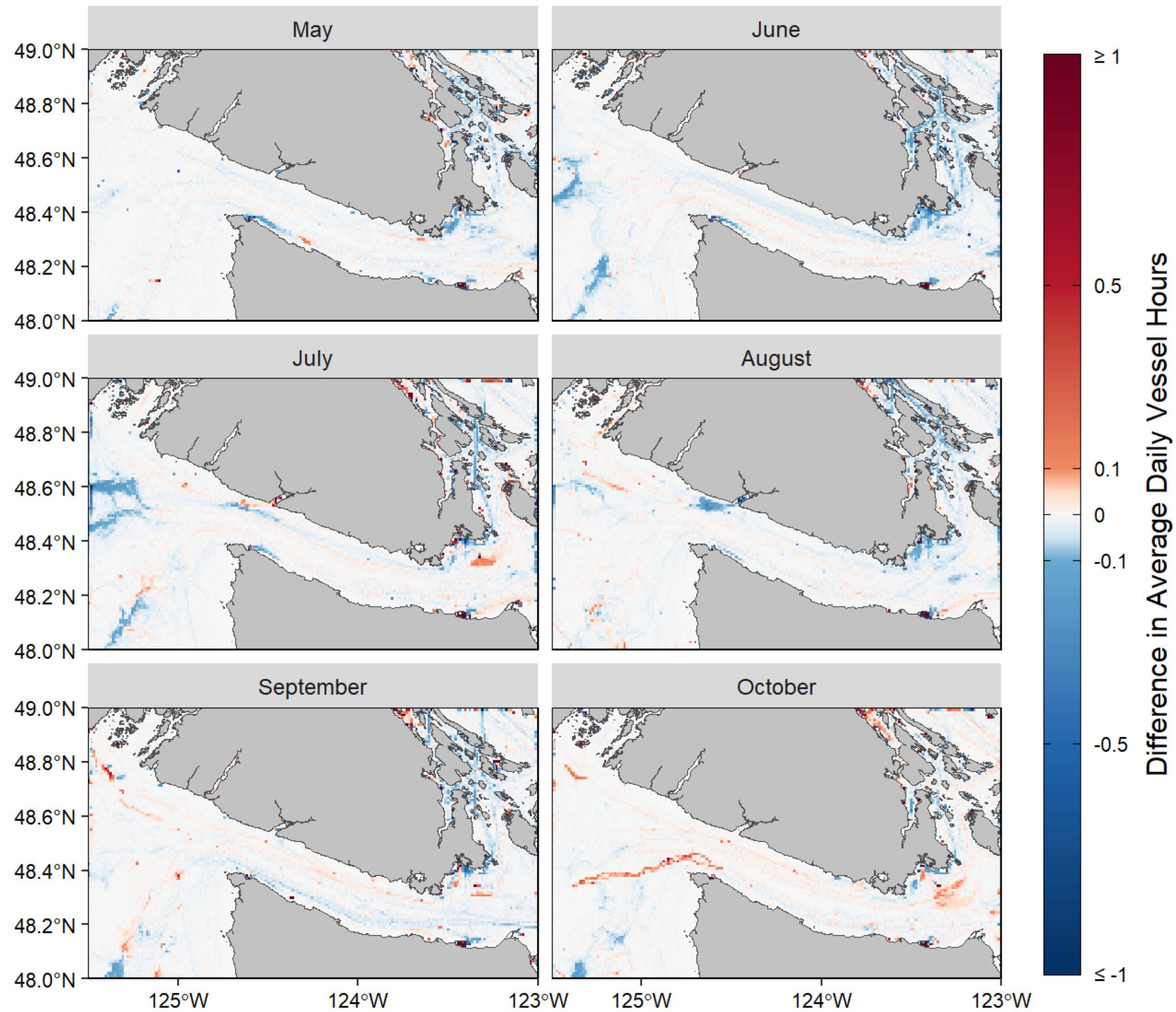

Figure 23: The change in average presence (hours/day/km^2) of AIS Class A (non-mandatory) small commercial and non-commercial vessels in 2020 compared to values for 2018 and 2019, expressed as a relative deviation. This includes tugs, fishing vessels, government/research vessels, vessels, naval vessels and other vessel types.

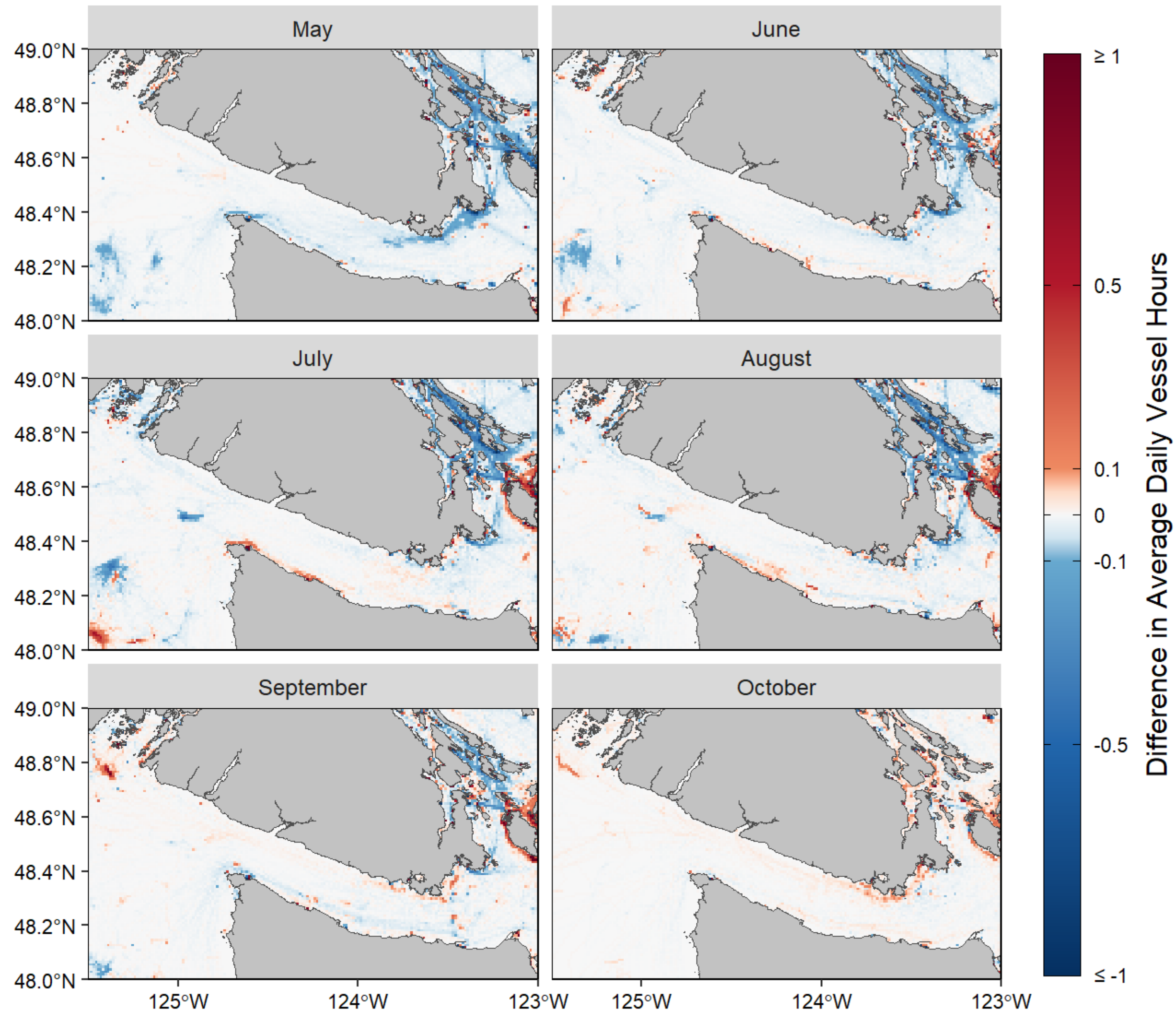

Figure 24: The change in daily presence (hours/day/km2) of AIS Class B vessels in 2020 compared to values for 2018 and 2019, expressed as a relative deviation. This includes recreational, small passenger, fishing vessels, and coast guard vessel, tugs and other vessel types.

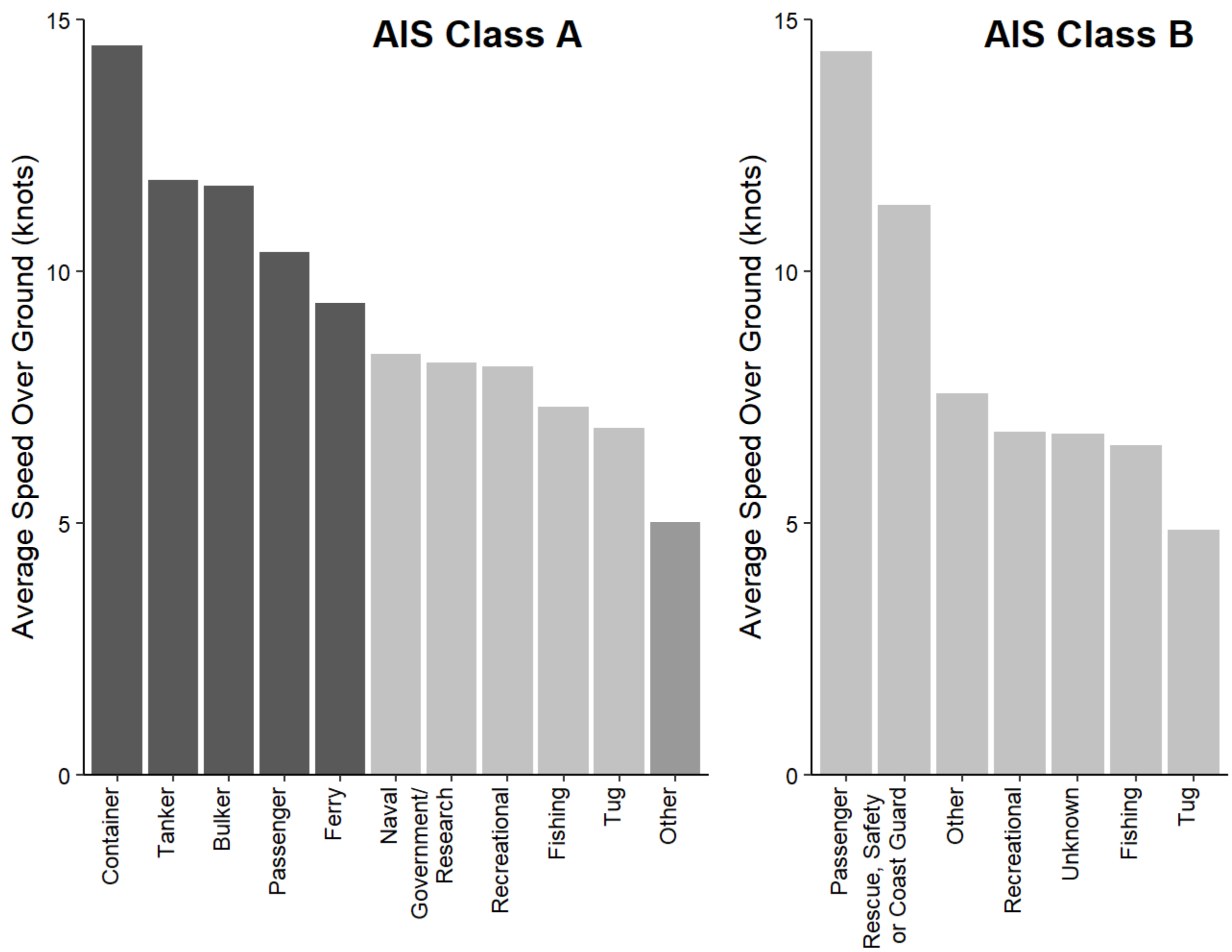

Figure 25: Average speed over ground (SOG) of AIS Class A and AIS Class B vessel presence by type in the study area, May through October, 2018-2020. AIS is generally mandatory for large commercial vessels (dark grey bars), but not for vessel types light grey bars. AIS Class A 'Other' vessels (mid-grey bar) represents large commercial vessels and other vessel types. The data were filtered to exclude vessels not making way (i.e. SOG < 1 knot). Only the top 10 Class A, and top 5 for Class B vessel types are shown, all others are represented as 'Other'.

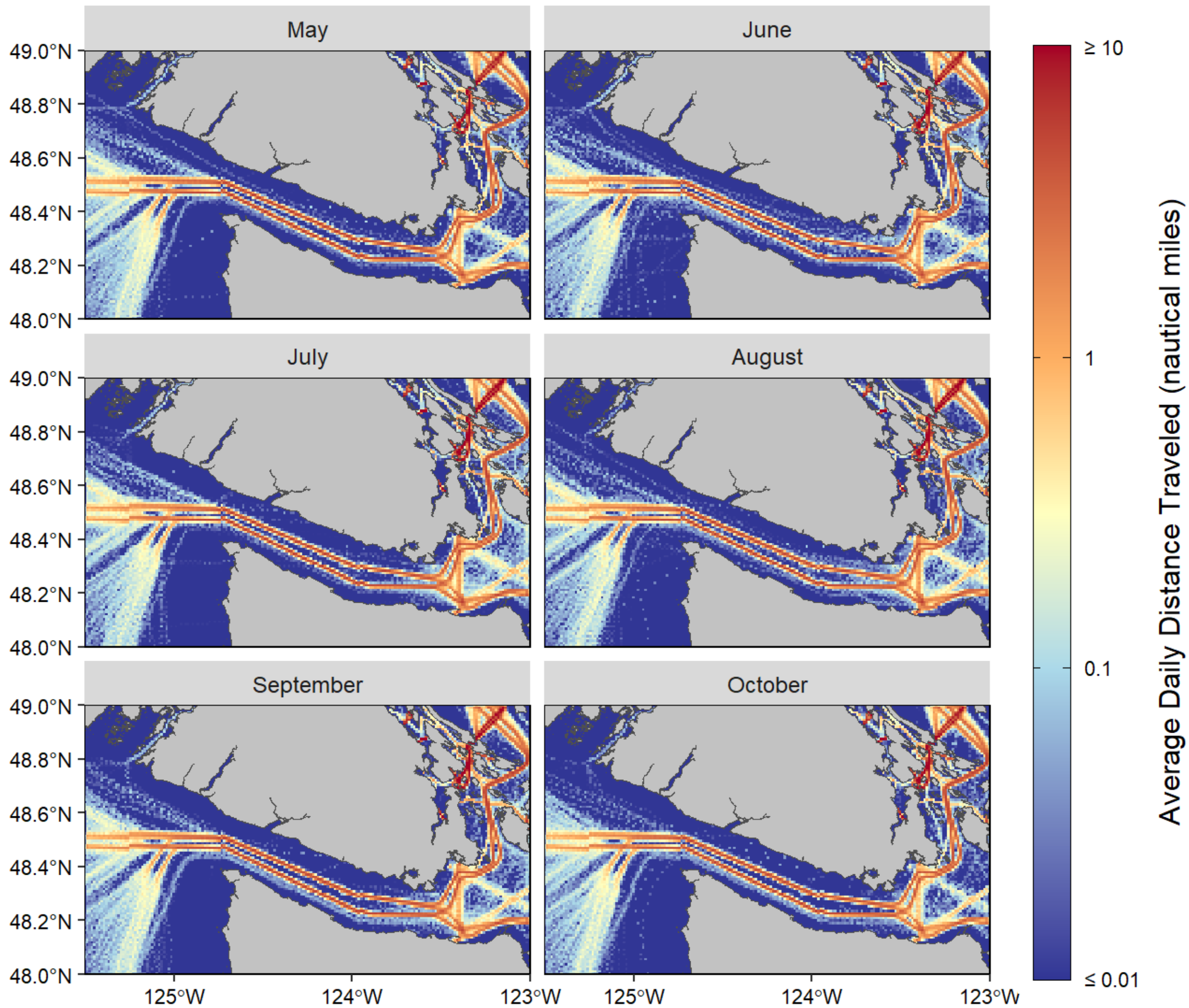

Figure 4: Average daily distance traveled by AIS Class A large commercial vessels in the Salish Sea, May through October, 2018-2020. This includes cargo vessels, tankers, ferries, and cruise ships. Distances were calculated from time and speed values.

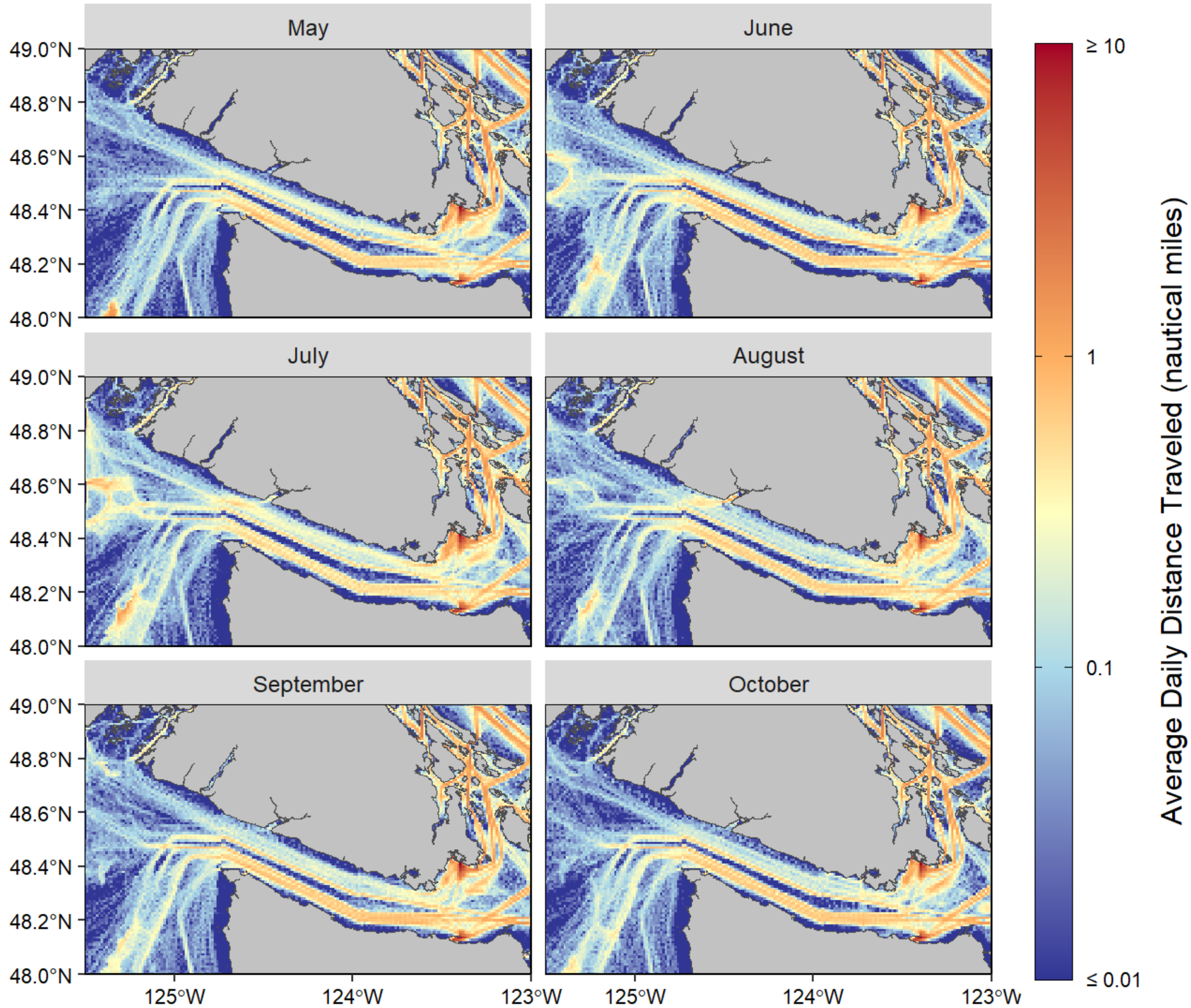

Figure 27: Average daily distance traveled by AIS Class A (non-mandatory) small commercial and non-commercial vessels in the Salish Sea, May through October, 2018-2020. This includes tugs, fishing vessels, government/research vessels, recreational vessels, naval vessels and other vessel types. These vessels are generally not required to carry AIS and so are incompletely captured here. Distances were calculated from time and speed values.

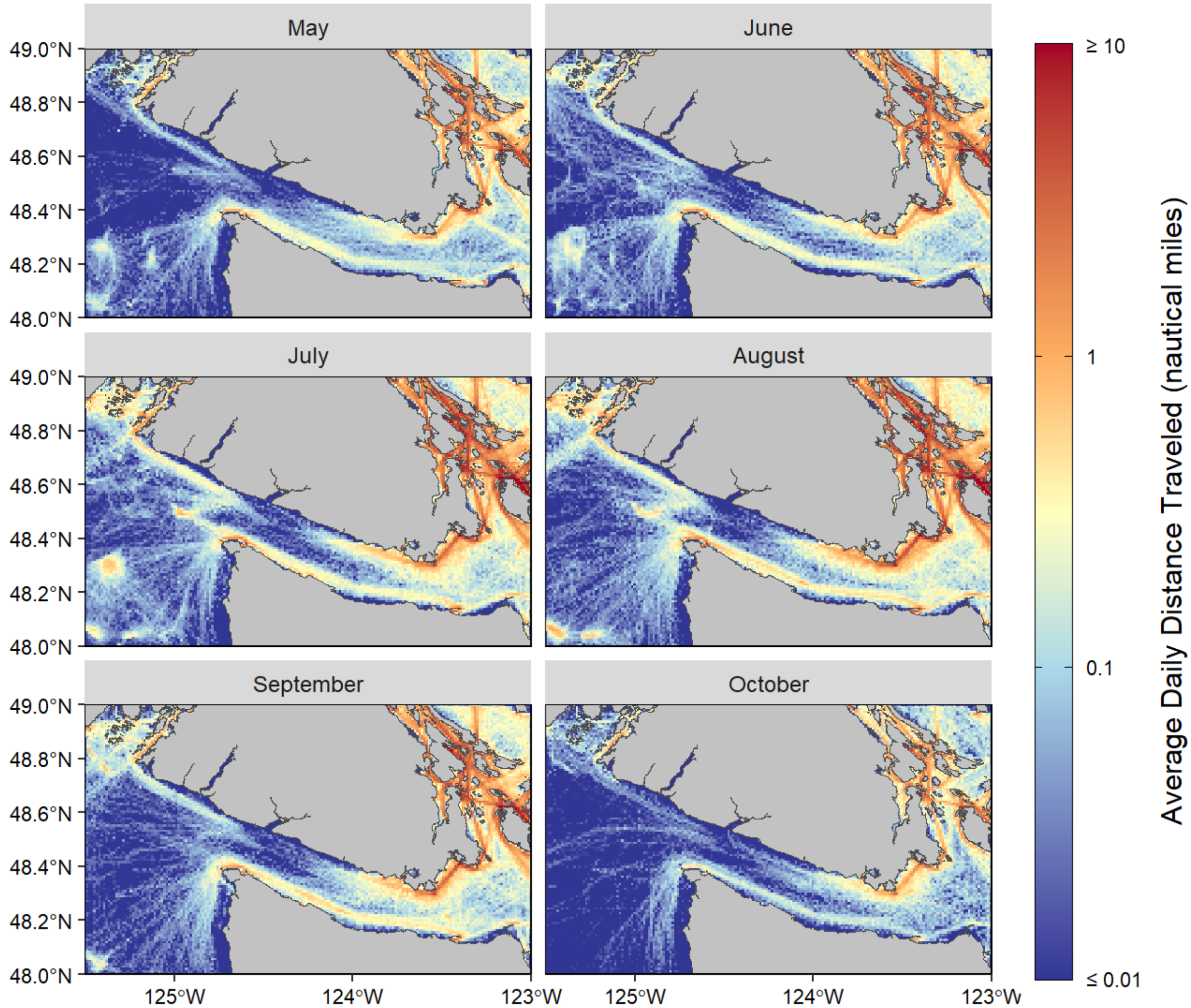

Figure 28: Average daily distance traveled by AIS Class B vessels in the Salish Sea, May through October, 2018-2020. This includes recreational, small passenger, fishing, and coast guard vessels, tugs and other vessel types. These vessels are generally not required to carry AIS and so are incompletely captured here. Distances were calculated from time and speed values.

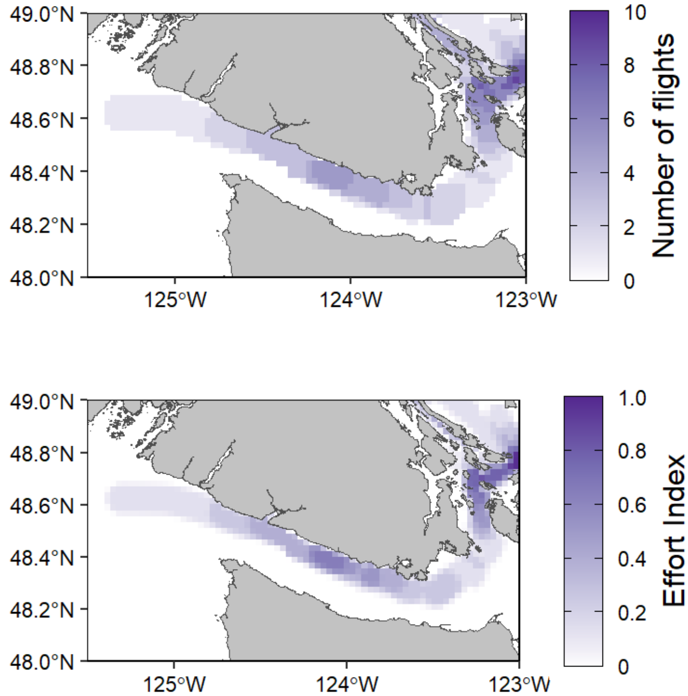

Figure 29: Survey coverage of National Aerial Surveillance Program flights in the study area, April through September, in 2015-2017. Adapted from Serra-Sogas et al., (2018).

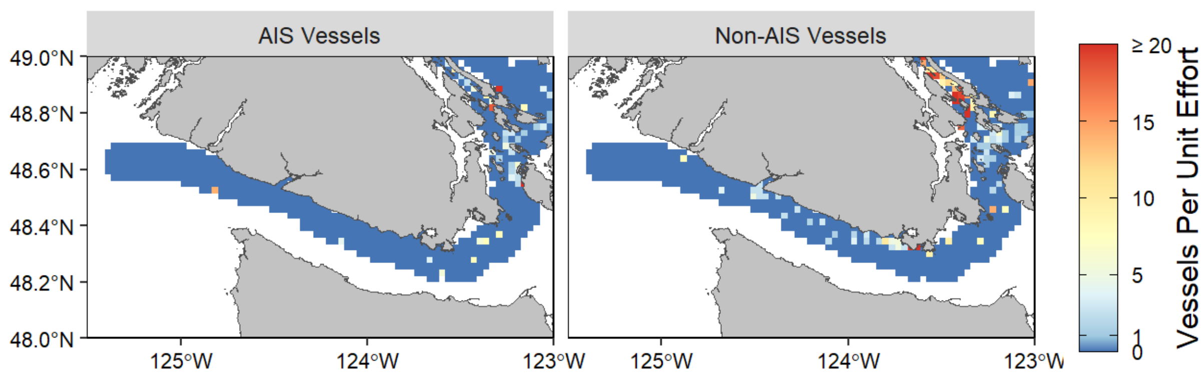

Figure 30: Vessel sightings per unit effort for National Aerial Surveillance Program flights in the study area, April through September, in 2015-2017. Vessels transmitting AIS (AIS Vessels, Left) and vessels not transmitting AIS (Non-AIS Vessels, Right) were mapped separately. Areas with no survey effort are shown in white. Data are from Serra-Sogas et al., (2018).

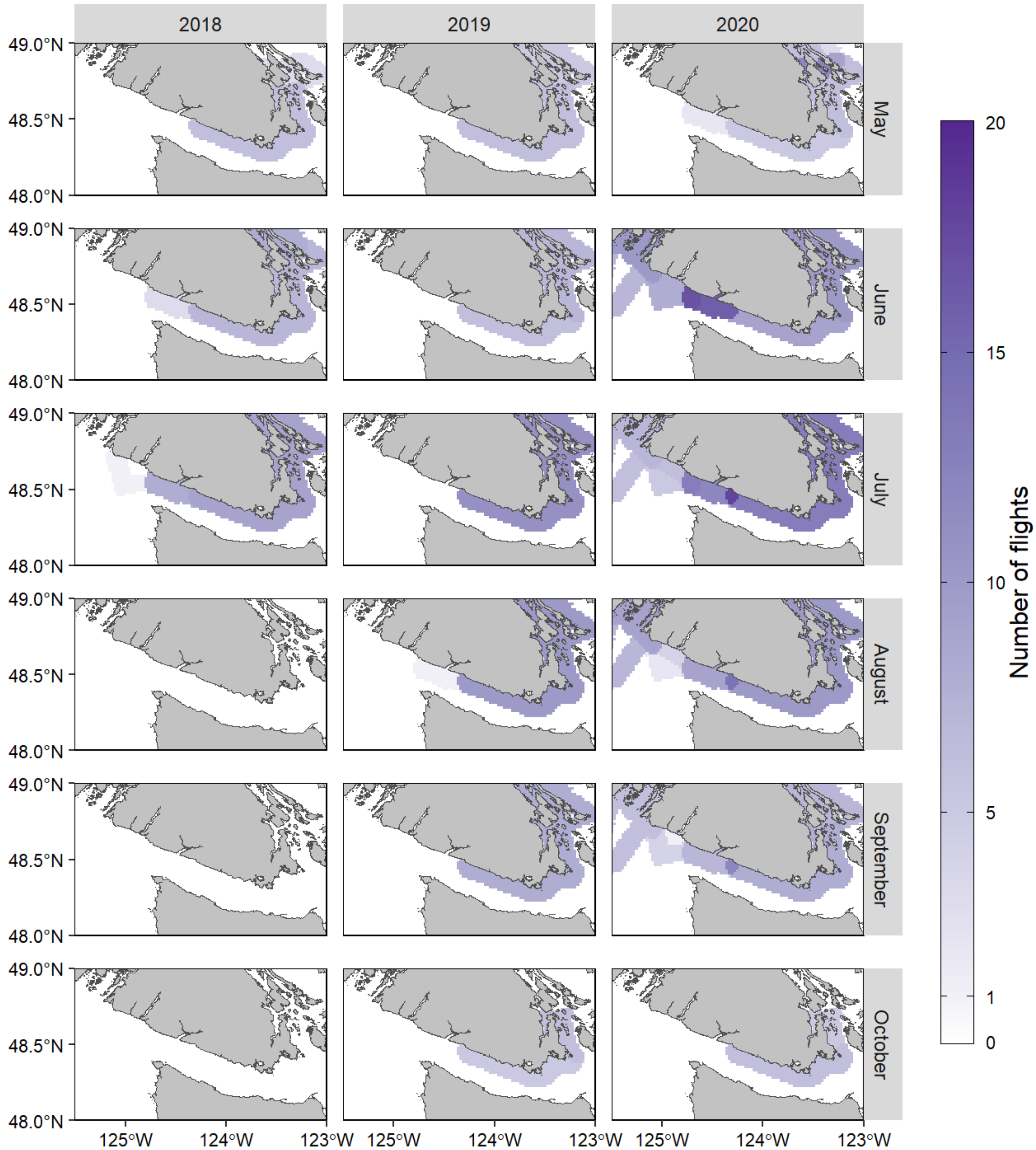

Figure 31: Approximated survey coverage of DFO Creel Survey overflights in the study area, May through October, in 2018-2020. Only flights for which vessel sightings have been digitized were included.

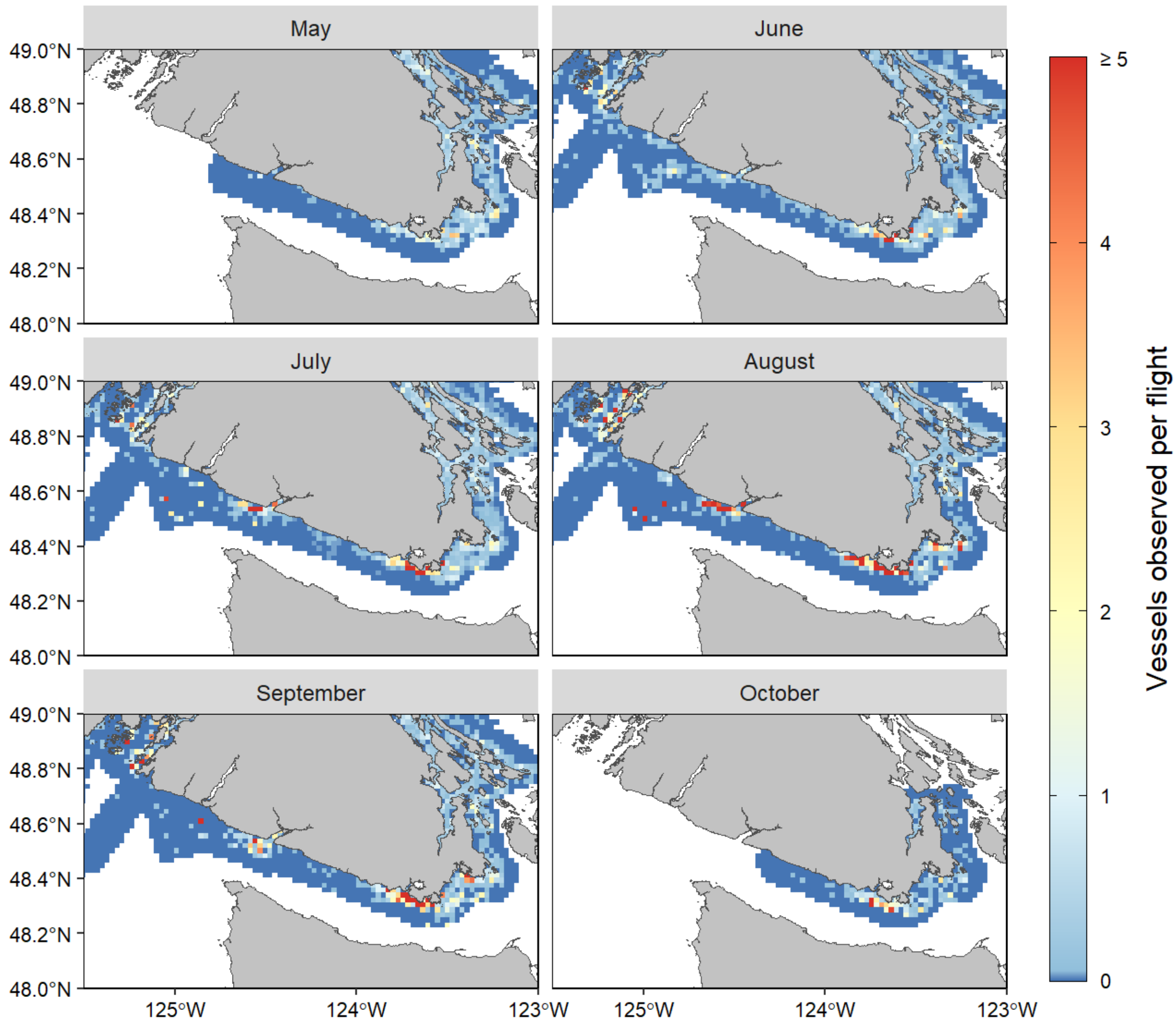

Figure 32: Average count of vessels observed per DFO Creel Survey overflight in the study area, May through October, in 2018-2020. Areas with no survey effort are shown in white.

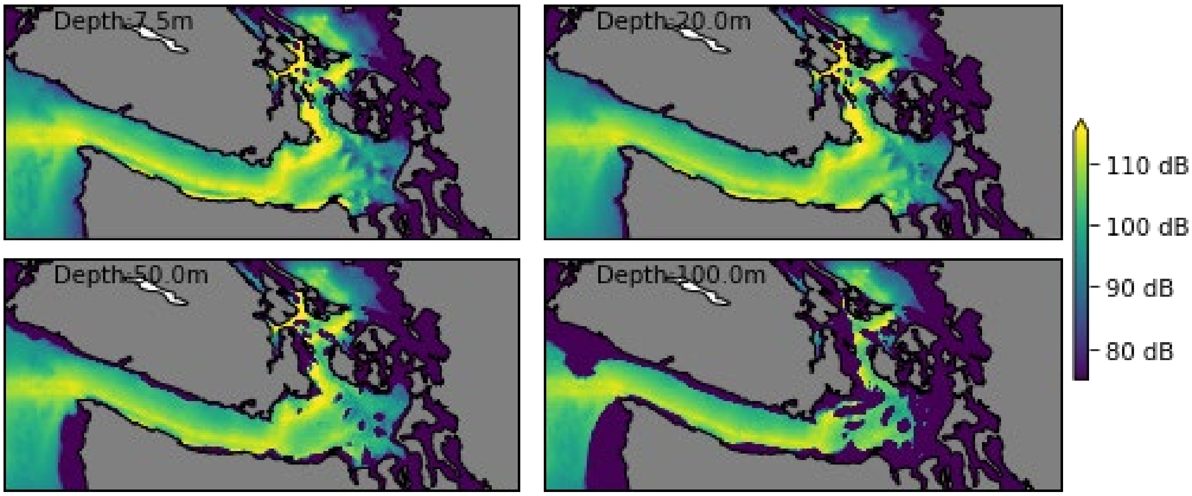

Figure 33: Example of vessel model output. The modelled SPL (95th percentile/L_5 exceedance level) values at 4 representative depths (7.5, 20, 50 and 100 m) for May 2018.

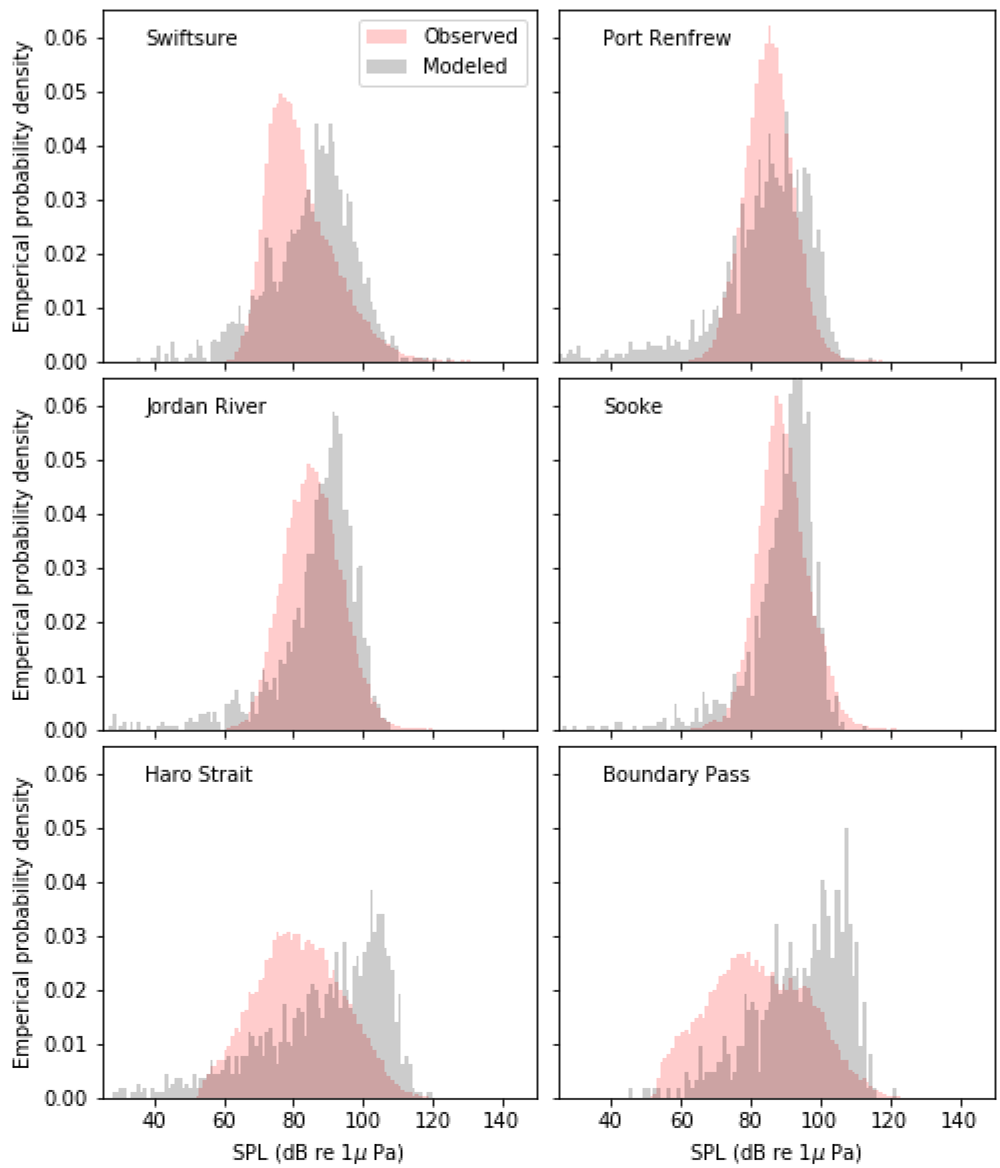

Figure 34: Comparison between the Empirical PDF of observed and simulated SPL at different mooring locations in the domain for the month of May 2018.

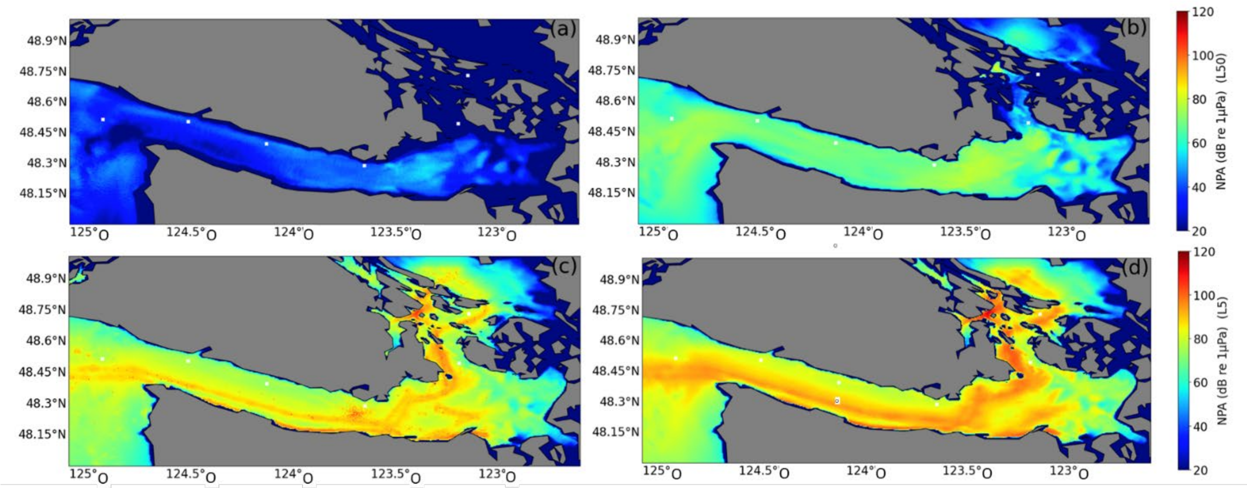

Figure 35: Vessel noise additions in the SRKW communication range (500 Hz to 15 kHz) for the L_{95} (a), L_{50} (b), L_{5} (c) exceedance levels and the arithmetic mean L_{eq} (d).

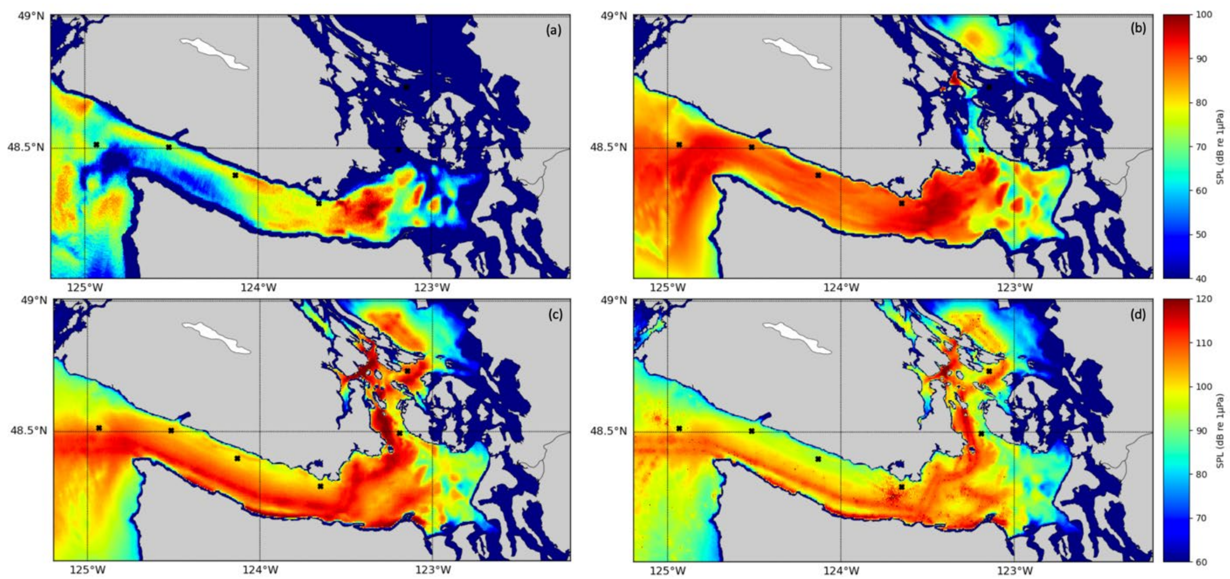

Figure 36: Vessel noise additions in the 50 kHz range for the L_{95} (a), L_{50} (b), L_{95} (c) exceedance levels and the arithmetic mean L_{eq} (d).

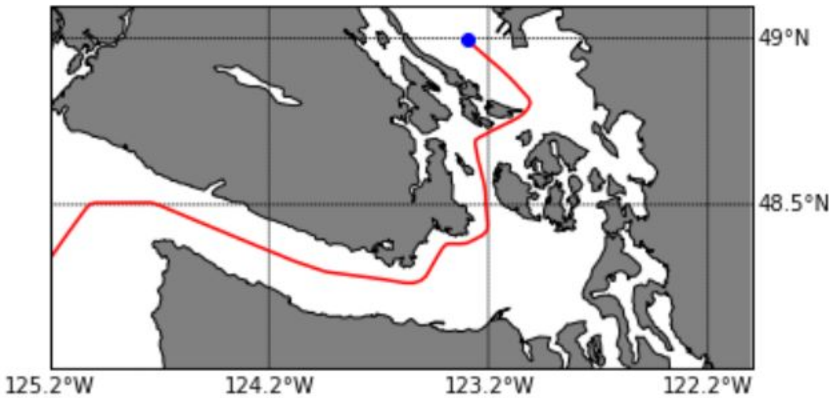

Figure 37: Track of additional (outgoing) TMX tankers. Starting point is marked with a blue circle.

8. REFERENCES CITED

Aarsæther, K.G., Moan, T. 2009. Estimating navigation patterns from AIS. Journal of Navigation. 62: 587–607.

Amitai, E., Nystuen, J.A., Anagnostou, E.N., Anagnostou, M.N. 2007. Comparison of deep underwater measurements and radar observations of rainfall. IEEE Geoscience and Remote Sensing Letters 4(3): 406–410.

Andrew, R.K., Howe, B.M., Mercer, J.A., Dzieciuch, M.A. 2002. Ocean ambient sound: comparing the 1960s with the 1990s for a receiver off the California coast. Acoustic Research Letters Online 3(2): 65–70.

Arveson, P.T. and Vendittis, D.J. 2000. Radiated noise characteristics of a modern cargo ship, Journal of the Acoustical Society of America 107: 118.

Au, W.W.L., Ford, J.K.B., Horne, J.K., Newman Allman, K.A. 2004. Echolocation signals of free-ranging killer whales (*Orcinus orca*) and modeling of foraging for chinook salmon (*Oncorhynchus tshawytscha*). Journal of the Acoustical Society of America 115, 901-909.

Aulanier, F., Simard, Y., Roy, N., Garvaise, C., Bander, M. 2017. Effects of shipping on marine acoustic habitats in Canadian Arctic estimated via probabilistic modeling and mapping. Marine Pollution Bulletin 125: 115–131.

Badino, A., Borelli, D., Gaggero, T., Rizzuto, E., Schenone, C. 2012. Noise emitted from ships: Impact inside and out- side the vessels. Proceedings of the Society of Behavioural Science 48:868–879.

Baird, R.W., Hanson, M.B., Ashe, E.E., Heithaus, M.R., Marshall, G.J. 2003. Studies of Foraging in ''Southern Resident'' Killer Whales During July 2002: Dive depths, bursts in speed, and the use of a ''crittercam'' system for examining sub- surface behavior (Report Order Number AB133F-02-SE-1744). National Marine Fisheries Service, National Marine Mammal Laboratory, Seattle, WA, p. 17. Available from: Cascadia Research, 218 1/2 W 4th Ave., Olympia, WA 98501.

Baird, R.W., Hanson, M.B., Dill, L.M. 2005. Factors influencing the diving behaviour of fish eating killer whales: sex differences and diel and interannual variation in diving rates. Canadian Journal of Zoology 83(2): 257–267.

Bates, A.E., Primack, R.B., Moraga, P., Duarte, C.M. 2020. COVID-19 pandemic and associated lockdown as a 'Global Human Confinement Experiment' to investigate biodiversity conservation. Biological Conservation 248:108665.

Branstetter, B., St. Leger, J., Acton, D., Stewart, J., Houser, D., Finneran, J.J., Jenkins, K. 2017. Killer whale (*Orcinus orca*) behavioral audiograms. Journal of the Acoustical Society of America 141: 2387.

Buckland,S. T., Anderson, D. R., Burnham, K. P., Laake, J. L., Borchers, D. L., Thomas, L. 2001. Introduction to distance sampling estimating abundance of biological populations. Oxford University Press, New York, NY, p. 432.

Burnham, R.E., Vagle, S., O'Neill, C. 2021. Spatiotemporal patterns in the natural and anthropogenic addtions to the soundscape in parts of the Salish Sea, British Columbia, 2018-2020. Marine Pollution Bulletin 170, 112647.

Carey, W.M., Fitzgerald, J.W., Monahan, E.C., Wang, Q. 1993. Measurement of the sound produced by a tipping trough with fresh and salt water. Journal of the Acoustical Society of America 93: 3178–3192.

Chapman, N.R., Price, A. 2011. Low frequency deep ocean ambient noise trend in the Northeast Pacific Ocean. Journal of the Acoustical Society of America 129, EL161–EL165.

Christiansen, F. Lusseau, D. 2014. Understanding the ecological effects of whale-watching on cetaceans. In: Whale-watching: Sustainable tourism and ecological management. J. Higham, L. Bejder, R. Williams, R. (Eds.), New York: Cambridge University Press. pp. 177–192.

Christiansen, F., Rasmussen, M., Lusseau, D. 2013. Whale watching disrupts feeding activities of minke whales on a feeding ground. Marine Ecological Progress Series 478: 239–251.

Coers, A., Bouton, N., Vincourt, D., Slaabbekoorn, H. 2008. Fluctuating noise conditions may limit acoustic communication distance in rock-pool blenny. Bioacoustics 17: 63–64.

Collins, M.D., 1993. A split-step Padé solution for the parabolic equation method Journal of the Acoustical Society of America 93: 1736–1742.

Cominelli, S., Devillers, R., Yurk, H., MacGillivray, A., McWhinnie, L., Canessa, R. 2018. Noise exposure from commercial shipping for the southern resident killer whale population. Marine Pollution Bulletin 136: 177–200.

COSEWIC 2001. COSEWIC assessment and update status report on the killer whale *Orcinus orca* in Canada. Committee on the status of endangered wildlife in Canada. Ottawa. 47 pp.

Dahlheim, M., Castellote, M. 2016. Changes in the acoustic behavior of gray whales (*Eschrichtius robustus*) in response to noise. Endangered Species Research 31: 227–242.

Dahlheim, M. E., Fisher, H. D. Schempp, J. D. (1984). Sound production by the gray whale and ambient noise levels in Laguna San Ignacio, Baja California Sue, Mexico. In: The gray whale, *Eschrichtius robustus*. M. L., Jones, S. L. Swartz, S. Leatherwood (Eds.), San Diego, California: Academic Press pp. 543–559.

DFO. 2017a. Identification of Habitats of Special Importance to Resident Killer Whales (*Orcinus orca*) off the West Coast of Canada. DFO Can. Sci. Advis. Sec. Sci. Advis. Rep. 2017/011.

DFO. 2017b. Evaluation of the scientific evidence to inform the probability of effectiveness of mitigation measures in reducing shipping-related noise levels by southern resident killer whales. DFO Can. Sci. Advis. Sec. Sci. Advis. Rep. 2017/041.

Erbe, C., MacGillivray, A., Williams, R. 2012. Mapping cumulative noise from shipping to inform marine spatial planning. Journal of the Acoustical Society of America. 132: EL423–EL428.

Erbe, C., Reichmuth, C., Cunningham, K., Lucke, K., Dooling, R. 2016. Communication masking in marine mammals: A review and research strategy. Marine Pollution Bulletin 103, 15–38.

Farina, A. 2014. Soundscape Ecology, Principles, Patterns, Methods and Applications. Dordrecht: Springer Science and Business Media.

Fisheries and Oceans Canada. 2018. Recovery Strategy for the Northern and Southern Resident Killer Whales (*Orcinus orca*) in Canada. Species at Risk Act Recovery Strategy Series, Fisheries & Oceans Canada. Ottawa, x + 84 pp.

Ford, J.K.B. 1989. Acoustic behaviour of resident killer whales (*Orcinus orca*) off Vancouver Island, British Columbia. Canadian Journal of Zoology, 67: 727–745.

Francois, R.E., and Garrison, G.R. 1982. Sound absorption based on ocean measurements. Part II: boric acid contribution and equation for total absorption. Journal of the Acoustical Society of America 72: 1879−1890.

Frisk, G.V. 2012. Noiseonomics: The relationship between ambient noise levels in the sea and global economic trends. Science Reports 2: 1–4.

Government of Canada. 2019. Regulations Amending the Navigation Safety Regulations (Automatic Identification Systems). SOR/2019-100.

Government of Canada. 2020. Navigation Safety Regulations. SOR/2020-216.

Gray L.M., and. Greeley, D.S. 1980. Source level model for propeller blade rate radiation for the world's merchant fleet. Journal of the Acoustical Society of America 67: 516–522

Haggarty, D., Gregr, E., Lessard, J., Fields, C., Davies, S. 2018. Deep substrate (100 m) for the Pacific Canadian Shelf. Published Sept 16, 2018. Data Distributor: J. Lessard, Fisheries and Oceans Canada, Nanaimo, BC.

Hamilton, E.L. 1980. Geoacoustic modeling of the sea floor. Journal of the Acoustical Society of America 65: 1313–1340.

Haugerud, R.A. 1999. Digital elevation model (DEM) of Cascadia, latitude 39N-53N, longitude 116W-133W. U.S. Geological Survey Open-File Report 99–369.

Hauser, D.D., Logsdon, M.G., Holmes, E.E., VanBlaricom, G.R., Osborne, R.W. 2007. Summer distribution patterns of southern resident killer whales *Orcinus orca*: core areas and spatial segregation of social groups. Marine Ecological Progress Series 351: 301.

Heise, K.A., Barrett-Lennard, L.G., Chapman, N.R., Dakin, D.T., Erbe, C., Hannay, D.E., Merchant, N.D., Pilkington, J.S., Thornton, S.J., Tollit, D.J., Vagle, S., Veirs, V.R., Vergara, V., Wood, J.D., Wright, B.M., Yurk, H. 2017. Proposed Metrics for the Management of Underwater Noise for Southern Resident Killer Whales. Coastal Ocean Report Series (2), Ocean Wise. Vancouver. 30 pp.

Hemmera Environchem Inc., SMRU Canada, Jasco Applied Sciences Canada. 2014. Roberts Bank Terminal 2, underwater noise and ship sound signature analysis study. Technical Data Report Prepared for Port Metro Vancouver (302-042.02), 154 pp.

Hijmans R.J. 2020. raster: Geographic Data Analysis and Modeling. R package version 3.1-5.

Hildebrand, J. 2009. Anthropogenic and natural sources of ambient noise in the ocean. Marine Ecological Progress Series 395: 5–20.

Holt, M.M., Noren, D.P., Veirs, V., Emmons, C.K., Veirs, S. 2009. Speaking up: Killer whales (*Orcinus orca*) increase their call amplitude in response to vessel noise. Journal of the Acoustical Society of America 125, EL27–EL32.

Jasny, M. 2005. Sounding the Depths. II: The rising toll of sonar, shipping and industrial ocean noise on marine life. Washington, DC: Natural Resource Defence Council.

Jensen, F.B., Porter, M.B., Kuperman, W.A., and Schmidt, H. 2011. Computational Ocean Acoustics. Springer, New York.

Jensen, F.H., Johnson, M., Ladegaard, M., Wisniewska, D.M., Madsen, P.T. 2018. Narrow acoustic field of view drives frequency scaling in toothed whale biosonar. Current Biology, 28: 3878–3885.

Ketten, D.R. 2002. Marine Mammal Auditory Sysytems: A summary of audiometric and anatomical data and implications for underwater acoustic impacts. Polarforshung 72: 79–92.

Knudsen, V.O., Alford R. S., Emling J.W. 1948. Underwater ambient noise. Journal of Marine Research (3): 410–429.

Konrad, C.M. 2020. Analysis of Automatic Identification System (AIS) data for the Eastern Shore Islands, Nova Scotia, 2017-2018. Can. Manuscr. Rep. Fish. Aquat. Sci. 3172: vi + 39 p.

Koski, K., Osborne, R., Tallmon, R. 2006. Soundwatch Public Outreach/Boater Education Project 2004–2005 Final Program Report, NMFS Contract No. AB133F-04-SE-0835 (Report No. NFFP 5000-4-00026), p. 25. The Whale Museum, Friday Harbor, WA. Available from: The Whale Museum, PO Box 945, Friday Harbor, WA 98250.

Ladich, F. 2013. Effects of noise on sound detection and acoustic communication in fishes. In Animal Communication and Noise. H. Brumm (Ed.) Berlin, Heidelberg: Springer Verlag, pp. 65–90.

Lammers, M.O., Au, W.W.L., Aubauer, R., Nachtigall, P.E. 2004. A comparative analysis of the pulsed emissions of free-ranging Hawaiian spinner dolphins (*Stenella longirostris*). In J.A. Thomas, C.F. Moss, M.Vater (Eds.), Echolocation in bats and dolphins. Chicago: The Unoversity of Chicago Press, pp. 414-419.

Lidtke, A.K., Humphrey, V.F., Turnock, S.R. 2016. Feasibility study into a computational approach for marine propeller noise and cavitation modelling. Ocean Engineering 120 : 152–159.

Lugli, M. 2010. Sounds of shallow water fishes pitch within the quiet window of the habitat ambient noise. Journal of Comparative Psychology A. 196: 439–451.

Ma, B.B., Nystuen, J.A. 2005. Passive Acoustic Detection and Measurement of Rainfall at Sea. Journal of Atmospheric and Oceanic Technology 22: 1225–1248.

Ma, B.B., Nystuen, J.A., Lien, R.-C. 2005. Prediction of underwater sound levels from rain and wind. Journal of the Acoustical Society of America 117: 3555–3565.

MacGillivray, A., Wood, M., Li, Z., Allen, A., Hannay, D. 2016. Regional ocean noise contributors analysis: Enhancing cetacean habitat and observation program. Document 01195, Version 3.0. Technical report by JASCO Applied Sciences for Vancouver Fraser Port Authority.

MacGillivray, A.M., Li, A. 2018. Vessel noise measurements from the ECHO slowdown trial: Final report. Document 01518, Version 3.0. Technical report by JASCO Applied Sciences for Vancouver Fraser Port Authority ECHO Program. Victoria, BC: JASCO Applied Sciences.

Madsen, P.T., Johnson, M., de Soto, N.A., Zimmer, W.A., Tyack, P. 2005. Biosonar performance of foraging beaked whales (*Mesoplodon densirostris*). Journal of Experimental Biology, 208: 181–194.

McGillivary, P. A., Schwehr, K. D., Fall, K. 2009. Enhancing AIS to improve whale-ship collision avoidance and maritime security. In: Proceedings of the OCEANS 2009, MTS/IEEE Biloxi - Marine Technology for Our Future: Global and Local Challenges, Biloxi, MS, 1–8.

McDonald, M.A., Hildebrand, J.A., Wiggins, S.M. 2006. Increases in deep ocean ambient noise in the Northeast Pacific west of San Nicolas Island, California. Journal of the Acoustical Society of America 120:711–718.

McDougall, T.J., Barker, P.M. 2011. Getting started with TEOS-10 and the Gibbs Seawater (GSW) oceanographic toolbox. In: SCOR/IAPSO WG127, p. 28 pp.

McKenna, M.F., Wiggins, S.M., Hildebrand, J.A. 2013. Relationship between container ship underwater noise levels and ship design, operational and oceanographic conditions. Science Reports 3:1760.

Medwin, H., Kurgan, A., Nystuen, J.A. 1990. Impact and bubble sound from raindrops at normal and oblique incidence. Journal of the Acoustical Society of America 88: 413–418.

Medwin, H., Nystuen, J.A., Jacobus, P.W., Ostwald, L.H., Snyder, D.E. 1992. The anatomy of underwater rain noise. Journal of the Acoustical Society of America 92: 1613–1623.

Merchant, N.D., Witt. M.J., Blondel, P., Godley, B.J., Smith, G.H. 2012. Assessing sound exposure from shipping in coastal waters using a single hydrophone and Automatic Identification System (AIS) data. Marine Pollution Bulletin 64: 132–139.

Merchant, N.D., Pirotta, E., Barton, T.R., Thompson, P.M, 2014. Monitoring ship noise to assess the impact of coastal developments on marine mammals. Marine Pollution Bulletin 78: 85–95.

Merchant, N.D., Fristrup, K.M., Johnson, M.P., Tyack, P.L., Witt, M.J., Blondel, P. Parks, S.E. 2015. Measuring acoustic habitats. Methods in Ecology and Evolution 6: 257–265.

Miller, P.J.O. 2002. Mixed-directionality of killer whale stereotyped calls: a direction of movement cue? Behavioral Ecology and Sociobiology 52(3): 262–270.

Miller, P.J.O. 2006. Diversity in sound pressure levels and estimated active space of resident killer whale vocalizations. Journal of Comparative Physiology A-Neuroethology Sensory Neural and Behavioral Physiology 192(5): 449–459.

Miller, P.J., Tyack, P.L. 1998. A small towed beamform array to identify vocalizing resident killer wales (*Orcinus orca*) concurrent with focal behavioural observations. Deep Sea Research II 45: 1389-1405.

Morete, M.E., Bisi, T.L., Rosso, S. 2007. Mother and calf humpback whale responses to vessels around the Abrolhos Archipelago, Bahia, Brazil. Journal of Cetacean Research and Management 9:241–248.

Morisaka, T., Karczmarski, L., Akamatsu, ., Sakai, M., Dawson, S., Thornton, M. 2011. Echolocation signals of Heaviside's dolphins (*Cephalorhynchus heavisidii*). Journal of the Acoustical Society of America 129: 449–457.

National Research Council, NRC. 2005. Marine Mammal Populations and Ocean Noise: Determining when noise causes biologically significant effects. Washington, DC: The National Academies Press.

Notarbartolo di Sciara, G. and Gordon, J. 1997. Bioacoustics: A tool for the conservation of cetaceans in the Mediterranean Sea. Marine and Freshwater Behaviour and Physiology, 30 (2): 125–146.

Nystuen, J.A. 1986. Rainfall measurements using underwater ambient noise. Journal of the Acoustical Society of America 79(4): 972–982.

Nystuen, J.A. 1993. An explanation of the sound generated in light in the presence of wind. In: Natural Physical Sources of Underwater Sound. B. R. Kerman (Ed.), Kluwer Academic Publishers, Boston, pp. 659–668.

Nystuen, J.A. 1996. Acoustic rainfall analysis: Rainfall drop size distribution using the underwater sound field. Journal of Atmospheric and Oceanic Technology 13, 74–84.

Nystuen, J.A., Ma, B. 2002. Using ambient sound to passively monitor sea surface processes. Proceedings of the Sixth Pan Ocean Remote Sensing Conference (PORSEC), B. P. Pasaribu, R. Kaswadji, I.W. Nurjava, J.L. Gaol (Eds.) PORSEC Association, 9–14.

Nystuen, J.A., Moore, S.E., Stabeno, P.J. 2010. A sound budget for the southeastern Bering Sea: measuring wind, rainfall, shipping, and other sources of underwater sound. Journal of the Acoustical Society of America 128: 58−65.

Olson, J.K., Wood, J., Osborne, R.W., Barrett-Lennard, L., Larson, S. 2018. Sightings of southern resident killer whales in the Salish Sea 1976−2014: The importance of a long-term opportunistic dataset. Endangered Species Research 37:105–118.

Pebesma, E. 2018. Simple Features for R: Standardized Support for Spatial Vector Data. The R Journal 10 (1): 439–446.

Pensieri, S. Bozzano, R., Nystuen, J.A, Anagnostou, E.N, Anagnostou, M. N., Bechini, R. 2015 Underwater acoustic measurements to estimate wind and rainfall in the Mediterranean Sea Advanced Meteorology 2015: 612512.

Pijanowski, B.C., Villanueva-Rivera, L.J., Dumyahn, S.L., Farina, A., Krause, B.L., Napoletano, B.M., Gage, S.H., Pieretti, N. 2011. Soundscape Ecology: The science of sound in the landscape. BioSciences 61(3): 203-216.

Pine, M.K., Jeffs, A.G., Wang, D., Radford, C.A. 2016. The potential for vessel noise to mask biologically important sounds within ecologically significant embayments. Ocean and Coastal Management 127: 63–73.

Quartly, G.D., Guymer, T.H., Birch, K.G., Smithers, J., Goy, K., Waddington, I. 2000. Listening for rain: theory and practice. In: Proceedings of the 5th European Conference on Underwater Acoustics, Lyon, France. pp. 723–728.

R Core Team. 2019. R: A language and environment for statistical computing. R Foundation for Statistical Computing, Vienna, Austria.

Raverty, S. St. Leger, J., Noren, D.P., Burek Huntington, K., Rotstein D.S., Gulland, F.M.D. Ford, J.K.B., Hanson, B., Lambourn, D.M., Huggins, J., Delaney, M.A., Spaven, L., Rowles, T., Gaydos, J.K. 2020 Pathology findings and correlations with body condition index in stranded killer whales (*Orcinus orca*) in the northeastern Pacific and Hawaii from 2004 to 2013. PLoS ONE 15(12):e0242505.

Richardson, W.J., Greene Jr., C.R., Malme, C.I., Thomson, D. 1995. Marine Mammals and Noise. San Diego, CA: Academic Press.

Robards, R.M., Silber, G., Adams, J., Arroyo, J., Lorenzini, D., Schwehr, K, Amos, J. 2016. Conservation science and policy applications of the marine vessel automatic identification system (AIS) – A review. Bulletin of Marine Science 92: 75–103.

Rolland, R.M., Parks, S.E., Hunt, K.E., Castellote, M., Corkeron, P.J., Nowacek, D.P., Wasser, S.K., Kraus, S.D. 2012. Evidence that ship noise increases stress in right whales. Proceeding in the Royal Society London B Biological Science 279:2363–2368.

Ross, D. 1976. Mechanics of Underwater Noise. Pergamon, New York.

Rutz, C. Loretto, M-C., Bates, A.E., Davidson, S.C., Duarte, C.M., Jetz, W., Johnson, M., Kato, A., Kays, R., Mueller, T., Primack, R.B., Ropert-Coudert, Y., Tucker, M.A., Wikelski, M., Cagnacci, F. 2020. COVID-19 lockdown allows research to quantify the effects of human activity on wildlife. Nature, Ecology and Evolution 4, 1156-1159.

Scrimger, J.A., Evans, D.J., Yee, W. 1989. Underwater noise due to rain – Open ocean measurements. Journal of the Acoustical Society of America 85, 726–731.

Serra-Sogas, N., Canessa, R., O'Hara, P. Smallshaw, L., Warrior, M. 2018. Small vessel traffic study in the Salish Sea and southern resident killer whale critical habitat, CORAL group. University of Victoria**:** 85 pp.

Shardlow, T.F., English, K.K., Hoyt, T, Gillespie, G.E., Calvin T.A. 1989. Strait of Georgia Creel Survey Sport Fishery Statistics, 1983. Canadian Manuscript Report of Fisheries and Aquatic Science 1872: vii + 53 p.

Siedlecki, S.A., Banas, N.S., Davis, K.A., Giddings, S., Hickey, B.M., MacCready, P., Connolly, T., Geier. S. 2015. Seasonal and inter-annual oxygen variability on the Washington and Oregon continental shelves. Journal of Geophysical Research, Oceans: 120.

Silber, G.K., Slutsky, J., Bettridge, S. 2010. Hydrodynamics of a ship/whale collision. Journal of Experimental Marine Biology and Ecology 391: 10-19.

Simard, Y., Roy, N., Gervaise, C., Chorus, C., Giard, S. 2016 Analysis and modelling of 225 source levels of merchant ships from an acoustic observatory along the St. Lawrence seaway. Journal of the Acoustical Society of America 140(3): 2002–2018.

Simmonds, M., Dolman, S., Weilgart, L. 2004. Oceans of Noise. A WDCS Science Report WDCS, the Whale and Dolphin Conservation Society, UK. 168.

Soontiens, N., Allen, S.E., Latornell, D., Le Souef, K., Machuca, I., Paquin, J-P, Lu, Y., Thompson, K., Korabel, V. 2016. Storm surges in the Strait of Georgia simulated with a regional model. Atmosphere-Ocean 54: 1–21.

Soontiens, N., Allen, S.E. 2017. Modelling sensitivities to mixing and advection in a sill-basin estuarine system. Ocean Modelling, 112: 17–32.

Southall, B.L., Bowles, A.E., Ellison, W.T., Finneran, J.J., Gentry, R.L., Greene Jr., C.R.. Kastak, D., Ketten, D.K., Miller, J.H., Nachtigall, P.E., Richardson, W.J., Thomas, J.A., Tyack. P.L. 2007. Marine Mammal noise exposure criteria: Initial scientific recommendations. Aquatic Mammals 33:412–522.

Sueur, J., Farina, A., 2015. Ecoacoustics: The ecological investigation and interpretation of environmental sound. Biosemiotics 8: 493–502.

Tasker, M., Amundin, M., André, M., Hawkins, A., Lang, W., Merck, T., Scholik- Schlomer, A., Teilmann, J., Thomsen, F., Werner, S., Zakharia, M. 2010. Marine Strategy Framework Directive G Task Group 11 Report Underwater noise and other forms of energy, EUR 24341 EN G Joint Research Centre, Luxembourg: Office for Official Publications of the European Communities, 55pp.

Tennessen, J.B., Holt, M.M., Hansen, M.B., Emmons, C.K., Giles, D.A., Hogan, J.T. 2019. Kinematic signatures of prey capture from archival tags reveal sex differences in killer whale foraging activity. Journal of Experimental Biology 222: 1–13.

Thomsen, F., Franck, D., Ford, J.K.B. 2001. Characteristics of whistles from the acoustic repertoire of resident killer whales (*Orcinus orca*) off Vancouver Island, British Columbia. Journal of the Acoustical Society of America 109: 1240–1246.

Tyack, P. 2008. Implications for marine mammals of large-scale changes in the marine acoustic environment Journal of Mammalogy 89(3):549–558.

Urick, R.J. 1983. Principles of Underwater Sound. McGraw-Hill, New York.

Vagle, S. 2020. Evaluation of the efficacy of the Juan de Fuca lateral displacement trial and Swiftsure Bank plus Swanson Channel interim sanctuary zones, 2019. Canadian Technical Report of Hydrography and Ocean Sciences. 332: vi + 60 p.

Vagle, S., Large, W. G., Farmer, D. M. 1990. An Evaluation of the WOTAN technique of inferring oceanic winds from underwater ambient sound. Journal of Atmospheric and Oceanic Technology 7: 576–595.

Vagle, S., Neves, M. 2019. Evaluation of the effects on underwater noise levels from shifting vessel traffic away from Southern Resident Killer Whale foraging areas in the Strait of Juan de Fuca in 2018. Canadian Technical Report of Hydrography and Ocean Sciences. 329 : vi + 64 p.

Veirs, S., Veirs, V., Wood, J. 2016. Ship noise in an urban estuary extends to frequencies used for echolocation by endangered killer whales. PeerJ PrePrints, 3: e955v3.

Veirs S., Veirs, V, Williams, R., Jasny, M., Wood, J. 2017. A key to quieter seas: half of ship noise comes from 15% of the fleet. Peer J. PrePrints e26525.

Veirs, V., Veirs, S. 2006. Average levels and power spectra of ambient sound in the habitat of Southern Resident orcas. Washington, D.C.: NOAA/NMFS/NWFSC.

Wellard, R., Pittman, R.L., Durban, J., Erbe, C. 2020. Cold call: The acoustic repertoire of Ross Sea killer whales (*Orcinus orca*, Type C) in McMurdo Sound, Antarctica. Royal Society Open Science 7: 191228.

Wenz, G.M. 1962. Acoustic ambient noise in the ocean: spectra and sources. Journal of the Acoustical Society of America 34: 1936–1956.

Williams, R., Erbe, C., Ashe, E., Beerman, A., Smith, J. 2014. Severity of killer whale behavioral responses to ship noise: a dose–response study. Marine Pollution Bulletin 79(1– 2):254–260.

Wysocki, L.E., Amoser, S. Ladich, F. 2007. Diversity in ambient noise in European freshwater habitats: Noise levels, spectral profiles, and impact on fishes. Journal of the Acoustical Society of America 121(5): 2559–2566.